SLAC-PUB--5558

DE91 013991

LIGHT-CONE QUANTIZATION OF QUANTUM CHROMODYNAMICS*

STANLEY J. BRODSKY

Stanford Linear Accelerator Center

Stanford University, Stanford, California 94309

and

HANS-CHRISTIAN PAULI

Max-Planck-Institut für Kernphysik,

D-6900 Heidelberg 1, Germany

Invited lectures presented at the

30th Schladming Winter School in Particle Physics: Field Theory

Schladming, Austria, March, 1991

* Work supported by the Department of Energy, contract DE-AC03-76SF00515.

ABSTRACT

We discuss the light-cone quantization of gauge theories from two perspectives: as a calculational tool for representing hadrons as QCD bound-states of relativistic quarks and gluons, and also as a novel method for simulating quantum field theory on a computer. The light-cone Fock state expansion of wavefunctions at fixed light cone time provides a precise definition of the parton model and a general calculus for hadronic matrix elements. We present several new applications of light-cone Fock methods, including calculations of exclusive weak decays of heavy hadrons, and intrinsic heavy-quark contributions to structure functions. A general non-perturbative method for numerically solving quantum field theories, "discretized light-cone quantization," is outlined and applied to several gauge theories, including QCD in one space and one time dimension, and quantum electrodynamics in physical space-time at large coupling strength. The DLCQ method is invariant under the large class of light-cone Lorentz transformations, and it can be formulated such that ultraviolet regularization is independent of the momentum space discretization. Both the bound-state spectrum and the corresponding relativistic light-cone wavefunctions can be obtained by matrix diagonalization and related techniques. We also discuss the construction of the light-cone Fock basis, the structure of the light-cone vacuum, and outline the renormalization techniques required for solving gauge theories within the light-cone Hamiltonian formalism.

Introduction

In quantum chromodynamics, hadrons are relativistic bound states of confined quark and gluon quanta. Although the momentum distributions of quarks in nucleons are well-determined experimentally from deep inelastic lepton scattering measurements, there has been relatively little progress in computing the basic wavefunctions of hadrons from first principles in QCD. The most interesting progress has come from lattice gauge theory[1,2] and QCD sum rule calculations,[3] both of which have given predictions for the lowest moments $\langle x_i^n \rangle$ of the proton's distribution amplitude, $\phi_p(x_i, Q)$. The distribution amplitude is the fundamental gauge invariant wavefunction which describes the fractional longitudinal momentum distributions of the valence quarks in a hadron integrated over transverse momentum up to the scale Q.[4] However, the results from the two analyses are in strong disagreement: The QCD sum rule analysis predicts a strongly asymmetric three-quark distribution (See Fig. 1), whereas the lattice results,[2] obtained in the quenched approximation, favor a symmetric distribution in the x_i. Models of the proton distribution amplitude based on a quark-di-quark structure suggest strong asymmetries and strong spin-correlations in the baryon wavefunctions.[5] Even less is known from first principles in non-perturbative QCD about the gluon and non-valence quark contributions to the proton wavefunction, although data from a number of experiments now suggest non-trivial spin correlations, a significant strangeness content, and a large x component to the charm quark distribution in the proton.[6]

There are many reasons why knowledge of hadron wavefunctions, particularly at the amplitude level, will be necessary for future progress in particle physics. For example, in electroweak theory, the central unknown required for reliable calculations of weak decay amplitudes are the hadronic matrix elements. The coefficient functions in the operator product expansion needed to compute many types of experimental quantities are essentially unknown and can only be estimated at this point. The calculation of form factors and exclusive scattering processes, in general, depend in detail on the basic amplitude structure of the scattering hadrons in a general Lorentz frame. Even the calculation of the magnetic moment of a proton requires wavefunctions in a boosted frame. We thus need a practical computational method for QCD which not only determines its spectrum, but also a method which can provide the non-perturbative hadronic matrix elements needed for general calculations in hadron physics.

It is clearly a formidable task to calculate the structure of hadrons in terms

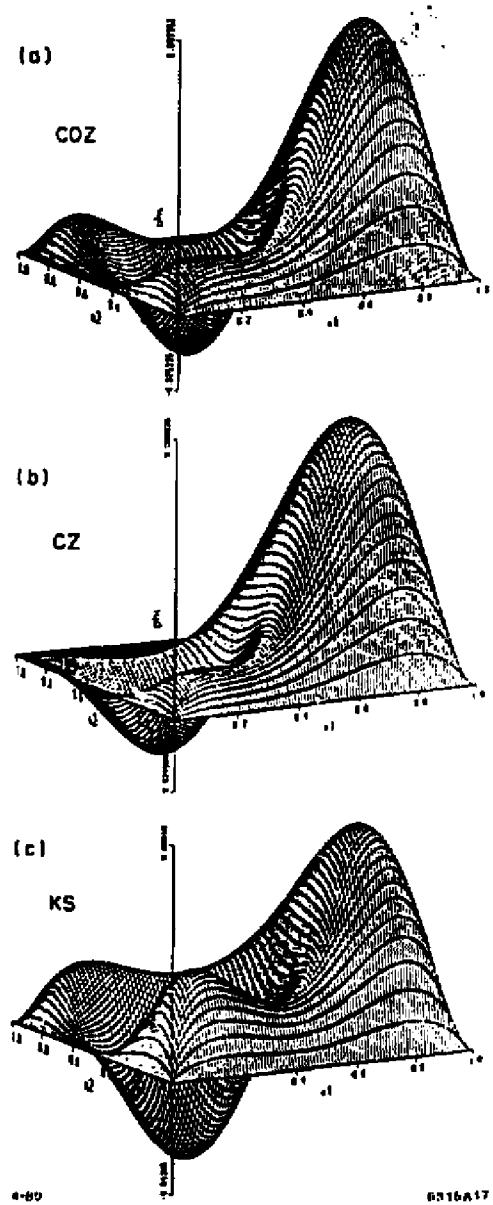

Figure 1. The proton distribution amplitude $\phi_P(x_i, \mu)$ evaluated at the scale $\mu \sim 1\ GeV$ from QCD sum rules.[3] The enhancement at large x_1 correspond to a strong correlation between the a high momentum u quark with spin parallel to the proton spin.

of their fundamental degrees of freedom in QCD. Even in the case of abelian

quantum electrodynamics, very little is known about the nature of the bound state solutions in the large α, strong-coupling, domain. A calculation of bound state structure in QCD has to deal with many complicated aspects of the theory simultaneously: confinement, vacuum structure, spontaneous breaking of chiral symmetry (for massless quarks), while describing a relativistic many-body system which apparently has unbounded particle number.

The first step is to find a language in which one can represent the hadron in terms of relativistic confined quarks and gluons. The Bethe-Salpeter formalism has been the central method for analyzing hydrogenic atoms in QED, providing a completely covariant procedure for obtaining bound state solutions. However, calculations using this method are extremely complex and appear to be intractable much beyond the ladder approximation. It also appears impractical to extend this method to systems with more than a few constituent particles.

An intuitive approach for solving relativistic bound-state problems would be to solve the Hamiltonian eigenvalue problem

$$H\,|\psi\rangle = \sqrt{\vec{P}^{\,2} + M^2}\,|\psi\rangle \tag{1}$$

for the particle's mass, M, and wavefunction, $|\psi\rangle$. Here, one imagines that $|\psi\rangle$ is an expansion in multi-particle occupation number Fock states, and that the operators H and $\vec{P}$ are second-quantized Heisenberg picture operators. Unfortunately, this method, as described by Tamm and Dancoff,[7] is severely complicated by its non-covariant structure and the necessity to first understand its complicated vacuum eigensolution over all space and time. The presence of the square root operator also presents severe mathematical difficulties. Even if these problems could be solved, the eigensolution is only determined in its rest system; determining the boosted wavefunction is as complicated as diagonalizing H itself.

Fortunately, "light-cone" quantization, the Lorentz-frame-independent method we shall emphasize in these lectures, offers an elegant avenue of escape.[8] The square root operator does not appear in light-cone formalism, and the vacuum structure is relatively simple; for example, there is no spontaneous creation of massive fermions in the light-cone quantized vacuum.

Quantization on the Light-Cone

There are, in fact, many reasons to quantize relativistic field theories at fixed light-cone time $\tau = t + z/c$. Dirac,[9] in 1949, showed that a maximum number of Poincare generators become independent of the dynamics in the "front form" formulation, including certain Lorentz boosts. In fact, unlike the traditional equal-time Hamiltonian formalism, quantization on the light-cone can be formulated without reference to the choice of a specific Lorentz frame; the eigensolutions of the light-cone Hamiltonian thus describe bound states of arbitrary four-momentum, allowing the computation of scattering amplitudes and other dynamical quantities. However, the most remarkable feature of this formalism is the apparent simplicity of the light-cone vacuum. In many theories the vacuum state of the free Hamiltonian is an eigenstate of the total light-cone Hamiltonian. The Fock expansion constructed on this vacuum state provides a complete relativistic many-particle basis for diagonalizing the full theory.

General Features of Light-Cone Quantization

In general, the Hamiltonian is the "time" evolution operator $H = i\frac{\partial}{\partial \tau}$ which propagates fields from one space-like surface to another. As emphasized by Dirac,[9] there are several choices for the evolution parameter τ. In the "Instant Form" $\tau = t$ is the ordinary Cartesian time. In the "Front Form," or light-cone quantization, one chooses $\tau = t + z/c$ as the light-cone coordinate with boundary conditions specified as a function of x, y, and $z^- = ct - z$. Another possible choice is the "point form," where $\tau = \sqrt{c^2t^2 - \vec{x}^2}$. Notice that all three forms become equivalent in the non-relativistic limit where, effectively, $c \to \infty$. A comparison of light-cone quantization with equal-time quantization is shown in Table 1.

Table 1. A comparison of light-cone and equal-time quantization.

	Instant Form	Front Form
Hamiltonian	$H = \sqrt{\vec{P}^2 + M^2} + V$	$P^- = \frac{P_\perp^2 + M^2}{P^+} + V$
Conserved quantities	$E, \quad \vec{P}$	$P^-, \quad P^+, \quad \vec{P}_\perp$
Momenta	$P_z <> 0$	$P^+ > 0$
Bound state equation	$H\psi = E\psi$	$P^+P^-\psi = M^2\psi$
Vacuum	Complicated	Trivial

Although the instant form is the conventional choice for quantizing field theory, it has many practical disadvantages. For example, given the wavefunction of an n-electron atom, $\psi_n(\vec{x}_i, t = 0)$, at initial time $t = 0$, then, in principle, one can use the Hamiltonian H to evolve $\psi_n(\vec{x}_i, t)$ to later times t. However, an experiment which could specify the initial wavefunction would require the simultaneous measurement of the positions of all of the bound electrons, such as by the simultaneous Compton scattering of n independent laser beams on the atom. In contrast, determining the initial wavefunction at fixed light-cone time $\tau = 0$ only requires an experiment which scatters one plane-wave laser beam, since the signal reaching each of the n electrons is received along the light front at the same light-cone time $\tau = t_i + z_i/c$.

As we shall discuss in these lectures, light cone quantization allows a precise definition of the notion that a hadron consists of confined quarks and gluons. In light-cone quantization, a free particle is specified by its four momentum $k^\mu = (k^+, k^-, k_\perp)$ where $k^\pm = k^0 \pm k^3$. If the particle is on its mass shell and has positive energy, its light-cone energy is also positive: $k^- = (k_\perp^2 + m^2)/k^+ > 0$. In perturbation theory, transverse momentum $\sum k_\perp$ and the plus momentum $\sum k^+$ are conserved at each vertex. The light-cone bound-state wavefunction thus describes constituents which are on their mass shell, but off the light-cone energy shell: $P^- < \sum k^- i$.

As we shall show explicitly, one can construct a complete basis of free Fock states (eigenstates of the free light-cone Hamiltonian) $|n\rangle\langle n| = I$ in the usual way by applying products of free field creation operators to the vacuum state $|0\rangle$:

$$\begin{aligned}
&|0\rangle \\
&|q\bar{q} : \underline{k}_i\lambda_i\rangle = b^\dagger(\underline{k}_1\lambda_1)\, d^\dagger(\underline{k}_2\lambda_2)\ |0\rangle \\
&|q\bar{q}g : \underline{k}_i\lambda_i\rangle = b^\dagger(\underline{k}_1\lambda_1)\, d^\dagger(\underline{k}_2\lambda_2)\, a^\dagger(\underline{k}_3\lambda_3)\ |0\rangle \\
&\vdots
\end{aligned} \tag{2}$$

where $b^\dagger$, $d^\dagger$ and $a^\dagger$ create bare quarks, antiquarks and gluons having three-momenta $\underline{k}_i$ and helicities λ_i.

Note, however, that in principle In the case of a theory such as QED, with massive fermions, all states containing particles have quanta with positive k^+, and the zero-particle state cannot mix with the other states in the basis.[10] The free vacuum in such theories is thus an exact eigenstate of H_{LC}. However, as we shall discuss in later sections, the vacuum in QCD is undoubtedly more complicated

due to the possibility of color-singlet states with $P^+ = 0$ built on four or more zero-mode massless gluon quanta.

The restriction $k^+ > 0$ for mass..e quanta is a key difference between light-cone quantization and ordinary equal-time quantization. In equal-time quantization, the state of a parton is specified by its ordinary three-momentum $\vec{k}_\perp = (k^1, k^2, k^3)$. Since each component of $\vec{k}_\perp$ can be either positive or negative, there exist zero total momentum Fock states of arbitrary particle number, and these will mix with the zero-particle state to build up the ground state. However, in light-cone quantization each of the particles forming a zero-momentum state must have vanishingly small k^+. Such a configuration represents a point of measure zero in the phase space, and therefore such states can usually be neglected.

Actually some care must be taken here, since there are operators in the theory that are singular at $k^+ = 0$—*e.g.* the kinetic energy $(\vec{k}_\perp^2 + M^2)/k^+$. In certain circumstances, states containing $k^+ \to 0$ quanta can significantly alter the ground state of the theory. One such circumstance is when there is spontaneous symmetry breaking. Another is the complication due to massless gluon quanta in a non-Abelian gauge theory. Nevertheless, the space of states that can play a role in the vacuum structure is much smaller for light-cone quantization than for equal-time quantization. This suggests that vacuum structure may be far simpler to analyze using the light-cone formulation.

Even in perturbation theory, light-cone quantization has overwhelming advantages over standard time-ordered perturbation theory. For example, in order to calculate a Feynman amplitude of order g^n in TOPTH one must suffer the calculation of the sum of n time-ordered graphs, each of which is a non-covariant function of energy denominators which, in turn, consist of sums of complicated square roots $p_i^0 = \sqrt{\vec{p}_i^2 + m_i^2}$. On the other hand, in light-cone perturbation theory (LCPTH), only a few graphs give non-zero contributions, and those that are non-zero have light-cone energy denominators which are simple sums of rational forms $p^- = (\vec{p}_{\perp i}^2 + m_i^2)/p_i^+$.

Probably the worst problem in TOPTH are the contributions from vacuum creation graphs, as illustrated for QED in Fig. 2(a). In TOPTH, all intermediate states contribute to the total amplitude as long as three-momentum is conserved; in this case $\vec{p}_1 + \vec{p}_2 + \vec{k} = \vec{0}$. The existence of vacuum creation and annihilation graphs implies that one cannot even compute any current matrix element without considering the effect of the currents arising from pair production from the vacuum. This is illustrated in Fig. 2(b). In contrast, in light-cone perturba-

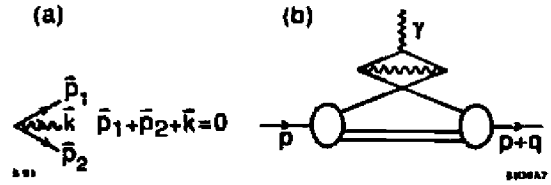

Figure 2. (a) Illustration of a vacuum creation graph in time-ordered perturbation theory. A corresponding contribution to the form factor of a bound state is shown in figure (b).

tion theory (LCPTH), an intermediate state contributes only if the total $\vec{p}_\perp$ and p^+ are conserved. In the case of vacuum creation graphs in QED, this implies $\vec{p}_{1\perp} + \vec{p}_{2\perp} + \vec{p}_{3\perp} = \vec{0}_\perp$ and $p_1^+ + p_2^+ + k_3^+ = 0$. However, the latter condition cannot be satisfied since each massive fermion has strictly positive $p_i^+ > 0$. Thus aside from theories which permit zero modes, there are no vacuum creation graphs in LCPTH.

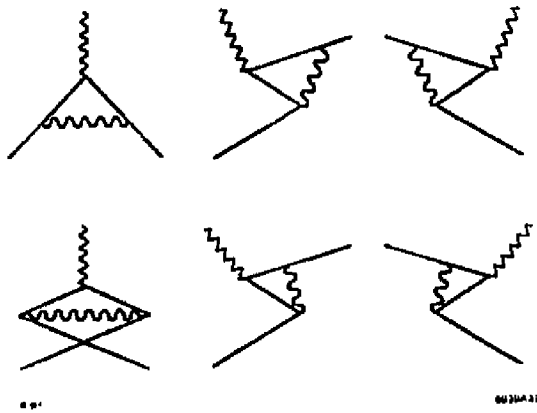

Figure 3. Time-ordered contributions to the electron's anomalous magnetic moment. In light-cone quantization with $q^+ = 0$, only graph (a) needs to be computed to obtain the Schwinger result.

In fact, light-cone perturbation theory is sufficiently simple that it provides in many cases a viable alternative to standard covariant (Feynman) perturbation theory. Each loop of a τ-ordered diagram requires a three-dimensional integration over the transverse momentum $d^2\vec{k}_{i\perp}$ and light-cone momentum fraction $x_i = k_i^+/p^+$ with $(0 < x_i < 1.)$ For example, the lowest order Schwinger contribution to the electron anomalous magnetic moment, $a = \frac{1}{2}(g-2) = \frac{\alpha}{2\pi}$, is easily computed

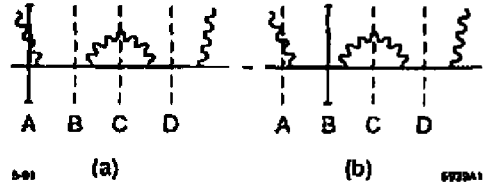

Figure 4. Construction of a renormalized amplitude in LCPTH using the method of alternating denominators.[11] The mass renormalization counterterm is constructed locally in momentum space in graph (b) by substituting the light-cone energy difference $P_C^- = P_B^-$ rather than $P_C^- - P_A^-$.

from just one LCPTH diagram. (See Fig. 3). Calculations of the higher order terms in α require renormalization in the context of light-cone Hamiltonian field theory. As shown in Ref. 11 renormalization in LCPTH can be carried out in close correspondence to Lagrangian methods. In the case of QED one can use the Pauli-Villars method to regulate the ultra-violet divergences. Then for each τ-ordered diagram with divergent subgraphs, the required local counter-term can be computed using the method of "alternating denominators."[11] A simple example for one LCPTH graph for Compton scattering is shown in Fig. 4. Additional divergences which occur due to the γ^- couplings (in covariant gauges) can be eliminated by subtraction of the divergent amplitude subgraph at $p^+ = 0$.[12]

One of the most interesting applications of LCPTH would be the perturbative calculation of the annihilation cross section $R_{e^+e^-}$, since one would automatically calculate, to the same order in perturbation theory, the quark and gluon jet distributions appearing in the final state. It is advantageous to use the light-cone gauge $A^+ = 0$ since one wants to describe gluon distributions with physical polarization. The extra complications in the renormalization procedure induced by a non-covariant axial gauge have recently been discussed by Langnau and Burkardt.[12] A non-perturbative light-cone quantization calculation of $R_{e^+e^-}$ for QED in one space and one time has been given by Hiller.[13] We will return to these developments in later sections.

Representation of Hadrons on the Light-Cone Fock Basis

One of the most important advantages of light-cone quantization is that the light-cone Fock expansion can be used as the basis for representing the physical states of QCD. For example, a pion with momentum $\underline{P} = (P^+, \vec{P}_\perp)$ is described by the expansion,

$$|\pi : \underline{P}) = \sum_{n,\lambda_i} \int \overline{\prod_i} \frac{dx_i d^2\vec{k}_{\perp i}}{\sqrt{x_i} 16\pi^3} \left| n : x_i P^+, x_i \vec{P}_\perp + \vec{k}_{\perp i}, \lambda_i \right\rangle \psi_{n/\pi}(x_i, \vec{k}_{\perp i}, \lambda_i) \quad (3)$$

where the sum is over all Fock states and helicities, and where

$$\begin{aligned} \overline{\prod_i} dx_i &\equiv \prod_i dx_i \, \delta\left(1 - \sum_j x_j\right) \\ \overline{\prod_i} d^2\vec{k}_{\perp i} &\equiv \prod_i d^2\vec{k}_{\perp i} \, 16\pi^3 \, \delta^2\left(\sum_j \vec{k}_{\perp j}\right). \end{aligned} \quad (4)$$

The wavefunction $\psi_{n/\pi}(x_i, \vec{k}_{\perp i}, \lambda_i)$ is thus the amplitude for finding partons in a specific light-cone Fock state n with momenta $(x_i P^+, x_i \vec{P}_\perp + \vec{k}_{\perp i})$ in the pion. The Fock state is off the light-cone energy shell: $\sum k_i^- > P^-$. The light-cone momentum coordinates x_i, with $\sum_{i=1}^n x_i$ and $\vec{k}_{\perp i}$, with $\sum_{i=1}^n \vec{k}_{\perp i} = \vec{0}_\perp$, are actually relative coordinates; *i.e.* they are independent of the total momentum P^+ and $P_\perp$ of the bound state. The special feature that light-cone wavefunctions do not depend on the total momentum is not surprising, since x_i is the longitudinal momentum fraction carried by the i^{th}-parton ($0 \leq x_i \leq 1$), and $\vec{k}_{\perp i}$ is its momentum "transverse" to the direction of the meson. Both of these are frame independent quantities. The ability to specify wavefunctions simultaneously in any frame is a special feature of light-cone quantization.

In the light-cone Hamiltonian quantization of gauge theories, one chooses the light-cone gauge, $\eta \cdot A = A^+ = 0$, for the gluon field. The use of this gauge results in well-known simplifications in the perturbative analysis of light-cone dominated processes such as high-momentum hadronic form factors. It is indispensable if one desires a simple, intuitive Fock-state basis since there are neither negative-norm

gauge boson states nor ghost states in $A^+ = 0$ gauge. Thus each term in the normalization condition

$$\sum_{n,\lambda_i} \int \prod_i \frac{dx_i d^2\vec{k}_{\perp i}}{16\pi^3} |\psi_{n/\pi}(x_i, \vec{k}_{\perp i}, \lambda_i)|^2 = 1 \tag{5}$$

is positive.

The coefficients in the light-cone Fock state expansion are the parton wavefunctions $\psi_{n/H}(x_i, \vec{k}_{\perp i}, \lambda_i)$ which describe the decomposition of each hadron in terms of its fundamental quark and gluon degrees of freedom. The light-cone variable $0 < x_i < 1$ is often identified with the constituent's longitudinal momentum fraction $x_i = k_i^z/P_z$, in a frame where the total momentum $P^z \to \infty$. However, in light-cone Hamiltonian formulation of QCD, x_i is the boost-invariant light cone fraction,

$$x_i \equiv \frac{k_i^+}{P^+} = \frac{k_i^0 + k_i^z}{P^0 + P^z}\,, \tag{6}$$

independent of the choice of Lorentz frame.

Calculation of Hadronic Processes from Light-Cone Wavefunctions

Given the light-cone wavefunctions, $\psi_{n/H}(x_i, \vec{k}_{\perp i}, \lambda_i)$, one can compute virtually any hadronic quantity by convolution with the appropriate quark and gluon matrix elements. For example, the leading-twist structure functions measured in deep inelastic lepton scattering are immediately related to the light-cone probability distributions:

$$2M\, F_1(x, Q) = \frac{F_2(x, Q)}{x} \approx \sum_a e_a^2\, G_{a/p}(x, Q) \tag{7}$$

where

$$G_{a/p}(x, Q) = \sum_{n,\lambda_i} \int \prod_i \frac{dx_i d^2\vec{k}_{\perp i}}{16\pi^3} |\psi_n^{(Q)}(x_i, \vec{k}_{\perp i}, \lambda_i)|^2 \sum_{b=a} \delta(x_b - x) \tag{8}$$

is the number density of partons of type a with longitudinal momentum fraction x in the proton. This follows from the observation that deep inelastic lepton

scattering in the Bjorken-scaling limit occurs if x_{bj} matches the light-cone fraction of the struck quark. (The $\sum_b$ is over all partons of type a in state n.) However, the light cone wavefunctions contain much more information for the final state of deep inelastic scattering, such as the multi-parton distributions, spin and flavor correlations, and the spectator jet composition.

As was first shown by Drell and Yan,[14] it is advantageous to choose a coordinate frame where $q^+ = 0$ to compute form factors $F_i(q^2)$, structure functions, and other current matrix elements at spacelike photon momentum. With such a choice the quark current cannot create pairs, and $\langle p'|j^+|p\rangle$ can be computed as a simple overlap of Fock space wavefunctions; all off-diagonal terms involving pair production or annihilation by the current or vacuum vanish. In the interaction picture one can equate the full Heisenberg current to the quark current described by the free Hamiltonian at $\tau = 0$. Accordingly, the form factor is easily expressed in terms of the pion's light cone wavefunctions by examining the $\mu = +$ component of this equation in a frame where the photon's momentum is transverse to the incident pion momentum, with $\vec{q}_\perp^{\,2} = Q^2 = -q^2$. The spacelike form factor is then just a sum of overlap integrals analogous to the corresponding nonrelativistic formula:[14] (See Fig. 5.)

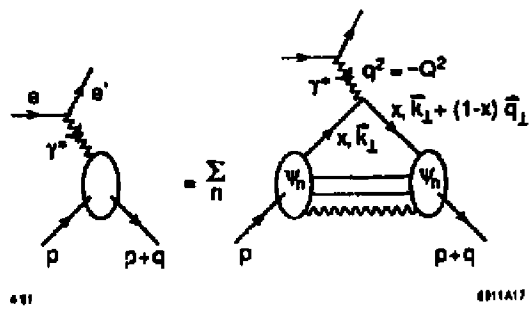

Figure 5. Calculation of the form factor of a bound state from the convolution of light-cone Fock amplitudes. The result is exact if one sums over all ψ_n.

$$F(Q^2) = \sum_{n,\lambda_i} \sum_a e_a \int \prod_i \frac{dx_i\, d^2\vec{k}_{\perp i}}{16\pi^3}\, \psi_n^{(\Lambda)*}(x_i, \vec{\ell}_{\perp i}, \lambda_i)\, \psi_n^{(\Lambda)}(x_i, \vec{k}_{\perp i}, \lambda_i). \qquad (9)$$

Here e_a is the charge of the struck quark, $\Lambda^2 \gg \vec{q}_\perp^{\,2}$, and

$$\vec{\ell}_{\perp i} \equiv \begin{cases} \vec{k}_{\perp i} - x_i \vec{q}_\perp + \vec{q}_\perp & \text{for the struck quark} \\ \vec{k}_{\perp i} - x_i \vec{q}_\perp & \text{for all other partons.} \end{cases} \tag{10}$$

Notice that the transverse momenta appearing as arguments of the first wavefunction correspond not to the actual momenta carried by the partons but to the actual momenta minus $x_i \vec{q}_\perp$, to account for the motion of the final hadron. Notice also that $\vec{\ell}_\perp$ and $\vec{k}_\perp$ become equal as $\vec{q}_\perp \to 0$, and that $F_\pi \to 1$ in this limit due to wavefunction normalization. All of the various form factors of hadrons with spin can be obtained by computing the matrix element of the plus current between states of different initial and final hadron helicities.[15]

As we have emphasized above, in principle, the light-cone wavefunctions determine all properties of a hadron. The general rule for calculating an amplitude involving wavefunction $\psi_n^{(\Lambda)}$, describing Fock state n in a hadron with $\underline{P} = (P^+, \vec{P}_\perp)$, has the form[4] (see Fig. 6):

$$\sum_{\lambda_i} \int \prod_i \frac{dx_i d^2\vec{k}_{\perp i}}{\sqrt{x_i} 16\pi^3} \psi_n^{(\Lambda)}(x_i, \vec{k}_{\perp i}, \lambda_i)\, T_n^{(\Lambda)}(x_i P^+, x_i \vec{P}_\perp + \vec{k}_{\perp i}, \lambda_i) \tag{11}$$

where $T_n^{(\Lambda)}$ is the irreducible scattering amplitude in LCPTh with the hadron replaced by Fock state n. If only the valence wavefunction is to be used, $T_n^{(\Lambda)}$ is irreducible with respect to the valence Fock state only; *e.g.* $T_n^{(\Lambda)}$ for a pion has no $q\bar{q}$ intermediate states. Otherwise contributions from all Fock states must be summed, and $T_n^{(\Lambda)}$ is completely irreducible.

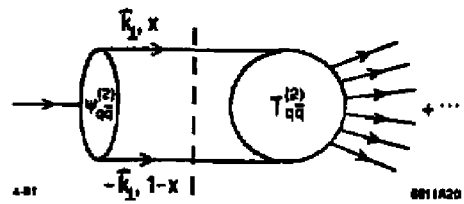

Figure 6. Calculation of hadronic amplitudes in the light-cone Fock formalism.

The leptonic decay of the $\pi^\pm$ is one of the simplest processes to compute since it involves only the $q\bar{q}$ Fock state. The sole contribution to π^- decay is from

$$\langle 0 \mid \bar{\psi}_u \gamma^+(1-\gamma_5)\psi_d \mid \pi^- \rangle = -\sqrt{2}P^+ f_\pi$$

$$= \int \frac{dx\, d^2\vec{k}_\perp}{16\pi^3}\, \psi^{(\Lambda)}_{d\bar{u}}(x,\vec{k}_\perp)\frac{\sqrt{n_c}}{\sqrt{2}}\left\{\frac{\bar{v}_\downarrow}{\sqrt{1-x}}\gamma^+(1-\gamma_5)\frac{u_\uparrow}{\sqrt{x}} + (\uparrow\leftrightarrow\downarrow)\right\} \tag{12}$$

where $n_c = 3$ is the number of colors, $f_\pi \approx 93$ MeV, and where only the $L_z = S_z = 0$ component of the general $q\bar{q}$ wavefunction contributes. Thus we have

$$\int \frac{dx\, d^2\vec{k}_\perp}{16\pi^3}\psi^{(\Lambda)}_{d\bar{u}}(x,\vec{k}_\perp) = \frac{f_\pi}{2\sqrt{3}}. \tag{13}$$

This result must be independent of the ultraviolet cutoff Λ of the theory provided Λ is large compared with typical hadronic scales. This equation is an important constraint upon the normalization of the $d\bar{u}$ wavefunction. It also shows that there is a finite probability for finding a π^- in a pure $d\bar{u}$ Fock state.

The fact that a hadron can have a non-zero projection on a Fock state of fixed particle number seems to conflict with the notion that bound states in QCD have an infinitely recurring parton substructure, both from the infrared region (from soft gluons) and the ultraviolet regime (from QCD evolution to high momentum). In fact, there is no conflict. Because of coherent color-screening in the color-singlet hadrons, the infrared gluons with wavelength longer than the hadron size decouple from the hadron wavefunction.

The question of parton substructure is related to the resolution scale or ultraviolet cut-off of the theory. Any renormalizable theory must be defined by imposing an ultraviolet cutoff Λ on the momenta occurring in theory. The scale Λ is usually chosen to be much larger than the physical scales μ of interest; however it is usually more useful to choose a smaller value for Λ, but at the expense of introducing new higher-twist terms in an effective Lagrangian:[16]

$$\mathcal{L}^{(\Lambda)} = \mathcal{L}_0^{(\Lambda)}(\alpha_s(\Lambda), m(\Lambda)) + \sum_{n=1}^{N}\left(\frac{\cdot}{\Lambda}\right)^n \delta\mathcal{L}_n^{(\Lambda)}(\alpha_s(\Lambda), m(\Lambda)) + \mathcal{O}\left(\frac{1}{\Lambda}\right)^{N+1} \tag{14}$$

where

$$\mathcal{L}_0^{(\Lambda)} = -\frac{1}{4}F^{(\Lambda)}_{\alpha\mu\nu}F^{(\Lambda)\alpha\mu\nu} + \bar{\psi}^{(\Lambda)}\left[i\not{\partial}^{(\Lambda)} - m(\Lambda)\right]\psi^{(\Lambda)}. \tag{15}$$

The neglected physics of parton momenta and substructure beyond the cutoff scale

has the effect of renormalizing the values of the input coupling constant $g(\Lambda^2)$ and the input mass parameter $m(\Lambda^2)$ of the quark partons in the Lagrangian.

One clearly should choose Λ large enough to avoid large contributions from the higher-twist terms in the effective Lagrangian, but small enough so that the Fock space domain is minimized. Thus if Λ is chosen of order 5 to 10 times the typical QCD momentum scale, then it is reasonable to hope that the mass, magnetic moment and other low momentum properties of the hadron could be well-described on a Fock basis of limited size. Furthermore, by iterating the equations of motion, one can construct a relativistic Schrödinger equation with an effective potential acting on the valence lowest-particle number state wavefunction.[4] Such a picture would explain the apparent success of constituent quark models for explaining the hadronic spectrum and low energy properties of hadron.

It should be emphasized that infinitely-growing parton content of hadrons due to the evolution of the deep inelastic structure functions at increasing momentum transfer, is associated with the renormalization group substructure of the quarks themselves, rather than the "intrinsic" structure of the bound state wavefunction.[17] The fact that the light-cone kinetic energy $\left\langle \frac{\vec{k}_\perp^2+m^2}{x} \right\rangle$ of the constituents in the bound state is bounded by Λ^2 excludes singular behavior of the Fock wavefunctions at $x \to 0$. There are several examples where the light-cone Fock structure of the bound state solutions is known. In the case of the super-renormalizable gauge theory, $QED(1+1)$, the probability of having non-valence states in the light-cone expansion of the lowest lying meson and baryon eigenstates to be less than 10^{-3}, even at very strong coupling.[18] In the case of QED(3+1), the lowest state of positronium can be well described on a light-cone basis with two to four particles, $|e^+e^-\rangle$, $|e^+e^-\gamma\rangle$, $|e^+e^-\gamma\gamma\rangle$, and $|e^+e^-e^+e^-\rangle$; in particular, the description of the Lamb-shift in positronium requires the coupling of the system to light-cone Fock states with two photons "in flight" in light-cone gauge. The ultraviolet cut-off scale Λ only needs to be taken large compared to the electron mass. On the other hand, a charged particle such as the electron does not have a finite Fock decomposition, unless one imposes an artificial infrared cut-off.

We thus expect that a limited light-cone Fock basis should be sufficient to represent bound color-singlet states of heavy quarks in QCD(3+1) because of the coherent color cancellations and the suppressed amplitude for transversely-polarized gluon emission by heavy quarks. However, the description of light hadrons is undoubtedly much more complex due to the likely influence of chiral symmetry breaking and zero-mode gluons in the light-cone vacuum. We return to this problem later.

Even without solving the QCD light-cone equations of motion, we can anticipate some general features of the behavior of the light-cone wavefunctions. Each Fock component describes a system of free particles with kinematic invariant mass squared:

$$\mathcal{M}^2 = \sum_i^n \frac{\vec{k}_{\perp i}^2 + m_i^2}{x_i}, \tag{16}$$

On general dynamical grounds, we can expect that states with very high $\mathcal{M}^2$ are suppressed in physical hadrons, with the highest mass configurations computable from perturbative considerations. We also note that $\ell n\, x_i = \ell n\, \frac{(k^0+k^z)_i}{(P^0+P^z)} = y_i - y_P$ is the rapidity difference between the constituent with light-cone fraction x_i and the rapidity of the hadron itself. Since correlations between particles rarely extend over two units of rapidity in hadron physics, this argues that constituents which are correlated with the hadron's quantum numbers are primarily found with $x > 0.2$.

The limit $x \to 0$ is normally an ultraviolet limit in a light-cone wavefunction. Recall, that in any Lorentz frame, the light-cone fraction is $x = k^+/p^+ = (k^0 + k^z)/(P^0 + P^z)$. Thus in a frame where the bound state is moving infinitely fast in the positive z direction ("the infinite momentum frame"), the light-cone fraction becomes the momentum fraction $x \to k^z/p^z$. However, in the rest frame $\vec{P} = \vec{0}$, $x = (k^0 + k^z)/M$. Thus $x \to 0$ generally implies very large constituent momentum $k^z \to -k^0 \to -\infty$ in the rest frame; it is excluded by the ultraviolet regulation of the theory—unless the particle has strictly zero mass and transverse momentum.

If a particle has non-relativistic momentum in the bound state, then we can identify $k^z \sim xM - m$. This correspondence is useful when one matches physics at the relativistic/non-relativistic interface. In fact, any non-relativistic solution to the Schrödinger equation can be immediately written in light-cone form by identifying the two forms of coordinates. For example, the Schrödinger solution for particles bound in a harmonic oscillator potential can be taken as a model for the light-cone wavefunction for quarks in a confining linear potential:[19]

$$\psi(x_i, \vec{k}_{\perp i}) = A \exp(-b\mathcal{M}^2) = \exp - \left(b \sum_i^n \frac{k_{\perp i}^2 + m_i^2}{x_i} \right) . \tag{17}$$

This form exhibits the strong fall-off at large relative transverse momentum and at the $x \to 0$ and $x \to 1$ endpoints expected for soft non-perturbative solutions in QCD. The perturbative corrections due to hard gluon exchange give amplitudes

suppressed only by power laws and thus will eventually dominate wavefunction behavior over the soft contributions in these regions. This *ansatz* is the central assumption required to derive dimensional counting perturbative QCD predictions for exclusive processes at large momentum transfer and the $x \to 1$ behavior of deep inelastic structure functions. A review is given in Ref. 20. A model for the polarized and unpolarized gluon distributions in the proton which takes into account both perturbative QCD constraints at large x and coherent cancellations at low x and small transverse momentum is given in Ref. 17.

The Light-Cone Hamiltonian Eigenvalue Problem

In principle, the problem of computing the spectrum in QCD and the corresponding light-cone wavefunctions for each hadron can be reduced to diagonalizing the QCD light cone Hamiltonian in Heisenberg quantum mechanics: Any hadron state must be an eigenstate of the light-cone Hamiltonian. For convenience we will work in the "standard" frame where $\underline{P}_\pi \equiv (P^+, P_\perp) = (1, 0_\perp)$ and $P_\pi^- = M_\pi^2$. Then the state $|\pi\rangle$ satisfies an equation

$$\left(M_\pi^2 - H_{LC}\right)|\pi\rangle = 0. \tag{18}$$

Projecting this onto the various Fock states $\langle q\bar{q}|$, $\langle q\bar{q}g|\ldots$ results in an infinite number of coupled integral eigenvalue equations,[4]

$$\begin{aligned}\left(M_\pi^2 - \sum_i \frac{\vec{k}_{\perp i}^2 + m_i^2}{x_i}\right)\begin{bmatrix}\psi_{q\bar{q}/\pi}\\ \psi_{q\bar{q}g/\pi}\\ \vdots\end{bmatrix} \\ = \begin{bmatrix}\langle q\bar{q}|V|q\bar{q}\rangle & \langle q\bar{q}|V|q\bar{q}g\rangle & \cdots\\ \langle q\bar{q}g|V|q\bar{q}\rangle & \langle q\bar{q}g|V|q\bar{q}g\rangle & \cdots\\ \vdots & \vdots & \ddots\end{bmatrix}\begin{bmatrix}\psi_{q\bar{q}/\pi}\\ \psi_{q\bar{q}g/\pi}\\ \vdots\end{bmatrix}\end{aligned} \tag{19}$$

where V is the interaction part of H_{LC}. Diagrammatically, V involves completely irreducible interactions—*i.e.* diagrams having no internal propagators—coupling Fock states. (See Fig. 7.) We will give the explicit forms of each matrix element of V in a later section.

In principle, these equations determine the hadronic spectrum and wavefunctions. However, even though the QCD potential is essentially trivial on the light-cone momentum space basis, the many channels required to describe a hadronic

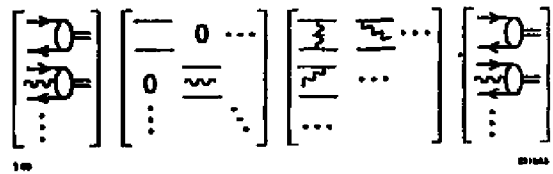

Figure 7. Coupled eigenvalue equations for the light-cone wavefunctions of a pion.

state make these equations very difficult to solve. For example, Fock states with two or more gluons are required just to represent the effects of the running coupling constant of QCD.

In the case of gauge theories in one space and one time dimension, there are no physical gluon degrees of freedom in light-cone gauge. The computational problem is thus much more tractable, and it is possible to explicitly diagonalize the light-cone Hamiltonian and thus solve these theories numerically. In this method, "discretized light-cone quantization" (DLCQ) the light-cone Fock state basis is rendered discrete by imposing periodic (or anti-periodic) boundary conditions.[21]

A central emphasis of these lectures will be the use of DLCQ methods to solve non-perturbative problems in gauge theory. This method was first used to obtain the mass spectrum and wavefunctions of Yukawa theory, $\bar{\psi}\psi\phi$, in one space and one time dimensions.[21] This success led to further applications including QED(1+1) for general mass fermions and the massless Schwinger model by Eller *et al.*,[22] ϕ^4 theory in 1+1 dimensions by Harindranath and Vary,[23] and QCD(1+1) for N_C = 2,3,4 by Hornbostel *et al.*[18] Complete numerical solutions have been obtained for the meson and baryon spectra as well as their respective light cone Fock state wavefunctions for general values of the coupling constant, quark masses, and color. Similar results for QCD(1+1) were also obtained by Burkardt[24] by solving the coupled light-cone integral equation in the low particle number sector. Burkardt was also able to study non-additive nuclear effects in the structure functions of nuclear states in QCD(1+1). In each of these applications, the mass spectrum and wavefunctions were successfully obtained, and all results agree with previous analytical and numerical work, where they were available. More recently, Hiller[13] has used DLCQ and the Lanczos algorithm for matrix diagonalization method to compute the annihilation cross section, structure functions and form factors in 1+1 theories. Although these are just toy models, they do exhibit confinement and are excellent tests of the light-cone Fock methods.

In addition to the above work on DLCQ, Wilson and his colleagues at Ohio State have developed a complimentary method, the Light-Front Tamm Damcoff approach.[25,26] which uses a fixed number Fock basis to truncate the theory. Wilson has also emphasized the potential advantages of using a Gaussian basis similar to that used in many-electron molecular systems, rather than the plane wave basis used in the DLCQ work.

The initial successes of DLCQ provide the hope that one can use this method for solving 3+1 theories. The application to higher dimensions is much more involved due to the expansion of the degrees of freedom and the need to introduce ultraviolet and infrared regulators and truncation procedures which minimize violations of gauge invariance and Lorentz invariance. This is in addition to the work involved implementing two extra dimensions with their added degrees of freedom. In these lectures, we will discuss some initial attempts to apply DLCQ to gauge theories in 3+1 dimensions.[27,28,29,30] We return to these applications in later sections.

The striking advantages of quantizing gauge theories on the light-cone have been realized by a number of authors, including Klauder, Leutwyler, and Streit,[31] Kogut and Soper,[32] Rohrlich,[33] Leutwyler,[34] Casher,[35] Chang, Root, and Yan,[36] Lepage and Brodsky,[4] Brodsky and Ji,[37] Lepage, Brodsky, Huang, and Mackenzie,[19] and McCartor.[38] Leutwyler recognized the utility of defining quark wavefunctions on the light-cone to give an unambiguous meaning to concepts used in the parton model. Casher gave the first construction of the light-cone Hamiltonian for non-Abelian gauge theory and gave an overview of important considerations in light-cone quantization. Chang, Root, and Yan demonstrated the equivalence of light-cone quantization with standard covariant Feynman analysis.

Franke,[39,40,41] Karmanov,[42,43] and Pervushin[44] have also done important work on light-cone quantization. The question of whether boundary conditions can be consistently set in light-cone quantization has been discussed by McCartor[45] and Lenz.[46] They have also shown that for massive theories that the energy and momentum derived using light-cone quantization are not only conserved, but also are equivalent to the energy and momentum one would normally write down in an equal-time theory.

The approach that we use in these lectures is closely related to the light-cone Fock methods used in Ref. 4 in the analysis of exclusive processes in QCD. The renormalization of light-cone wavefunctions and the calculation of physical observables in the light-cone framework is also discussed in that paper. The analysis of light-cone perturbation theory rules for QED in light-cone gauge used here is sim-

ilar to that given in Ref. 19. A number of other applications of QCD in light-cone quantization are reviewed in Ref. 20.

A mathematically similar but conceptually different approach to light-cone quantization is the "infinite momentum frame" formalism. This method involves observing the system in a frame moving past the laboratory close to the speed of light. The first developments were given by Weinberg.[47] Although light-cone quantization is similar to infinite momentum frame quantization, it differs since no reference frame is chosen for calculations, and it is thus manifestly Lorentz covariant. The only aspect that "moves at the speed of light" is the quantization surface. Other works in infinite momentum frame physics include Drell, Levy, and Yan,[48] Susskind and Frye,[49] Bjorken, Kogut, and Soper,[50] and Brodsky, Roskies, and Suaya.[51] This last reference presents the infinite momentum frame perturbation theory rules for QED in Feynman gauge, calculates one-loop radiative corrections, and demonstrates renormalizability.

Light-Cone Wavefunctions and High Momentum-Transfer Exclusive Processes

Exclusive Processes and Light-Cone Wavefunctions

One of the major advantages of the light-cone formalism is that many properties of large momentum transfer exclusive reactions can be calculated without explicit knowledge of the form of the non-perturbative light-cone wavefunctions. The main ingredients of this analysis are asymptotic freedom, and the power-law scaling relations and quark helicity conservation rules of perturbative QCD. For example, consider the light-cone expression (9) for a meson form factor at high momentum transfer Q^2. If the internal momentum transfer is large then one can iterate the gluon-exchange term in the effective potential for the light-cone wavefunctions. The result is the hadron form factors can be written in a factorized form as a convolution of quark "distribution amplitudes" $\phi(x_i, Q)$, one for each hadron involved in the amplitude, with a hard-scattering amplitude T_H.[4,52] The pion's electromagnetic form factor, for example, can be written as[4,52,53]

$$F_\pi(Q^2) = \int_0^1 dx \int_0^1 dy\, \phi_\pi^*(y,Q)\, T_H(x,y,Q)\, \phi_\pi(x,Q) \left(1 + \mathcal{O}\left(\frac{1}{Q}\right)\right). \qquad (20)$$

Here T_H is the scattering amplitude for the form factor but with the pions replaced by collinear $q\bar{q}$ pairs—*i.e.* the pions are replaced by their valence partons. We can

also regard T_H as the free particle matrix element of the order $1/Q^2$ term in the effective Lagrangian for $\gamma^* q\bar{q} \to q\bar{q}$.[6]

The process-independent distribution amplitude[4] $\phi_\pi(x,Q)$ is the probability amplitude for finding the $q\bar{q}$ pair in the pion with $x_q = x$ and $x_{\bar{q}} = 1-x$. It is directly related to the light-cone valence wavefunction:

$$\phi_\pi(x,Q) = \int \frac{d^2\vec{k}_\perp}{16\pi^3} \psi^{(Q)}_{q\bar{q}/\pi}(x,\vec{k}_\perp) \tag{21}$$

$$= P^+_\pi \int \frac{dz^-}{4\pi} e^{ixP^+_\pi z^-/2} \langle 0|\overline{\psi}(0)\frac{\gamma^+\gamma_5}{2\sqrt{2n_c}}\psi(z)|\pi\rangle^{(Q)}\Big|_{z^+=\vec{z}_\perp=0} . \tag{22}$$

The $\vec{k}_\perp$ integration in Eq. (21) is cut off by the ultraviolet cutoff $\Lambda = Q$ implicit in the wavefunction; thus only Fock states with invariant mass squared $\mathcal{M}^2 < Q^2$ contribute. We will return later to the discussion of ultraviolet regularization in the light-cone formalism.

It is important to note that the distribution amplitude is gauge invariant. In gauges other than light-cone gauge, a path-ordered "string operator" $P\exp(\int_0^1 ds\, ig\, A(sz)\cdot z)$ must be included between the $\overline{\psi}$ and ψ. The line integral vanishes in light-cone gauge because $A\cdot z = A^+z^-/2 = 0$ and so the factor can be omitted in that gauge. This (non-perturbative) definition of ϕ uniquely fixes the definition of T_H which must itself then be gauge invariant.

The above result is in the form of a factorization theorem; all of the non-perturbative dynamics is factorized into the non-perturbative distribution amplitudes, which sums all internal momentum transfers up to the scale Q^2. On the other hand, all momentum transfers higher than Q^2 appear in T_H, which, because of asymptotic freedom, can be computed perturbatively in powers of the QCD running coupling constant $\alpha_s(Q^2)$.

Given the factorized structure, one can read off a number of general features of the PQCD predictions; *e.g.* the dimensional counting rules, hadron helicity conservation, color transparency, etc.[20] In addition, the scaling behavior of the exclusive amplitude is modified by the logarithmic dependence of the distribution amplitudes in $\ell n\ Q^2$ which is in turn determined by QCD evolution equations.[4]

An important application of the PQCD analysis is exclusive Compton scattering and the related cross process $\gamma\gamma \to \bar{p}p$. Each helicity amplitude for $\gamma p \to \gamma p$ can be computed at high momentum transfer from the convolution of the proton

distribution amplitude with the $O(\alpha_s^2)$ amplitudes for $qqq\gamma \to qqq\gamma$. The result is a cross section which scales as

$$\frac{d\sigma}{dt}(\gamma p \to \gamma p) = \frac{F(\theta_{CM}, \ell n\ s)}{s^6} \tag{23}$$

if the proton helicity is conserved. The helicity-flip amplitude and contributions involving more quarks or gluons in the proton wavefunction are power-law suppressed. The nominal s^{-6} fixed angle scaling follows from dimensional counting rules.[54] It is modified logarithmically due to the evolution of the proton distribution amplitude and the running of the QCD coupling constant.[4] The normalization, angular dependence, and phase structure are highly sensitive to the detailed shape of the non-perturbative form of $\phi_p(x_i, Q^2)$. Recently Kronfeld and Nizic[55] have calculated the leading Compton amplitudes using model forms for ϕ_p predicted in the QCD sum rule analyses;[3] the calculation is complicated by the presence of integrable poles in the hard-scattering subprocess T_H. The results for the unpolarized cross section are shown in Fig. 8.

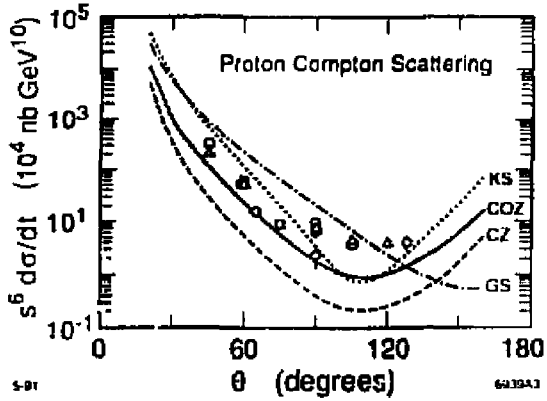

Figure 8. Comparison[85] of the order α_s^4/s^6 PQCD prediction for proton Compton scattering with the available data. The calculation assumes PQCD factorization and distribution amplitudes computed from QCD sum rule moments.[3].

There also has been important progress testing PQCD experimentally using measurements of the $p \to N^*$ form factors. In a recent new analysis of existing SLAC data, Stoler[56] has obtained measurements of several transition form factors of the proton to resonances at $W = 1232, 1535$, and $1680\ MeV$. As is the case of

the elastic proton form factor, the observed behavior of the transition form factors to the $N^*(1535)$ and $N^*(1680)$ are each consistent with the Q^{-4} fall-off and dipole scaling predicted by PQCD and hadron helicity conservation over the measured range $1 < Q^2 < 21\ GeV^2$. In contrast, the $p \to \Delta(1232)$ form factor decreases faster than $1/Q^4$ suggesting that non-leading processes are dominant in this case. Remarkably, this pattern of scaling behavior is what is expected from PQCD and the QCD sum rule analyses,[3] since, unlike the case of the proton and its other resonances, the distribution amplitude $\phi_{N^*}(x_1, x_2, x_3, Q)$ of the Δ resonance is predicted to be nearly symmetric in the x_i, and a symmetric distribution leads to a strong cancellation[57] of the leading helicity-conserving terms in the matrix elements of the hard scattering amplitude for $qqq \to \gamma^* qqq$.

These comparisons of the proton form factor and Compton scattering predictions with experiment are very encouraging, showing agreement in both the fixed-angle scaling behavior predicted by PQCD and the normalization predicted by QCD sum rule forms for the proton distribution amplitude. Assuming one can trust the validity of the leading order analysis, a systematic series of polarized target and beam Compton scattering measurements on proton and neutron targets and the corresponding two-photon reactions $\gamma\gamma \to p\bar{p}$ will strongly constrain a fundamental quantity in QCD, the nucleon distribution amplitude $\phi(x_i, Q^2)$. It is thus imperative for theorists to develop methods to calculate the shape and normalization of the non-perturbative distribution amplitudes from first principles in QCD.

Is PQCD Factorization Applicable to Exclusive Processes?

One of the concerns in the derivation of the PQCD results for exclusive amplitudes is whether the momentum transfer carried by the exchanged gluons in the hard scattering amplitude T_H is sufficiently large to allow a safe application of perturbation theory.[58] The problem appears to be especially serious if one assumes a form for the hadron distribution amplitudes $\phi_H(x_i, Q^2)$ which has strong support at the endpoints, as in the QCD sum rule model forms suggested by Chernyak and Zhitnitskii and others.[3]

This problem has now been clarified by two groups: Gari *et al.*[59] in the case of baryon form factors, and Mankiewicz and Szczepaniak,[60] for the case of meson form factors. Each of these authors has pointed out that the assumed non-perturbative input for the distribution amplitudes must vanish strongly in the endpoint region; otherwise, there is a double-counting problem for momentum transfers occurring

in the hard scattering amplitude and the distribution amplitudes. Once one enforces this constraint, (*e.g.* by using exponentially suppressed wavefunctions[19]) on the basis functions used to represent the QCD moments, or uses a sufficiently large number of polynomial basis functions, the resulting distribution amplitudes do not allow significant contribution to the high Q^2 form factors to come from soft gluon exchange region. The comparison of the PQCD predictions with experiment thus becomes phenomenologically and analytically consistent. An analysis of exclusive reactions on the effective Lagrangian method[61] is also consistent with this approach. In addition, as discussed by Botts,[62] potentially soft contributions to large angle hadron-hadron scattering reactions from Landshoff pinch contributions[63] are strongly suppressed by Sudakov form factor effects.

The empirical successes of the PQCD approach, together with the evidence for color transparency in quasi-elastic pp scattering[20] gives strong support for the validity of PQCD factorization for exclusive processes at moderate momentum transfer. It seems difficult to understand this pattern of form factor behavior if it is due to simple convolutions of soft wavefunctions. Thus it should be possible to use these processes to empirically constrain the form of the hadron distribution amplitudes, and thus confront non-perturbative QCD in detail.

Light-Cone Quantization and Heavy Particle Decays

One of the most interesting applications of the light-cone PQCD formalism is to large momentum transfer exclusive processes to heavy quark decays. For example, consider the decay $\eta_c \to \gamma\gamma$. If we can choose the Lagrangian cutoff $\Lambda^2 \sim m_c^2$, then to leading order in $1/m_c$, all of the bound state physics and virtual loop corrections are contained in the $c\bar{c}$ Fock wavefunction $\psi_{\eta_c}(x_i, k_{\perp i})$. The hard scattering matrix element of the effective Lagrangian coupling $c\bar{c} \to \gamma\gamma$ contains all of the higher corrections in $\alpha_s(\Lambda^2)$ from virtual momenta $|k^2| > \Lambda^2$. Thus

$$\begin{aligned} \mathcal{M}(\eta_c \to \gamma\gamma) &= \int d^2k_\perp \int_0^1 dx\, \psi_{\eta_c}^{(\Lambda)}(x, k_\perp)\, T_H^{(\Lambda)}(c\bar{c} \to \gamma\gamma) \\ &\Rightarrow \int_0^1 dx\, \phi(x, \Lambda)\, T_H^{(\Lambda)}(c\bar{c} \to \gamma\gamma) \end{aligned} \tag{24}$$

where $\phi(x, \Lambda^2)$ is the η_c distribution amplitude. This factorization and separation of scales is shown in Fig. 9. Since the η_c is quite non-relativistic, its distribution

amplitude is peaked at $x = 1/2$, and its integral over x is essentially equivalent to the wavefunction at the origin, $\psi(\vec{r} = \vec{0})$.

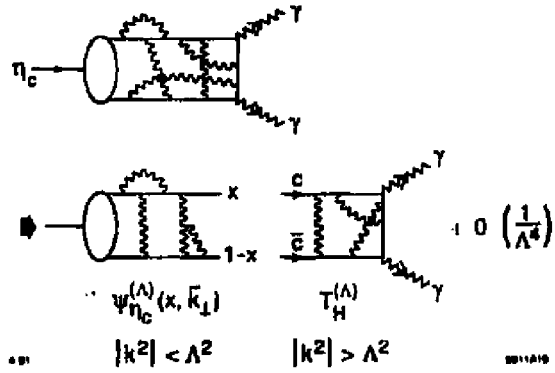

Figure 9. Factorization of perturbative and non-perturbative contributions to the decay $\eta_c \to \gamma\gamma$.

Another interesting calculational example of quarkonium decay in PQCD is the annihilation of the J/ψ into baryon pairs. The calculation requires the convolution of the hard annihilation amplitude $T_H(c\bar{c} \to ggg \to uud\,uud)$ with the J/ψ, baryon, and anti-baryon distribution amplitudes.[4,3] (See Fig. 10.) The magnitude of the computed decay amplitude for $\psi \to \bar{p}p$ is consistent with experiment assuming the proton distribution amplitude computed from QCD sum rules.[3] The angular distribution of the proton in $e^+e^- \to J/\psi \to p\bar{p}$ is also consistent with the hadron helicity conservation rule predicted by PQCD; *i.e.* opposite proton and anti-proton helicity.

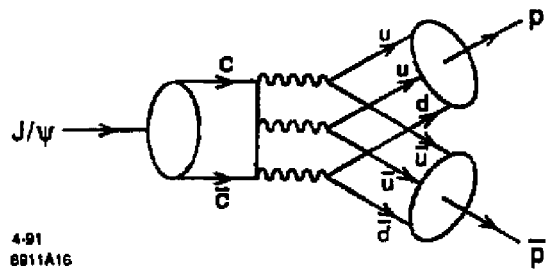

Figure 10. Calculation of $J/\psi \to p\bar{p}$ in PQCD.

The effective Lagrangian method was used by Lepage, Caswell, and Thacker[16] to systematically compute the order $\alpha_s(\hat{Q})$ corrections to the hadronic and photon decays of quarkonium. The scale $\hat{Q}$ can then be set by incorporating vacuum polarization corrections into the running coupling constant.[64] A summary of the results can be found in Ref. 65.

Exclusive Weak Decays of Heavy Hadrons

An important application of the PQCD effective Lagrangian formalism is to the exclusive decays of heavy hadrons to light hadrons, such as $B^0 \to \pi^+\pi^-$, K^+, K^-.[66] To a good approximation, the decay amplitude $\mathcal{M} = \langle B|H_{W_k}|\pi^+\pi^-\rangle$ is caused by the transition $\bar{b} \to W^+\bar{u}$; thus $\mathcal{M} = f_\pi p_\pi^\mu \frac{G_F}{\sqrt{2}} \langle \pi^-|J_\mu|B^0\rangle$ where J_μ is the $\bar{b} \to \bar{u}$ weak current. The problem is then to recouple the spectator d quark and the other gluon and possible quark pairs in each B^0 Fock state to the corresponding Fock state of the final state π^-. (See Fig. 11.) The kinematic constraint that $(p_B - p_\pi)^2 = m_\pi^2$ then demands that at least one quark line is far off shell: $p_{\bar{u}}^2 = (yp_B - p_\pi)^2 \sim -\mu m_B \sim -1.5\, GeV^2$, where we have noted that the light quark takes only a fraction $(1-y) \sim \sqrt{(k_\perp^2 + m_d^2)}/m_B$ of the heavy meson's momentum since all of the valence quarks must have nearly equal velocity in a bound state. In view of the successful applications[56] of PQCD factorization to form factors at momentum transfers in the few GeV^2 range, it is reasonable to assume that $\langle|p_{\bar{u}}^2|\rangle$ is sufficiently large that we can begin to apply perturbative QCD methods.

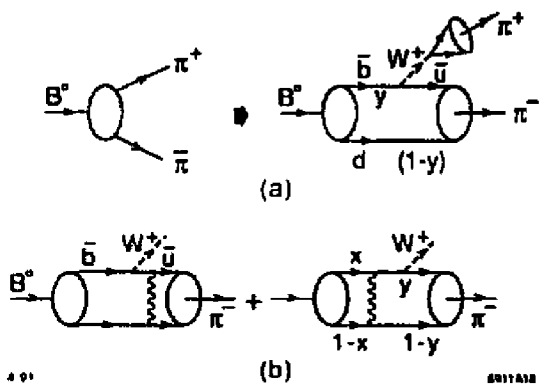

Figure 11. Calculation of the weak decay $B \to \pi\pi$ in the PQCD formalism of Ref. 66. The gluon exchange kernel of the hadron wavefunction is exposed where hard momentum transfer is required.

The analysis of the exclusive weak decay amplitude can be carried out in parallel to the PQCD analysis of electroweak form factors[67] at large Q^2. The first step is to iterate the wavefunction equations of motion so that the large momentum transfer through the gluon exchange potential is exposed. The heavy quark decay amplitude can then be written as a convolution of the hard scattering amplitude for $Q\bar{q} \to W^+ q\bar{q}$ convoluted with the B and π distribution amplitudes. The minimum number valence Fock state of each hadron gives the leading power law contribution. Equivalently, we can choose the ultraviolet cut-off scale in the Lagrangian at ($\Lambda^2 < \mu m_B$) so that the hard scattering amplitude $T_H(Q\bar{q} \to W^+ q\bar{q})$ must be computed from the matrix elements of the order $1/\Lambda^2$ terms in $\delta\mathcal{L}$. Thus T_H contains all perturbative virtual loop corrections of order $\alpha_s(\Lambda^2)$. The result is the factorized form:

$$\mathcal{M}(B \to \pi\pi) = \int_0^1 dx \int_0^1 dy \phi_B(y,\Lambda) T_H \phi_\pi(x,\Lambda) \tag{25}$$

which is expected to be correct up to terms of order $1/\Lambda^4$. All of the non-perturbative corrections with momenta $|k^2| < \Lambda^2$ are summed in the distribution amplitudes.[68]

In order to make an estimate of the size of the $B \to \pi\pi$ amplitude, in Ref. 66 we have taken the simplest possible forms for the required wavefunctions

$$\phi_\pi(y) \propto \gamma_5 \not{p}_\pi y(1-y) \tag{26}$$

for the pion and

$$\phi_B(x) \propto \frac{\gamma_5[\not{p}_B + m_B g(x)]}{\left[1 - \frac{1}{x} - \frac{\epsilon^2}{(1-x)}\right]^2} \tag{27}$$

for the B, each normalized to its meson decay constant. The above form for the heavy quark distribution amplitude is chosen so that the wavefunction peaks at equal velocity; this is consistent with the phenomenological forms used to describe heavy quark fragmentation into heavy hadrons. We estimate $\epsilon \sim 0.05$ to 0.10. The functional dependence of the mass term $g(x)$ is unknown; however, it should be reasonable to take $g(x) \sim 1$ which is correct in the weak binding approximation.

One now can compute the leading order PQCD decay amplitude

$$\mathcal{M}(B^0 \to \pi^-\pi^+) = \frac{G_F}{\sqrt{2}} V_{ud}^* V_{ub}\, P_{\pi^+}^{\mu} \langle \pi^- \mid V^{\mu} \mid B^0 \rangle \tag{28}$$

where

$$\begin{aligned}\langle \pi^- \mid V^{\mu} \mid B^0 \rangle = \frac{8\pi\alpha_s(Q^2)}{3} \int_0^1 dx \int_0^{1-x} dy\, \phi_B(x)\, \phi_\pi(y) \\ \times \frac{\mathrm{Tr}[\not{P}_\pi - \gamma_5 \gamma^\nu \not{k}_1 \gamma^\mu (\not{P}_B + M_B g(x)) \gamma_5 \gamma_\nu]}{k_1^2 Q^2} \\ + \frac{\mathrm{Tr}[\not{P}_\pi - \gamma_5 \gamma^\nu (\not{k}_2 + M_B) \gamma^\nu (\not{P}_B + M_B g(x)) \gamma_5 \gamma_\nu]}{(k_2^2 - M_B^2) Q^2}\end{aligned} \tag{29}$$

Numerically, this gives the branching ratio

$$BR(B^0 \to \pi^+\pi^-) \sim 10^{-8} \xi^2 N \tag{30}$$

where $\xi = 10|V_{ub}/V_{cb}|$ is probably less than unity, and N has strong dependence on the value of g: $N = 180$ for $g = 1$ and $N = 5.8$ for $g = 1/2$. The present experimental limit[69] is

$$BR(B^0 \to \pi^+\pi^-) < 3 \times 10^{-4}. \tag{31}$$

A similar PQCD analysis can be applied to other two-body decays of the B; the ratios of the widths will not be so sensitive to the form of the distribution amplitude, allowing tests of the flavor symmetries of the weak interaction.

Light-Cone Quantization of Gauge Theory

In this section we will outline the canonical quantization of QCD in $A^+ = 0$ gauge, following the discussion in Refs. 4 and 19. The quantization proceeds in several steps. First we identify the independent dynamical degrees of freedom in the Lagrangian. The theory is quantized by defining commutation relations for

these dynamical fields at a given light-cone time $\tau = t + z$ (we choose $\tau = 0$). These commutation relations lead immediately to the definition of the Fock state basis. Expressing the dependent fields in terms of the independent fields, we then derive a light-cone Hamiltonian, which determines the evolution of the state space with changing τ. Finally we derive the rules for τ-ordered perturbation theory.

The purpose of this exercise is to illustrate the origins and nature of the Fock state expansion, and of light-cone perturbation theory in QCD. In this section we will ignore the subtleties to the zero-mode large scale structure of non-Abelian gauge fields. Although these have a profound effect on the structure of the vacuum, the theory can still be described with a Fock state basis and some sort of effective light-cone Hamiltonian. At the least, this procedure should be adequate to describe heavy quark systems. Furthermore, the short distance interactions of the theory are unaffected by this structure, according to the central ansatz of perturbative QCD.

The Lagrangian (density) for QCD can be written

$$\mathcal{L} = -\frac{1}{2}\,\mathrm{Tr}\,(F^{\mu\nu}F_{\mu\nu}) + \overline{\psi}(i\not{D} - m)\psi \tag{32}$$

where $F^{\mu\nu} = \partial^\mu A^\nu - \partial^\nu A^\mu + ig[A^\mu, A^\nu]$ and $iD^\mu = i\partial^\mu - gA^\mu$. Here the gauge field A^μ is a traceless 3×3 color matrix ($A^\mu \equiv \sum_a A^{a\mu}T^a$, $\mathrm{Tr}(T^aT^b) = 1/2\delta^{ab}$, $[T^a, T^b] = ic^{abc}T^c, \ldots$), and the quark field ψ is a color triplet spinor (for simplicity, we include only one flavor). In order to maintain charge conjugation symmetry in the construction of the Hamiltonian, it is understood that this expression is averaged with its Hermetian conjugate.

Given the Lagrangian density, one can calculate the energy momentum tensor and stress tensor in the usual way from the independent dynamical fields and their conjugate momenta. At a given light-cone time, say $\tau = 0$, the independent dynamical fields are $\psi_+ \equiv \Lambda_+\psi$ and $A^i_\perp$ with conjugate fields $i\psi^\dagger_+$ and $\partial^+ A^i_\perp$, where $\Lambda_\pm = \gamma^0\gamma^\pm/2$ are projection operators ($\Lambda_+\Lambda_- = 0$, $\Lambda^2_\pm = \Lambda_\pm$, $\Lambda_+ + \Lambda_- = 1$) and $\partial^\pm = \partial^0 \pm \partial^3$. Using the equations of motion, the remaining fields in $\mathcal{L}$ can be expressed in terms of ψ_+, $A^i_\perp$:

$$\psi_- \equiv \Lambda_- \psi = \frac{1}{i\partial^+}\left[i\vec{D}_\perp \cdot \vec{\alpha}_\perp + \beta m\right]\psi_+$$

$$= \tilde{\psi}_- - \frac{1}{i\partial^+}\, g\,\vec{A}_\perp \cdot \vec{\alpha}_\perp \psi_+ \,,$$

$$A^+ = 0 \,, \tag{33}$$

$$A^- = \frac{2}{i\partial^+}\, i\vec{\partial}_\perp \cdot \vec{A}_\perp + \frac{2g}{(i\partial^+)^2}\left\{\left[i\partial^+ A^i_\perp, A^i_\perp\right] + 2\psi^\dagger_+ T^a \psi_+ T^a\right\}$$

$$\equiv \tilde{A}^- + \frac{2g}{(i\partial^+)^2}\left\{\left[i\partial^+ A^i_\perp, A^i_\perp\right] + 2\psi^\dagger_+ T^a \psi_+ T^a\right\} \,,$$

with $\beta = \gamma^a$ and $\vec{\alpha}_\perp = \gamma^o \vec{\gamma}$.

To quantize, we expand the fields at $\tau = 0$ in terms of creation and annihilation operators,

$$\psi_+(x) = \int_{k^+>0} \frac{dk^+ d^2k_\perp}{k^+ 16\pi^3} \sum_\lambda \left\{b(\underline{k},\lambda)\; u_+(\underline{k},\lambda)\; e^{-ik\cdot x}\right.$$

$$\left. + d^\dagger(\underline{k},\lambda)\; v_+(\underline{k},\lambda)\; e^{ik\cdot x}\right\} \,, \quad \tau = x^+ = 0 \tag{34}$$

$$A^i_\perp(x) = \int_{k^+>0} \frac{dk^+ d^2k_\perp}{k^+ 16\pi^3} \sum_\lambda \left\{a(\underline{k},\lambda)\; \epsilon^i_\perp(\lambda)\; e^{-ik\cdot x} + c.c.\right\} \,, \quad \tau = x^+ = 0 \,,$$

with commutation relations ($\underline{k} = (k^+, \vec{k}_\perp)$):

$$\left\{b(\underline{k},\lambda),\; b^\dagger(\underline{p},\lambda)\right\} = \left\{d(\underline{k},\lambda),\; d^\dagger(\underline{p},\lambda')\right\}$$

$$= \left[a(\underline{k},\lambda),\; a^\dagger(\underline{p},\lambda')\right] \tag{35}$$

$$= 16\pi^3 k^+ \delta^3(\underline{k}-\underline{p})\,\delta_{\lambda\lambda'} \,,$$

$$\{b,b\} = \{d,d\} = \ldots = 0 \,,$$

where λ is the quark or gluon helicity. These definitions imply canonical commutation relations for the fields with their conjugates ($\tau = x^+ = y^+ = 0$, $\underline{x} =$

$(x^-, x_\perp), \ldots)$:

$$\left\{\psi_+(\underline{x}),\ \psi_+^\dagger(\underline{y})\right\} = \Lambda_+\,\delta^3(\underline{x}-\underline{y})\,,$$
$$\left[A^i(\underline{x}),\ \partial^+ A^j_\perp(\underline{y})\right] = i\delta^{ij}\,\delta^3(\underline{x}-\underline{y})\,. \tag{36}$$

It should be emphasized that these commutation relations are not new; they are the usual commutation relation for free fields evaluated at fixed light-cone rather than ordinary time.

The creation and annihilation operators define the Fock state basis for the theory at $\tau = 0$, with a vacuum $|0\rangle$ defined such that $b\,|0\rangle = d\,|0\rangle = a\,|0\rangle = 0$. The evolution of these states with τ is governed by the light-cone Hamiltonian, $H_{LC} = P^-$, conjugate to τ. The Hamiltonian can be readily expressed in terms of ψ_+ and $A^i_\perp$:

$$H_{LC} = H_0 + V\,, \tag{37}$$

where

$$\begin{aligned} H_0 &= \int d^3x \left\{ \mathrm{Tr}\left(\partial^i_\perp A^j_\perp \partial^i_\perp A^j_\perp\right) + \psi_+^\dagger\,(i\partial_\perp\cdot\alpha_\perp + \beta m)\,\frac{1}{i\partial^+}\,(i\partial_\perp\cdot\alpha_\perp + \beta m)\,\psi_+ \right\} \\ &= \sum_{\substack{\lambda \\ \text{colors}}} \int \frac{dk^+\,d^2k_\perp}{16\pi^3\,k^+} \left\{ a^\dagger(\underline{k},\lambda)\,a(\underline{k},\lambda)\frac{k_\perp^2}{k^+} + b^\dagger(\underline{k},\lambda)\,b(\underline{k},\lambda) \right. \\ &\quad \left. \times\ \frac{k_\perp^2+m^2}{k^+} + d^\dagger(\underline{k},\lambda)\,b(\underline{k},\lambda)\,\frac{k_\perp^2+m^2}{k^+} \right\} + \text{constant} \end{aligned} \tag{38}$$

is the free Hamiltonian and V the interaction:

$$\begin{aligned} V = \int d^3x\ \Big\{ & 2g\ \mathrm{Tr}\left(i\partial^\mu \widetilde{A}^\nu \left[\widetilde{A}_\mu, \widetilde{A}_\nu\right]\right) - \frac{g^2}{2}\,\mathrm{Tr}\left(\left[\widetilde{A}^\mu, \widetilde{A}^\nu\right]\left[\widetilde{A}_\mu, \widetilde{A}_\nu\right]\right) \\ & + g\overline{\widetilde{\psi}}\ \widetilde{\not{A}}\,\widetilde{\psi} + g^2\,\mathrm{Tr}\left(\left[i\partial^+\widetilde{A}^\mu, \widetilde{A}_\mu\right]\frac{1}{(i\partial^+)^2}\left[i\partial^+\widetilde{A}^\nu, \widetilde{A}_\nu\right]\right) \\ & + g^2\overline{\widetilde{\psi}}\ \widetilde{\not{A}}\,\frac{\gamma^+}{2i\partial^+}\ \widetilde{\not{A}}\,\widetilde{\psi} - g^2\overline{\widetilde{\psi}}\gamma^+\left(\frac{1}{(i\partial^+)^2}\left[i\partial^+\widetilde{A}^\nu, \widetilde{A}_\nu\right]\right)\widetilde{\psi} \\ & + \frac{g^2}{2}\ \overline{\psi}\gamma^+\,T^a\psi\,\frac{1}{(i\partial^+)^2}\,\overline{\psi}\gamma^+\,T^a\psi \Big\}\,, \end{aligned} \tag{39}$$

with $\tilde{\psi} = \tilde{\psi}_- + \psi_+$ ($\to \psi$ as $g \to 0$) and $\tilde{A}^\mu = (0, \tilde{A}^-, A^i_\perp)$ ($\to A^\mu$ as $g \to 0$). The Fock states are obviously eigenstates of H_0 with

$$H_0 \left| n : k_i^+, k_{\perp i} \right\rangle = \sum_i \left(\frac{k_\perp^2 + m^2}{k^+} \right)_i \left| n : k_i^+, k_{\perp i} \right\rangle \ . \tag{40}$$

It is equally obvious that they are not eigenstates of V, though any matrix element of V between Fock states is trivially evaluated.

The first three terms in V correspond to the familiar three and four gluon vertices, and the gluon-quark vertex [Fig. 12(a)]. The remaining terms represent new four-quanta interactions containing instantaneous fermion and gluon propagators [Fig. 12(b)]. All terms conserve total three-momentum $\underline{k} = (k^+, \vec{k}_\perp)$, because of the integral over $\underline{x}$ in V.

The matrix elements of the light-cone Hamiltonian for the continuum case can be found in Refs. [19,28,27]. For the sake of completeness, the explicit expressions are compiled in Tables 2a-d for the vertex V, the contraction C, and the seagull interaction S, respectively, to the extent they are needed in the present context. The light cone Hamiltonian $H_{\rm LC} = T + V + S + C$ is the sum of these three interactions and of the free or 'kinetic' energy

$$T = \sum_q \left(\frac{m_{\rm F}^2 + \vec{k}_\perp^2}{x} \right)_q (b_q^\dagger b_q + d_q^\dagger d_q) \ + \ \sum_q \left(\frac{\vec{k}_\perp^2}{x} \right)_1 a_q^\dagger a_q .$$

The creation operators $b_q^\dagger$, $d_q^\dagger$ and $a_q^\dagger$ create plane wave states for the electrons, positrons, and photons, respectively, characterized by the four kinematical quantum numbers $q \equiv (x, \vec{k}_\perp, \lambda)$, and the destruction operators b_q, d_q and a_q destroy them correspondingly. They obey the usual (anti-)commutation relations. Each single particle carries thus a longitudinal momentum fraction x, transverse momentum $\vec{k}_\perp$, and helicity λ. The fermions have mass $m_{\rm F}$ and kinetic energy $\frac{m_{\rm F}^2 + \vec{k}_\perp^2}{x}$, the photons are massless. The symbol $\sum_q$ denotes summation over the entire range of the quantum numbers. In the continuum limit sums are replaced by integrals, i.e. $\sum_q \longrightarrow C_L \int dq$, where

$$C_L \equiv \frac{\Omega P^+}{16\pi^3} \quad \text{and} \quad \int dq \equiv \sum_{\lambda = \pm 1} \int_0^1 dx \int_{-\infty}^{+\infty} d(\vec{k}_\perp)_x \int_{-\infty}^{+\infty} d(\vec{k}_\perp)_y \ .$$

The normalization volume is denoted by $\Omega \equiv 2L_\parallel (2L_\perp)^2$, and the total longitudinal momentum by P^+.

Table 2a: The matrix elements of the vertex interaction V. — The transversal polarisation vector is defined as $\vec{\epsilon}_\perp(\lambda) = (-\lambda\hat{x} - i\hat{y})/\sqrt{2}$. The coupling constant g is hidden in $\widetilde{g}$, with $\widetilde{g}^2 = g^2\,\frac{2}{P^+\Pi}$. In the continuum limit one replaces sums by integrals and $\beta = \widetilde{g}^2$ by $\widetilde{\beta} \equiv C_L\beta = \frac{\alpha}{2\pi^2}$, since $g^2 \equiv 4\pi\alpha$ in our units. — The Gell-Mann matrices are denoted by $T^a_{c_1c_2}$, and the totally anti-symmetric structure constants of SU(N_c) by $C^a_{bc} \equiv c^{abc}$. The are related by $\left[T^a, T^b\right] = ic^{abc}T^c$.

Graph	Matrix Element = Momentum×Helicity×Flavor×Color Factor				
$V_{q\to qg}(1;2,3)$ 	$=$	$+\widetilde{g}\sqrt{\frac{1}{x_3}}\, m_F \left[\frac{1}{x_1} - \frac{1}{x_2}\right]$	$\delta^{\lambda_2}_{-\lambda_1}\,\delta^{\lambda_3}_{\lambda_1}$	$\delta^{f_2}_{f_1}$	$T^{a_3}_{c_1c_2}$
		$+\widetilde{g}\sqrt{\frac{2}{x_3}}\, \vec{\epsilon}_\perp(\lambda_3)\cdot\left[\left(\frac{\vec{k}_\perp}{x}\right)_3 - \left(\frac{\vec{k}_\perp}{x}\right)_2\right]$	$\delta^{\lambda_2}_{+\lambda_1}\,\delta^{\lambda_3}_{\lambda_1}$	$\delta^{f_2}_{f_1}$	$T^{a_3}_{c_1c_2}$
		$+\widetilde{g}\sqrt{\frac{2}{x_3}}\, \vec{\epsilon}_\perp(\lambda_3)\cdot\left[\left(\frac{\vec{k}_\perp}{x}\right)_3 - \left(\frac{\vec{k}_\perp}{x}\right)_1\right]$	$\delta^{\lambda_2}_{+\lambda_1}\,\delta^{\lambda_3}_{-\lambda_1}$	$\delta^{f_2}_{f_1}$	$T^{a_3}_{c_1c_2}$
$V_{g\to q\bar{q}}(1;2,3)$ 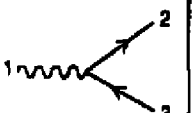	$=$	$+\widetilde{g}\frac{1}{\sqrt{x_1}}\, m_F \left[\frac{1}{x_2} + \frac{1}{x_3}\right]$	$\delta^{\lambda_3}_{+\lambda_2}\,\delta^{\lambda_3}_{+\lambda_1}$	$\delta^{f_3}_{f_2}$	$T^{a_1}_{c_2c_3}$
		$+\widetilde{g}\sqrt{\frac{2}{x_1}}\, \vec{\epsilon}_\perp(\lambda_1)\cdot\left[\left(\frac{\vec{k}_\perp}{x}\right)_1 - \left(\frac{\vec{k}_\perp}{x}\right)_3\right]$	$\delta^{\lambda_3}_{-\lambda_2}\,\delta^{\lambda_3}_{-\lambda_1}$	$\delta^{f_3}_{f_2}$	$T^{a_1}_{c_2c_3}$
		$+\widetilde{g}\sqrt{\frac{2}{x_1}}\, \vec{\epsilon}_\perp(\lambda_1)\cdot\left[\left(\frac{\vec{k}_\perp}{x}\right)_1 - \left(\frac{\vec{k}_\perp}{x}\right)_2\right]$	$\delta^{\lambda_3}_{-\lambda_2}\,\delta^{\lambda_3}_{+\lambda_1}$	$\delta^{f_3}_{f_2}$	$T^{a_1}_{c_2c_3}$
$V_{g\to gg}(1;2,3)$ 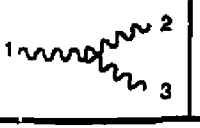	$= -\widetilde{g}\sqrt{\frac{x_3}{2x_1x_2}}\, \vec{\epsilon}^{\,*}_\perp(\lambda_1)\cdot\left[\left(\frac{\vec{k}_\perp}{x}\right)_1 - \left(\frac{\vec{k}_\perp}{x}\right)_3\right]$		$\delta^{\lambda_3}_{-\lambda_2}$	1	$iC^{a_1}_{a_2a_3}$
	$-\widetilde{g}\sqrt{\frac{x_1}{2x_2x_3}}\, \vec{\epsilon}_\perp(\lambda_3)\cdot\left[\left(\frac{\vec{k}_\perp}{x}\right)_3 - \left(\frac{\vec{k}_\perp}{x}\right)_2\right]$		$\delta^{\lambda_2}_{\lambda_1}$	1	$iC^{a_1}_{a_2a_3}$
	$-\widetilde{g}\sqrt{\frac{x_2}{2x_3x_1}}\, \vec{\epsilon}_\perp(\lambda_3)\cdot\left[\left(\frac{\vec{k}_\perp}{x}\right)_3 - \left(\frac{\vec{k}_\perp}{x}\right)_1\right]$		$\delta^{\lambda_2}_{\lambda_1}$	1	$iC^{a_1}_{a_2a_3}$

$$
\begin{aligned}
V = &\sum_{q_1,q_2,q_3} \left(b_1^\dagger b_2 a_3 - d_1^\dagger d_2 a_3\right)\, V_{q\to qg}(1;2,3) \\
&+ \sum_{q_1,q_2,q_3} \left(a_3^\dagger b_2^\dagger b_1 - a_3^\dagger d_2^\dagger d_1\right)\, V^*_{q\to qg}(1;2,3) \\
&+ \sum_{q_1,q_2,q_3} \left(a_1^\dagger d_2 b_3\, V_{g\to q\bar{q}}(1;2,3) + b_3^\dagger d_2^\dagger a_1\, V^*_{g\to q\bar{q}}(1;2,3)\right) \\
&+ \sum_{q_1,q_2,q_3} \left(a_1^\dagger a_2 a_3\, V_{g\to gg}(1;2,3) + a_3^\dagger a_2^\dagger a_1\, V^*_{g\to gg}(1;2,3)\right)
\end{aligned}
$$

Table 2b: The matrix elements of the contraction energy C. — The effective coupling constant g is given by $\widetilde{g}^2 = g^2 \frac{2}{P^+ 0}$. The color coefficient for the quarks are given by $C_F \equiv \sum_{a,c}(T^a T^a)_{cc'} = (N_c^2 - 1)/2N_c$, and for the gluons by $C_G \equiv \sum_{a,a'} \mathrm{Tr}(T^a T^{a'}) = N_f/2$, respectively.

Graph	Matrix Element as Infinite Sums	as Finite Sums
	$C_q^{(g)} = \widetilde{g}^2 C_F \sum_{x,\vec{k}_\perp} \left[\frac{1}{(x_1-x)^2} - \frac{1}{(x_1+x)^2} \right]$	$= 2\widetilde{g}^2 C_F \sum_{\vec{n}_\perp, n=1}^{n_1} \left(\frac{LP^+}{2\pi n} \right)^2$
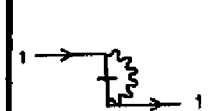	$C_q^{(q)} = \widetilde{g}^2 \frac{C_F}{2} \sum_{x,\vec{k}_\perp} \left[\frac{1}{x(x_1+x)} + \frac{1}{x(x_1-x)} \right]$	$= \widetilde{g}^2 \frac{C_F}{x_1} \sum_{\vec{n}_\perp, n=1}^{n_1} \frac{LP^+}{2\pi n}$
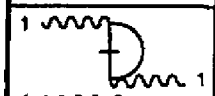	$C_g^{(g)} = \widetilde{g}^2 C_G \sum_{x,\vec{k}_\perp} \left[\frac{-1}{x_1(x+x_1)} + \frac{-1}{x_1(x-x_1)} \right]$	$= -2\widetilde{g}^2 \frac{C_G}{x_1} \sum_{\vec{n}_\perp, n=1}^{n_1} \frac{LP^+}{2\pi n}$
	$C_g^{(q)} = \widetilde{g}^2 \frac{N_c}{4} \sum_{x,\vec{k}_\perp} \left[\frac{2(x-x_1)}{x(x+x_1)^2} - \frac{(x+x_1)^2}{xx_1(x-x_1)^2} \right]$	
	$C_g^{(n)} = \quad 0$	
$C = \sum_{q_1} a_1^\dagger a_1 \left[C_g^{(g)}(1) + C_g^{(q)}(1) + C_g^{(n)}(1) \right] + (b_1^\dagger b_1 + d_1^\dagger d_1) \left[C_q^{(g)}(1) + C_q^{(q)}(1) \right]$		

Table 2c: The matrix elements of the seagull interaction S. — The coupling constant g is hidden in $\widetilde{g}^2 = g^2 \frac{2}{p^+q^+}$. In the continuum limit one replaces sums by integrals and $\widetilde{g}^2$ by $\widetilde{g}^2 C_L = \frac{\alpha}{2\pi^2}$, since $g^2 \equiv 4\pi\alpha$ in our units.

Type	Graph	Element = Momentum×Helicity×Flavor×Color Factor			
S_1		$S_{qq\to qq} = -\widetilde{g}^2 \frac{1}{(x_1-x_3)^2}$	$\delta^{\lambda_3}_{\lambda_1}\delta^{\lambda_4}_{\lambda_2}$	$\delta^{f_3}_{f_1}\delta^{f_4}_{f_2}$	$T^a_{c_1c_3}T^a_{c_2c_4}$
S_3	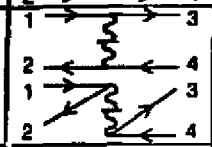	$S^{(s)}_{q\bar{q}\to q\bar{q}} = \widetilde{g}^2 \frac{2}{(x_1-x_3)^2}$	$\delta^{\lambda_3}_{\lambda_1}\delta^{\lambda_4}_{\lambda_2}$	$\delta^{f_3}_{f_1}\delta^{f_4}_{f_2}$	$T^a_{c_1c_3}T^a_{c_4c_2}$
		$S^{(a)}_{q\bar{q}\to q\bar{q}} = -\widetilde{g}^2 \frac{2}{(x_1+x_2)^2}$	$\delta_{-\lambda_1}^{\lambda_2}\delta_{-\lambda_3}^{\lambda_4}$	$\delta^{f_2}_{f_1}\delta^{f_4}_{f_3}$	$T^a_{c_1c_2}T^a_{c_4c_3}$
S_5	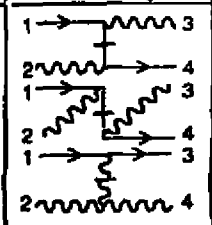	$S^{(s)}_{qg\to qg} = \widetilde{g}^2 \frac{1}{x_1-x_4}\frac{1}{\sqrt{x_2x_4}}$	$\delta^{\lambda_3}_{\lambda_1}\delta^{\lambda_4}_{\lambda_2}\delta^{\lambda_2}_{\lambda_1}$	$\delta^{f_3}_{f_1}$	$T^{a_4}_{c_1c}T^{a_2}_{cc_3}$
		$S^{(a)}_{qg\to qg} = \widetilde{g}^2 \frac{1}{x_1+x_2}\frac{1}{\sqrt{x_2x_4}}$	$\delta^{\lambda_3}_{\lambda_1}\delta^{\lambda_4}_{\lambda_2}\delta_{-\lambda_1}^{\lambda_2}$	$\delta^{f_3}_{f_1}$	$T^{a_2}_{c_1c}T^{a_4}_{cc_3}$
		$S^{(n)}_{qg\to qg} = \widetilde{g}^2 \frac{1}{(x_1-x_2)^2}\frac{(x_2+x_4)}{\sqrt{x_2x_4}}$	$\delta^{\lambda_3}_{\lambda_1}\delta^{\lambda_4}_{\lambda_2}$	$\delta^{f_3}_{f_1}$	$iT^a_{c_1c_2}C^a_{a_2a_4}$
S_7	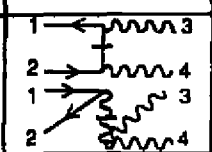	$S_{q\bar{q}\to gg} = \widetilde{g}^2 \frac{1}{x_1-x_3}\frac{1}{\sqrt{x_3x_4}}$	$\delta_{-\lambda_1}^{\lambda_2}\delta_{-\lambda_3}^{\lambda_4}\delta^{\lambda_3}_{\lambda_1}$	$\delta^{f_2}_{f_1}$	$T^{a_3}_{c_1c}T^{a_4}_{cc_2}$
		$S^{(n)}_{q\bar{q}\to gg} = \widetilde{g}^2 \frac{1}{(x_1+x_2)^2}\frac{(x_3-x_4)}{\sqrt{x_3x_4}}$	$\delta_{-\lambda_1}^{\lambda_2}\delta_{-\lambda_3}^{\lambda_4}$	$\delta^{f_2}_{f_1}$	$iT^a_{c_1c_2}C^a_{a_3a_4}$
S_9	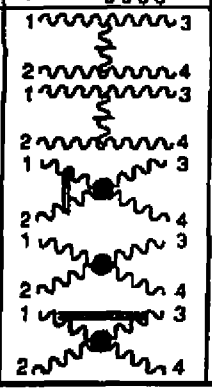	$S^{(s)}_{gg\to gg} = -\widetilde{g}^2 \frac{(x_1+x_3)}{4(x_1-x_3)^2}\frac{(x_2+x_4)}{\sqrt{x_1x_2x_3x_4}}$	$\delta^{\lambda_2}_{\lambda_1}\delta^{\lambda_4}_{\lambda_2}$	1	$C^a_{a_1a_2}C^a_{a_2a_4}$
		$S^{(a)}_{gg\to gg} = \widetilde{g}^2 \frac{1}{2(x_1+x_2)^2}\sqrt{\frac{x_1x_3}{x_2x_4}}$	$\delta_{-\lambda_1}^{\lambda_2}\delta_{-\lambda_3}^{\lambda_4}$	1	$C^a_{a_1a_2}C^a_{a_3a_4}$
		$S^{(na)}_{gg\to gg} = \widetilde{g}^2 \frac{1}{4\sqrt{x_1x_2x_3x_4}}$	$\delta^{\lambda_2}_{\lambda_1}\delta^{\lambda_4}_{\lambda_2}$	1	$C^a_{a_1a_2}C^a_{a_3a_4}$
		$S^{(nb)}_{gg\to gg} = \widetilde{g}^2 \frac{1}{4\sqrt{x_1x_2x_3x_4}}$	$\delta^{\lambda_3}_{\lambda_1}\delta^{\lambda_4}_{\lambda_2}$	1	$C^a_{a_1a_4}C^a_{a_3a_2}$
		$S^{(nc)}_{gg\to gg} = \widetilde{g}^2 \frac{1}{4\sqrt{x_1x_2x_3x_4}}$	$\delta_{-\lambda_1}^{\lambda_2}\delta_{-\lambda_3}^{\lambda_4}$	1	$C^a_{a_1a_3}C^a_{a_2a_4}$

$$
\begin{aligned}
S = &\sum_{q_1,q_2,q_3,q_4} (b_1^\dagger b_2^\dagger b_3 b_4 + d_1^\dagger d_2^\dagger d_3 d_4)\; S_1(1,2;3,4)\\
&+ \sum_{q_1,q_2,q_3,q_4} b_1^\dagger d_2^\dagger b_3 d_4 \;\; S_3(1,2;3,4)\\
&+ \sum_{q_1,q_2,q_3,q_4} (b_1^\dagger a_2^\dagger b_3 a_4 + d_1^\dagger a_2^\dagger d_3 a_4)\; S_5(1,2;3,4)\\
&+ \sum_{q_1,q_2,q_3,q_4} (b_1^\dagger d_2^\dagger a_3 a_4 + a_4^\dagger a_3^\dagger d_2 b_1)\; S_7(1,2;3,4)\\
&+ \sum_{q_1,q_2,q_3,q_4} a_1^\dagger a_2^\dagger a_3 a_4 \;\; S_9(1,2;3,4)
\end{aligned}
$$

Table 2d: The matrix elements of the fork interaction F. — The coupling constant g is hidden in $\widetilde{g}^2 = g^2 \frac{2}{P^+\Omega}$.

Type	Graph	Momentum × Helicity × Flavor × Color Factor
F_3	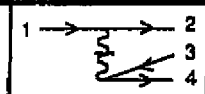	$F_{q\to qq\bar{q}} = \widetilde{g}^2 \frac{2}{(x_1-x_2)^2}$ $\delta^{\lambda_2}_{\lambda_1}\delta^{\lambda_4}_{-\lambda_3}$ $\delta^{f_2}_{f_1}\delta^{f_4}_{f_3}$ $T^a_{c_1c_2}T^a_{c_3c_4}$
F_5	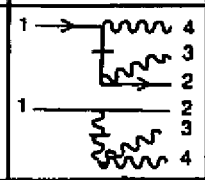	$F^{(q)}_{q\to qgg} = \widetilde{g}^2 \frac{1}{(x_1-x_4)}\frac{1}{\sqrt{x_3x_4}}$ $\delta^{\lambda_2}_{\lambda_1}\delta^{\lambda_4}_{-\lambda_3}\delta^{\lambda_4}_{+\lambda_1}$ $\delta^{f_2}_{f_1}$ $T^{a_3}_{c_1c}T^{a_4}_{cc_2}$
		$F^{(g)}_{q\to qgg} = \widetilde{g}^2 \frac{1}{(x_1-x_2)^2}\sqrt{\frac{x_3}{x_4}}$ $\delta^{\lambda_2}_{\lambda_1}\delta^{\lambda_4}_{-\lambda_3}$ $\delta^{f_2}_{f_1}$ $iT^a_{c_1c_2}C^a_{a_3a_4}$
F_7	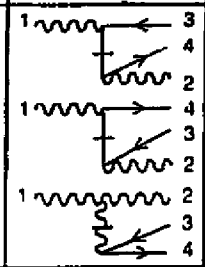	$F^{(qq\bar{q})}_{g\to qq\bar{q}} = \widetilde{g}^2 \frac{1}{(x_1-x_3)}\frac{1}{\sqrt{x_1x_2}}$ $\delta^{\lambda_2}_{\lambda_1}\delta^{\lambda_4}_{-\lambda_3}\delta^{\lambda_4}_{-\lambda_3}$ $\delta^{f_4}_{f_3}$ $T^{a_1}_{c_3c}T^{a_2}_{cc_4}$
		$F^{(qe)}_{g\to qq\bar{q}} = -\widetilde{g}^2 \frac{1}{(x_1-x_4)}\frac{1}{\sqrt{x_1x_2}}$ $\delta^{\lambda_2}_{\lambda_1}\delta^{\lambda_4}_{-\lambda_3}\delta^{\lambda_4}_{+\lambda_1}$ $\delta^{f_4}_{f_3}$ $T^{a_2}_{c_3c}T^{a_1}_{cc_4}$
		$F^{(g)}_{g\to qq\bar{q}} = \widetilde{g}^2 \frac{1}{(x_1-x_2)^2}\frac{(x_1+x_2)}{\sqrt{x_1x_2}}$ $\delta^{\lambda_2}_{\lambda_1}\delta^{\lambda_4}_{-\lambda_3}$ $\delta^{f_4}_{f_3}$ $iC^a_{a_1a_2}T^a_{c_3c_4}$
F_9	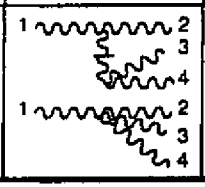	$F^{(g)}_{g\to ggg} = \widetilde{g}^2 \frac{1}{2(x_1-x_2)^2}\frac{(x_1+x_2)x_3}{\sqrt{x_1x_2x_3x_4}}$ $\delta^{\lambda_2}_{\lambda_1}\delta^{\lambda_4}_{-\lambda_3}$ 1 $C^a_{a_1a_2}C^a_{a_3a_4}$
		$F^{(n)}_{g\to ggg} = \widetilde{g}^2 \frac{1}{2\sqrt{x_1x_2x_3x_4}}$ $\delta^{\lambda_3}_{\lambda_1}\delta^{\lambda_4}_{-\lambda_2}$ 1 $C^a_{a_1a_2}C^a_{a_3a_4}$

$$
\begin{aligned}
F = &\sum_{q_1,q_2,q_3,q_4} (b_1^\dagger b_2 d_3 b_4 + d_1^\dagger d_2 b_3 d_4)\; F_3(1;2,3,4) + \text{h.c.} \\
&+ \sum_{q_1,q_2,q_3,q_4} (b_1^\dagger b_2 a_3 a_4 + d_1^\dagger d_2 a_3 a_4)\; F_5(1;2,3,4) + \text{h.c.} \\
&+ \sum_{q_1,q_2,q_3,q_4} a_1^\dagger a_2 d_3 b_4 \;\; F_7(1;2,3,4) + \text{h.c.} \\
&+ \sum_{q_1,q_2,q_3,q_4} a_1^\dagger a_2 a_3 a_4 \;\; F_9(1;2,3,4) + \text{h.c.}
\end{aligned}
$$

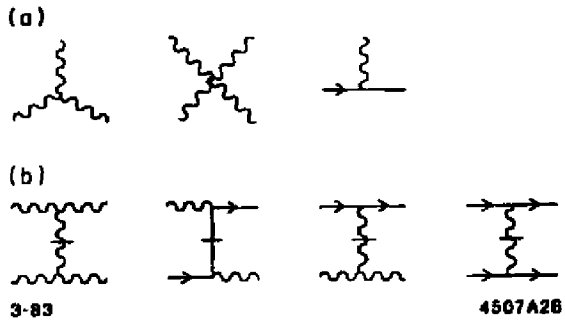

Figure 12. Diagrams which appear in the interaction Hamiltonian for QCD on the light cone. The propagators with horizontal bars represent "instantaneous" gluon and quark exchange which arise from reduction of the dependent fields in $A^+ = 0$ gauge. (a) Basic interaction vertices in QCD. (b) "Instantaneous" contributions.

Light-Cone Perturbation Theory for Gauge Theory

The light-cone Green's functions are the probability amplitudes that a state starting in Fock state $|i\rangle$ ends up in Fock state $|f\rangle$ a (light-cone) time τ later

$$\begin{aligned} \langle f|i\rangle\ G(f,i;\tau) &\equiv \langle f|e^{-iH_{LC}\tau/2}|i\rangle \\ &= i\int \frac{d\epsilon}{2\pi}\, e^{-i\epsilon\tau/2}\, G(f,i;\epsilon)\,\langle f|i\rangle\ , \end{aligned} \tag{41}$$

where Fourier transform $G(f,i;\epsilon)$ can be written

$$\begin{aligned} \langle f|i\rangle\ G(f,i;\epsilon) &= \left\langle f\left|\frac{1}{\epsilon - H_{LC} + i0_+}\right|i\right\rangle \\ &= \left\langle f\left|\frac{1}{\epsilon - H_{LC} + i0_+} + \frac{1}{\epsilon - H_0 + i0_+}V\frac{1}{\epsilon - H_0 + i0_+}\right.\right. \\ &\quad \left.\left. + \frac{1}{\epsilon - H_0 + i0_+}V\frac{1}{\epsilon - H_0 + i0_+}V\frac{1}{\epsilon - H_0 + i0_+} + \ldots\right|i\right\rangle . \end{aligned} \tag{42}$$

The rules for τ-ordered perturbation theory follow immediately when $(\epsilon - H_0)^{-1}$ is replaced by its spectral decomposition.

$$\frac{1}{\epsilon - H_0 + i0_+} = \sum_{n,\lambda_i}\int \tilde{\prod}\, \frac{dk_i^+\, d^2k_{\perp i}}{16\pi^3\, k_i^+}\, \frac{|n:\underline{k}_i,\lambda_i\rangle\ \langle n:\underline{k}_i,\lambda_i|}{\epsilon - \sum_i (k^2+m^2)_i/k_i^+ + i0_+} \tag{43}$$

The sum becomes a sum over all states n intermediate between two interactions.

To calculate $G(f,i;\epsilon)$ perturbatively then, all τ-ordered diagrams must be considered, the contribution from each graph computed according to the following rules:

1. Assign a momentum k^μ to each line such that the total $k^+, k_\perp$ are conserved at each vertex, and such that $k^2 = m^2$, i.e. $k^- = (k^2 + m^2)/k^+$. With fermions associate an on-shell spinor.

$$u(\underline{k},\lambda) = \frac{1}{\sqrt{k^+}}\left(k^+ + \beta m + \vec{\alpha}_\perp \cdot \vec{k}_\perp\right) \begin{cases} \chi(\uparrow) & \lambda = \uparrow \\ \chi(\downarrow) & \lambda = \downarrow \end{cases} \tag{44}$$

or

$$v(\underline{k},\lambda) = \frac{1}{\sqrt{k^+}}\left(k^+ - \beta m + \vec{\alpha}_\perp \cdot \vec{k}_\perp\right) \begin{cases} \chi(\downarrow) & \lambda = \uparrow \\ \chi(\uparrow) & \lambda = \downarrow \end{cases} \tag{45}$$

where $\chi(\uparrow) = 1/\sqrt{2}\,(1,0,1,0)$ and $\chi(\downarrow) = 1/\sqrt{2}\,(0,1,0,-1)^T$. For gluon lines, assign a polarization vector $\epsilon^\mu = (0,\ 2\vec{\epsilon}_\perp \cdot \vec{k}_\perp/k^+,\ \vec{\epsilon}_\perp)$ where $\vec{\epsilon}_\perp(\uparrow) = -1/\sqrt{2}\,(1,i)$ and $\vec{\epsilon}_\perp(\downarrow) = 1/\sqrt{2}\,(1,-i)$.

2. Include a factor $\theta(k^+)/k^+$ for each internal line.

3. For each vertex include factors as illustrated in Fig. 13. To convert incoming into outgoing lines or vice versa replace

$$u \leftrightarrow v\,, \qquad \overline{u} \leftrightarrow -\overline{v}\,, \qquad \epsilon \leftrightarrow \epsilon^* \tag{46}$$

in any of these vertices.

4. For each intermediate state there is a factor

$$\frac{1}{\epsilon - \sum_{\text{interm}} k^- + i0_+} \tag{47}$$

where ϵ is the incident P^-, and the sum is over all particles in the intermediate state.

5. Integrate $\int dk^+ d^2k_\perp/16\pi^3$ over each independent k, and sum over internal helicities and colors.

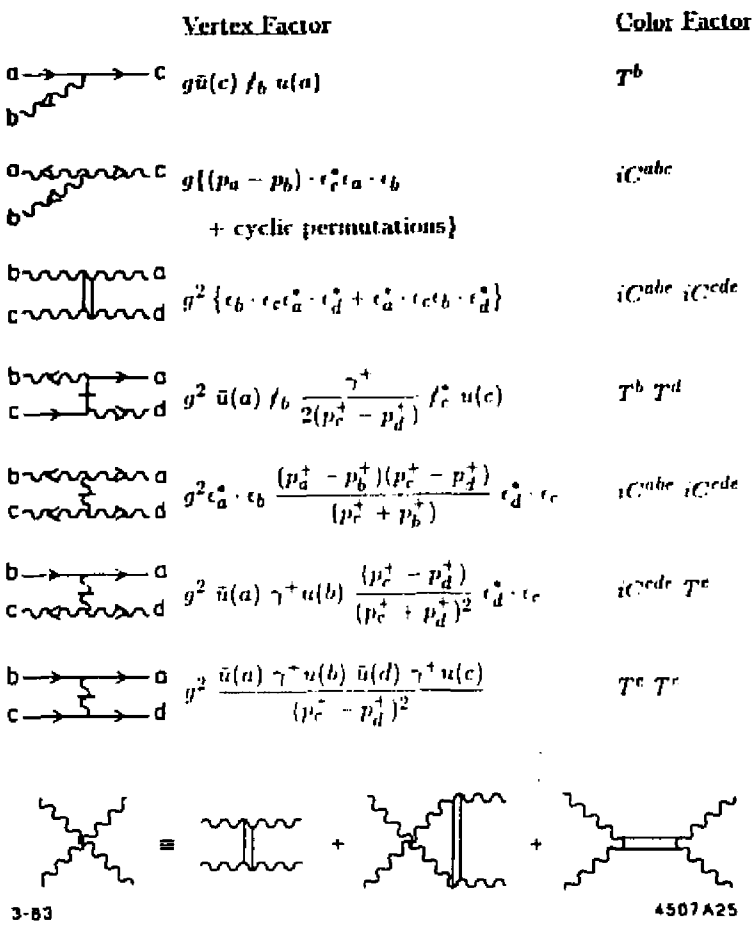

Figure 13. Graphical rules for QCD in light-cone perturbation theory.

6. Include a factor -1 for each closed fermion loop, for each fermion line that both begins and ends in the initial state (*i.e.* $\bar{v}\ldots u$), and for each diagram in which fermion lines are interchanged in either of the initial or final states.

As an illustration, the second diagram in Fig. 13 contributes

$$\frac{1}{\epsilon - \sum_{i=b,d}\left(\frac{k_\perp^2+m^2}{k^+}\right)_i}\cdot\frac{\theta(k_a^+ - k_b^+)}{k_a^+ - k_b^+}$$

$$\times\frac{g^2\sum_\lambda \overline{u}(b)\,\epsilon^*(\underline{k}_a-\underline{k}_b,\lambda)\,u(a)\,\overline{u}(d)\;\not{\epsilon}(\underline{k}_a-\underline{k}_b,\lambda)\,u(c)}{\epsilon - \sum_{i=b,c}\left(\frac{k_\perp^2+m^2}{k^+}\right)_i - \frac{(k_{\perp a}-k_{\perp b})^2}{k_a^+-k_b^+}}\cdot\frac{1}{\epsilon - \sum_{i=a,c}\left(\frac{k_\perp^2+m^2}{k^+}\right)_i} \tag{48}$$

(times a color factor) to the $q\overline{q} \to q\overline{q}$ Green's function. (The vertices for quarks and gluons of definite helicity have very simple expressions in terms of the momenta of the particles.) The same rules apply for scattering amplitudes, but with propagators omitted for external lines, and with $\epsilon = P^-$ of the initial (and final) states.

The light-cone Fock state representation can thus be used advantageously in perturbation theory. The sum over intermediate Fock states is equivalent to summing all $\tau-$ordered diagrams and integrating over the transverse momentum and light-cone fractions x. Because of the restriction to positive x, diagrams corresponding to vacuum fluctuations or those containing backward-moving lines are eliminated. For example, such methods can be used to compute perturbative contributions to the annihilation ratio $R_{e\overline{e}} = \sigma(e\overline{e} \to \text{hadrons})/\sigma(e\overline{e} \to \mu^+\mu^-)$ as well as the quark and gluon jet distribution. The computed distributions are functions of the light-cone variables, x, $k_\perp$, λ, which are the natural covariant variables for this problem. Since there are no Faddeev-Popov or Gupta-Bleuler ghost fields in the light-cone gauge $A^+ = 0$, the calculations are explicitly unitary. It is hoped that one can in this way check the three-loop calculation of Gorishny, *et al.*[70]

The Lorentz Symmetries of Light-Cone Quantization

It is important to notice that the light-cone quantization procedure and all amplitudes obtained in light-cone perturbation theory (graph by graph!) are manifestly invariant under a large class of Lorentz transformations:

1. boosts along the 3-direction — *i.e.* $p^+ \to Kp^+$, $p^- \to K^{-1}p^-$, $p_\perp \to p_\perp$ for each momentum;
2. transverse boosts — *i.e.* $p^+ \to p^+$, $p^- \to p^- + 2p_\perp \cdot Q_\perp + p^+Q_\perp^2$, $p_\perp \to p_\perp + p^+Q_\perp$ for each momentum ($Q_\perp$ like K is dimensionless);
3. rotations about the 3-direction. It is these invariances which also lead to the

frame independence of the Fock state wave functions.

More generally, we can understand these properties from the fact that the maximum number (seven) of the ten Poincare generators are kinematic in light-cone and thus leave the state unchanged at $\tau = 0$.[9,71]

Light-Cone Poincare Generators

The seven generators that commute with the light-cone energy

$$P^- = P^0 - P^3 \,, \tag{49}$$

are the three momenta,

$$P^+ = P^0 + P^3, \quad P_\perp = (P_1, P_2) \,, \tag{50}$$

the longitudinal rotation and boost operators,

$$J_3, \quad K_3 \,, \tag{51}$$

and the light-cone boost operators,

$$B_{\perp 1} = \frac{(K_1 + J_2)}{\sqrt{2}} \,, \qquad B_{\perp 2} = \frac{(K_2 - J_1)}{\sqrt{2}} \,. \tag{52}$$

Thus one can diagonalize the light cone energy P^- within a Fock basis where the constituents have fixed total $P^+, P_\perp$, and J_3. For convenience we shall define the light cone Hamiltonian as the operator

$$H_{LC} = P^- P^+ - P_\perp^2 \tag{53}$$

so that the eigenvalues of H_{LC} correspond to the invariant spectrum $\mathcal{M}^2$ of the theory.

The boost invariance of the eigensolutions of H_{LC} reflects the fact that the boost operators $K_3, B_{\perp 1}$ and $B_{\perp 2}$ are kinematical. The remaining Poincare generators, the light-cone angular momentum operators,

$$S_{\perp 1} = \frac{(K_1 - J_2)}{\sqrt{2}}, \quad \text{and} \quad S_{\perp 2} = \frac{(K_2 + J_1)}{\sqrt{2}} \tag{54}$$

are dynamical and do not commute with P^- or H_{LC}.

In order to understand these features better, we shall discuss the construction of the LC Fock basis for mesons in QCD in some detail. It is easiest to start in a "standard frame" with total momentum $P^+_{\rm std} = 1$, $\vec{P}_{\perp \rm std} = \vec{0}_\perp$ (in any units!) and then boost to a general frame.[71] To simplify the notation we shall write the conserved three momenta in the form $\underline{k_i} \equiv (k_i^+, \vec{k}_{\perp i})$ which becomes $(x_a, \vec{k}_{\perp i})$ in the standard frame. We can then build the light-cone Fock states by applying the free quark, anti-quark, and gluon field operators to the free vacuum:

$$|a\rangle = b^\dagger(\underline{k_a}, \lambda_a) d^\dagger(\underline{k_b}, \lambda_b) a^\dagger(\underline{k_c}, \lambda_c) |0\rangle \ , \tag{55}$$

where $\sum x_i = 1, \sum k_{\perp i} = 0_\perp$, and $\sum \lambda_i = \lambda$, since

$$J_3 \left| P^+ = 1, \vec{P}_\perp = \vec{0}_\perp, \lambda \right\rangle = \lambda \left| P^+ = 1, \vec{P}_\perp = 0_\perp, \lambda \right\rangle \ . \tag{56}$$

In addition, in each Fock state the color indices of the quark and gluon quanta can be combined to form $SU(3)_C$ color-singlet representations. (A general group theory procedure for finding all such irreducible representations is given by Kaluža.[30]) Since the Fock basis is complete, we can write the eigensolution to the pion wavefunction in the standard frame in the form

$$\begin{aligned} |\Psi_\pi(P^+ = 1, P_\perp = 0_\perp)\rangle = \sum_{\lambda_i} \int_0^1 \frac{1}{\sqrt{x}\sqrt{1-x}} \int \frac{d^2k_\perp}{2(2\pi)^3} \psi_{q\bar{q}}(x, k_\perp, \lambda_i) \\ \times b^\dagger(x, k_\perp, \lambda_1) d^\dagger(1-x, -k_\perp, -\lambda_1) |0\rangle \\ + \sum \int \psi_{q\bar{q}g} b^\dagger d^\dagger a^\dagger |0\rangle + \ \ldots \ . \end{aligned} \tag{57}$$

Thus with this construction $\vec{P}_\perp |\Psi_\pi\rangle = \vec{0}_\perp$, and $P^+ |\Psi_\pi\rangle = 1 |\Psi_\pi\rangle$. The eigenvalue problem for the pion in QCD is then

$$P^- |\Psi_\pi\rangle = m_\pi^2 |\Psi_\pi\rangle \ . \tag{58}$$

which in the Fock basis reduces to the problem of diagonalizing the Heisenberg

matrix:

$$\sum_n \langle m|H_{LC}|n\rangle \langle n|\Psi_\pi\rangle = m_\pi^2 \langle m|\Psi_\pi\rangle \ . \tag{59}$$

The eigensolutions then determine the complete Fock representation of the pion light-cone wavefunction.

Given the pion eigensolution in the standard frame, we can immediately construct the pion wavefunction at any total three-momentum $\underline{Q} = (Q^+, Q_\perp)$ since the boost operators $K_3, B_{\perp 1}$, and $B_{\perp 2}$ can all be constructed from the free quark and gluon fields. The boost operators have the action

$$e^{-i\omega K_3} P^+ e^{i\omega K_3} = e^{\omega} P^+ \ , \tag{60}$$

and

$$e^{-i\vec{V}_\perp \cdot \vec{B}_\perp} \vec{P}_\perp = \vec{P}_\perp + P^+ \vec{V}_\perp \ . \tag{61}$$

Thus we define the boost operator

$$U(Q^+, \vec{Q}_\perp) = e^{-i\frac{\vec{Q}_\perp}{Q^+}\cdot \vec{B}_\perp} e^{-\ell n\, Q^+ K_3} \ , \tag{62}$$

so that

$$U(Q^+, \vec{Q}_\perp) b^\dagger(x, \vec{k}_\perp, \lambda) U^{-1}(Q^+, \vec{Q}_\perp) = b^\dagger(xQ, \vec{k}_\perp + x\vec{Q}_\perp, \lambda) \ , \tag{63}$$

etc. Thus the pion wavefunction in a general frame is

$$\Psi_\pi(Q^+, \vec{Q}_\perp) = U(Q^+, \vec{Q}_\perp) \Psi_\pi(Q^+ = 1, \vec{Q}_\perp = \vec{0}_\perp), \tag{64}$$

since $\sum_i (\vec{k}_{\perp i} + x_i \vec{Q}_\perp) = \vec{Q}_\perp$, and $\sum_i x_i Q^+ = Q^+$. Since U is only a function of the free fields, the result is the Fock expansion of Eq. (4). Thus, as emphasized above, the light-cone wavefunctions $\psi_n(x_i, \vec{k}_{\perp i}, \lambda_i)$ and its relative coordinates x_i and $\vec{k}_{\perp i}$ are independent of the total momenta Q^+, $\vec{Q}_\perp$. The actual particle momenta are with plus momentum $k^+ = x_i Q^+$, transverse momentum $\vec{k}_{\perp i} + x_i \vec{Q}_\perp$ and spin projection $J_3 = \lambda_i$. The spinors and polarization vectors for such particles are given explicitly in the proceeding section.

Spin on the Light-Cone[71]

If a theory is rotational invariant, then each eigenstate of the Hamiltonian which describes a state of nonzero mass can be classified in its rest frame by its spin eigenvalues

$$J^2 \left| P^0 = M, \vec{P} = \vec{0} \right\rangle = s(s+1) \left| P^0 = M, \vec{P} = \vec{0} \right\rangle \ , \tag{65}$$

and

$$J_z \left| P^0 = M, \vec{P} = \vec{0} \right\rangle = s_z \left| P^0 = M, \vec{P} = \vec{0} \right\rangle \ . \tag{66}$$

This procedure is more complicated in the light-cone scheme since the angular momentum operator does not commute with H_{LC}. Nevertheless, one can construct light-cone operators[71] $\mathcal{J}^2 = \mathcal{J}_3^2 + \mathcal{J}_\perp^2$ and $\mathcal{J}_3$ where

$$\mathcal{J}_3 = J_3 + \epsilon_{ij} B_{\perp i} P_{\perp j} / P^+ \ , \tag{67}$$

and

$$\mathcal{J}_\perp = \frac{1}{M} \epsilon_{k\ell} (S_{\perp \ell} P^+ - B_{\perp \ell} P^- - K_3 P_{\perp \ell} + \mathcal{J}_3 \epsilon_{\ell m} P_{\perp m}) \ , \tag{68}$$

which, in principle, could be applied to an eigenstate $\left| P^+, \vec{P}_\perp \right\rangle$ to obtain the rest frame spin quantum numbers. This is straightforward for $\mathcal{J}_3$ since it is kinematical; in fact, $\mathcal{J}_3 = J_3$ in a frame with $\vec{P}_\perp = \vec{0}_\perp$. However, $\mathcal{J}_\perp$ is dynamical and depends on the interactions. Thus it is generally difficult to explicitly compute the total spin of a state using light-cone quantization. Nevertheless, this is not a problem in practice since, given the spectrum of the light-cone Hamiltonian, one can identify the rest-frame spin of each eigenstate simply by counting the number of degenerate levels appearing at each value of J_3.

Discrete Light-Cone Symmetries

The QCD Hamiltonian has a number of global symmetries which are also characteristic of its eigensolutions. It is thus useful to pre-diagonalize the Light-Cone Fock state basis with respect to all of the operators which commute with H_{LC} and then diagonalize H_{LC} within each super–selection sector. The most important global symmetries are[71]

Light-Cone Parity,

$$I_P^{LC} = e^{-i\pi J_3} I_P \ , \tag{69}$$

where

$$I_P^{LC} \psi_{q\bar{q}}(x, k_{\perp 1}, k_{\perp 2}, \lambda_i) = \psi_{q\bar{q}}(x, -k_{\perp 1}, k_{\perp 2}, -\lambda_i) \ ; \tag{70}$$

Light-Cone Time-Reversal,

$$I_T^{LC} = e^{-i\pi J_3} I_P I_T \ , \tag{71}$$

where

$$I_P^{LC} \psi_{q\bar{q}}(x, \vec{k}_\perp \lambda_i) = \psi^*_{q\bar{q}}(x, -\vec{k}_\perp, \lambda_i) \ ; \tag{72}$$

and *Light-Cone Charge-Conjugation*:

$$I_P^{LC} \psi_{q\bar{q}}(x, \vec{k}_\perp, \lambda_1, \lambda_2) = -\psi_{q\bar{q}}(1-x, -\vec{k}_\perp, \lambda_2, \lambda_1) \ . \tag{73}$$

By pre-diagonalizing in the eigensectors of these symmetries, one reduces the matrix size of the representations of H_{LC} by a factor of two for each symmetry.

Renormalization and Ultra-Violet Regulation of Light-Cone-Quantized Gauge Theory

An important element in the light-cone Hamiltonian formulation of quantum field theories is the regulation of the ultraviolet region. In order to define a renormalizable theory, a covariant and gauge invariant procedure is required to eliminate states of high virtuality. The physics beyond the scale Λ is contained in the normalization of the mass $m(\Lambda)$ and coupling constant $g(\Lambda)$ parameters of the theory, modulo negligible corrections of order $1/\Lambda^n$ from the effective Lagrangian.

The logarithmic dependence of these input parameters is determined by the renormalization group equations. In Lagrangian field theories the ultraviolet cut-off is usually introduced via a spectrum of Pauli-Villars particles or dimensional regulation. Another interesting possibility is to work with a super-symmetric extension of theory which is finite, and then introduce soft symmetry breaking to give the super-partners large mass of order Λ.

An analogous ultraviolet regularization must also can also be followed in the case of quantization in the light-cone Hamiltonian framework. For example, one can construct the ultraviolet regulated Hamiltonian H_{LC}^{Λ} for QED(3+1) directly from the Lagrangian using Pauli-Villars regulation for both the ultraviolet and infrared regions. The Pauli-Villars spectral conditions must be chosen to eliminate both logarithmic and potentially quadratic divergences.

As an example of this procedure, we have shown in Ref. 28 that the lepton mass renormalization counterterms computed in LCPTH using discretization is identical to that of the Lagrangian perturbation theory in the continuum limit. It was also verified numerically (to 12 significant figures) that this procedure is also consistent within the context of the non-perturbative diagonalization of the light-cone Hamiltonian for the electron state within a truncated Fock space basis $|e\rangle$, $|e\gamma\rangle$.

The Pauli-Villars regulation allows a complete implementation of time-ordered Hamiltonian perturbation theory at $P \to \infty$, in a form which is essentially equivalent to LCPTH.[51] The renormalized amplitudes can be explicitly constructed in each order in perturbation theory simply by subtracting local mass vertex and wavefunction renormalization counterterms defined using the "alternating denominators" method. (See Fig. 4). In addition, it is shown in Ref. 51 that Z-graphs or instantaneous fermion exchange contributions can be automatically included leading to a numerator factor from each time ordering identical to the numerator of the corresponding Feynman amplitude. These methods have been successfully applied to the calculation of the electron magnetic moment to two and three loop order. More recently, Langnau[72] has extended the $g-2$ calculations in LCPTH using dimensional regulation for the transverse momentum integrations in both Feynman and light-cone gauge.

The above method for ultraviolet regulation is not sufficient for non-perturbative problems, such as the diagonalization of the light-cone Hamiltonian. In the previous sections we have discussed the discretization of the light-cone Fock basis using DLCQ. In such methods, one needs to provide *a priori* some type of truncation of the Fock state basis. Since wavefunctions and Green's functions decrease with

virtuality, one expects that states very far off the light-cone energy shell will have no physical effect on a system, except for renormalization of the coupling constant and mass parameters. Thus it is natural to introduce a "global" cut-off such that a Fock state $|n\rangle$ is retained only if

$$\sum_{i\in n} \frac{\vec{k}_{\perp i}^2 + m_i^2}{x_i} - M^2 < \Lambda^2 \,. \tag{74}$$

Here M is the mass of the system in the case of the bound state problem, or the total invariant mass $\sqrt{s}$ of the initial state in scattering theory. One can also limit the growth of the Fock state basis by introducing a "local" cutoff on each matrix element $\langle n|H_{LC}|m\rangle$ by requiring that the change in invariant mass squared

$$\left| \sum_{i\in n} \frac{\vec{k}_{\perp i}^2 + m_i^2}{x_i} - \sum_{i\in m} \frac{\vec{k}_{\perp i}^2 + m_i^2}{x_i} \right| < \Lambda^2 \,. \tag{75}$$

Similarly, one can use a lower cutoff on the invariant mass difference to regulate the infrared region.[73]

The global and local cutoff methods were used in Ref. 4 to derive factorization theorems for exclusive and inclusive processes at large momentum transfer in QCD. In particular, the global cut-off defines the Fock-state wavefunctions $\psi^\Lambda(x, \vec{k}_\perp, \lambda)$ and distribution amplitude $\phi(x, \Lambda)$, the non-perturbative input for computing hadronic scattering amplitudes. The renormalization group properties of the light-cone wavefunctions and the resulting evolution equations for the structure functions and distribution amplitudes are also discussed in Ref. 4. The calculated anomalous dimensions γ_n for the moments of these quantities agree with results obtained using the operator product expansion.[74]

The global cut-off conveniently truncates the ultraviolet and infrared regions of the Fock space basis, and it is easily implemented in practice. However, there several complicating features if this method is used as the sole ultraviolet cut-off of the field theory:

- Gauge-invariance is obviously destroyed by the implementation of a strict cut-off in momentum space. In fact, this problem can be largely avoided by using the following "gauge principle":[28] the matrix element of an instantaneous gluon exchange four-point interaction is nonzero only if the corresponding three-point gluon exchange interactions are allowed by the Fock

space cutoff. Similarly, instantaneous fermion exchange matrix elements are non-zero only if the corresponding propagating fermion interactions are permitted. One can easily check that this principle retains gauge invariance in tree diagrams in gauge theory and preserves the boost invariance of the light-cone Hamiltonian theory.

- Use of the global cut-off alone implies that the cut-off of a self-energy insertion counterterm for any particle depends on the invariant mass of the entire Fock state. This implies that the renormalization counterterms for a given particle depends on the kinematics of the spectators appearing in that Fock state.[28] Formally, this dependence is power-law suppressed by at least a power of $1/\Lambda^2$, but in practice, it is advantageous to keep Λ^2 of reasonable size. The spectator problem is avoided if one uses the local cut-off.
- In general, light-cone quantization using the global or local cutoff can lead to terms in H^{Λ}_{LC} of the form $\delta m\bar{\psi}\frac{\gamma^+}{i\partial^+}\psi$. Although such a term is invariant under the large class of light-cone Lorentz transformations, it is not totally invariant. For example, such terms arise in order g^2 as a result of normal-ordering of the four-point interaction terms. (Note that this complication does not occur in a strictly covariant regulation procedure such as Pauli-Villars.) Thus in this cut-off procedure one has to allow for an extra mass counterterm insertions in the numerator matrix elements of the light-cone interaction Hamiltonian. Burkardt and Langnau[12] have suggested that the extra counterterms can be fixed by *a posteriori* imposing rotational symmetry on the bound state solutions, so that all Lorentz symmetries are restored.

Each of the proposed cut-offs thus have advantages and disadvantages for the DLCQ program. A global cut-off is necessary to limit the size of the Fock space for the numerical diagonalization of the light-cone Hamiltonian or to truncate it to a finite set of equations of motion. However, for the purpose of renormalization, it is possibly advantageous to simultaneously implement other regulators, such as the local cut-off, a Pauli-Villars spectrum, supersymmetric partners, etc.

Ideally, one can apply all of this to QCD(3+1). Once one has defined the regulated light-cone Hamiltonian, solved for its spectrum, as in the DLCQ procedure, the mass $m(\Lambda)$ and coupling constant $g(\Lambda)$ parameters can be fitted by normalizing the output mass and charge radius of the proton state, say, to experiment. Non-perturbative QCD would then be tested by comparison with the remaining hadron and nuclear spectrum and wavefunctions. We discuss the beginning of the application of this program to three-space one-time theories in the following sections.

Discretized Light-Cone Quantization: Applications to QCD(1+1)

As we have seen in the proceeding sections, QCD dynamics takes a rather simple form when quantized at equal light-cone "time" $\tau = t + z/c$. In light-cone gauge $A^+ = A^0 + A^z = 0$, the QCD light-cone Hamiltonian

$$H_{\rm QCD} = H_0 + gH_1 + g^2 H_2 \tag{76}$$

contains the usual 3-point and 4-point interactions plus induced terms from instantaneous gluon exchange and instantaneous quark exchange diagrams. The perturbative vacuum serves as the lowest state in constructing a complete basis set of color-singlet Fock states of H_0 in momentum space. Solving QCD is then equivalent to solving the eigenvalue problem:

$$H_{\rm QCD}|\Psi>= M^2|\Psi> \tag{77}$$

as a matrix equation on the free Fock basis. The set of eigenvalues $\{M^2\}$ represents the spectrum of the color-singlet states in QCD. The Fock projections of the eigenfunction corresponding to each hadron eigenvalue gives the quark and gluon Fock state wavefunctions $\psi_n(x_i, k_{\perp i}, \lambda_i)$ required to compute structure functions, distribution amplitudes, decay amplitudes, etc. For example, the e^+e^- annihilation cross section into a given $J = 1$ hadronic channel can be computed directly from its $\psi_{q\bar{q}}$ Fock state wavefunction.

The basic question is whether one can actually solve the light-cone Hamiltonian eigenvalue problem, even numerically. This is the goal of the DLCQ method.[21] We first observe that the light-cone momentum space Fock basis becomes discrete and amenable to computer representation if one chooses (anti-)periodic boundary conditions for the quark and gluon fields along the $z^- = z - ct$ and $z_\perp$ directions. In the case of renormalizable theories, a covariant ultraviolet cutoff Λ is introduced which limits the maximum invariant mass of the particles in any Fock state. One thus obtains a finite matrix representation of $H_{\rm QCD}^{(\Lambda)}$ which has a straightforward continuum limit. The entire analysis is frame independent, and fermions present no special difficulties.

Construction of the Discrete LC Fock Basis

The key step in obtaining a discrete representation of the light-cone Hamiltonian in a form amenable to numerical diagonalization, is the construction of a complete, countable, Fock state basis,

$$\sum_n |n\rangle \langle n| = I \ . \tag{78}$$

This can be explicitly done in QCD by constructing a complete set of color-singlet eigenstates of the free Hamiltonian as products of representations of free quark and gluon fields. The states are chosen as eigenstates of the constants of the motion, P^+, $\vec{P}_\perp$, J_z, and the conserved charges. In addition, one can pre-diagonalize the Fock representation by classifying the states according to their discrete symmetries, as described in the previous section. This step alone reduces the size of the matrix representations by as much as a factor of 16.

The light-cone Fock representation can be made discrete by choosing periodic (or, in the case of fermions, anti-periodic) boundary conditions on the fields:

$$\psi(x^-) = \pm\psi(x^- - L) \ , \tag{79}$$

$$\psi(x_\perp) = \psi(x_\perp - L_\perp) \tag{80}$$

Thus in each Fock state,

$$P^+ = \frac{2\pi}{L} K \ , \tag{81}$$

and each constituent

$$k_i^+ = \frac{2\pi}{L} n_i \ , \tag{82}$$

where the positive integers n_i satisfy

$$\sum_i n_i = K \ . \tag{83}$$

Similarly

$$\vec{k}_{\perp i} = \frac{\pi}{L_\perp} \vec{n}_{\perp i} \ , \tag{84}$$

where the vector integers sum to $\vec{0}_\perp$ in the standard frame.

The positive integer K is called the "harmonic resolution." Notice that for any choice of K, there are only a finite number of partitions of the plus momenta, and thus only a finite set of rational values of $x_i = k_i^+/P^+ = n_i/K$ appear:

$$x_i = \frac{1}{K}, \quad \frac{2}{K}, \quad \cdots \frac{K-1}{K}. \tag{85}$$

Thus eigensolutions obtained by diagonalizing H_{LC} on this basis determine the deep inelastic structure functions $F_I(x)$ only at the set of rational discrete points x_i. The continuum limit thus requires extrapolation to $K \to \infty$. Note that the value of L is irrelevant, since it can always be scaled away by a Lorentz boost. Since H_{LC}, P^+, $\vec{P}_\perp$, and the conserved charges all commute, H_{LC} is block diagonal.

The DLCQ program becomes especially simple for gauge theory in one-space one-time dimensions because of the absence of transverse momenta but also because there are no gluon degrees of freedom. In addition, for a given value of the harmonic resolution K the Fock basis becomes restricted to finite dimensional representations. The dimension of the representation corresponds to the number of partitions of the integer K as a sum of positive integers n. The eigenvalue problem thus reduces to the diagonalization of a finite Hermitian matrix. The continuum limit is clearly $K \to \infty$.

Since continuum scattering states as well as single hadron color-singlet hadronic wavefunctions are obtained by the diagonalization of H_{LC}, one can also calculate scattering amplitudes as well as decay rates from overlap matrix elements of the interaction Hamiltonian for the weak or electromagnetic interactions. In principle, all higher Fock amplitudes, including spectator gluons, can be kept in the light-cone quantization approach; such contributions cannot generally be neglected in decay amplitudes involving light quarks.

One of the first applications[22] of DLCQ to local gauge theory was to QED in one-space and one-time dimensions. Since $A^+ = 0$ is a physical gauge, there are no photon degrees of freedom. Explicit forms for the matrix representation of H_{QED} are given in Ref. 22, The QED results agree with the Schwinger solution at zero fermion mass, or equivalently, infinite coupling strength.

More recently DLCQ[18] has been used to obtain the complete color-singlet spectrum of QCD in one space and one time dimension for $N_C = 2, 3, 4$.[75] The hadronic spectra are obtained as a function of quark mass and QCD coupling constant (see Fig. 14).

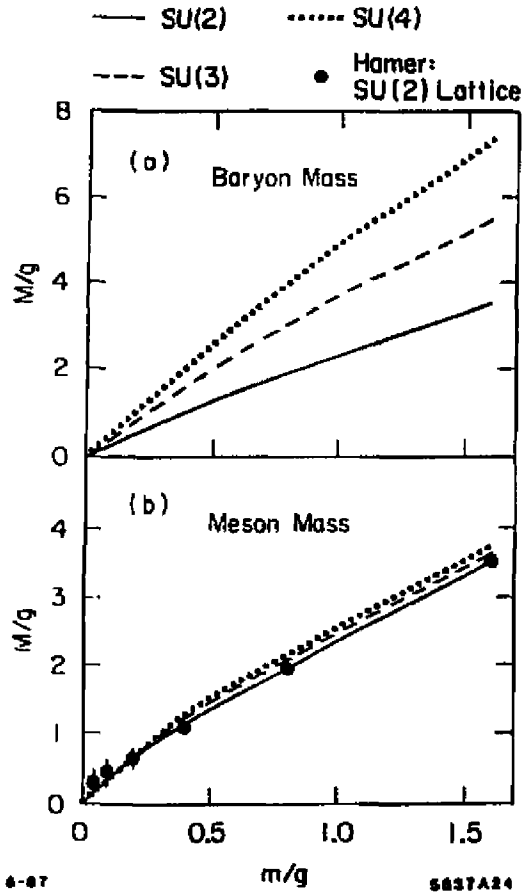

Figure 14. The baryon and meson spectrum in QCD(1+1) computed in DLCQ for $N_C = 2, 3, 4$ as a function of quark mass and coupling constant.[16]

Where they are available, the spectra agree with results obtained earlier; in particular, the lowest meson mass in SU(2) agrees within errors with lattice Hamiltonian results.[76] The meson mass at $N_C = 4$ is close to the value predicted by 't Hooft[75] in the large N_C limit. The DLCQ method also provides the first results for the baryon spectrum in a non-Abelian gauge theory. The lowest baryon mass is shown in Fig. 14 as a function of coupling constant. The ratio of meson to baryon mass as a function of N_C also agrees at strong coupling with results obtained by Frishman and Sonnenschein.[77] Precise values for the mass eigenvalue can be obtained by extrapolation to large K by fitting to forms with the correct functional dependence in $1/K$.

QCD(1+1) in the $m/g \to 0$ Limit

It is interesting to see how one QCD(1+1) and QED(1+1) become equivalent to theories of non-interacting hadrons theories in the Schwinger zero quark mass limit. The emergence of massless hadrons at zero quark mass in the non-Abelian theory may be understood[18] by studying the momentum space transforms of the $SU(N)$ currents (at $x^+ = 0$)

$$V_k^a = \frac{1}{2} \int_{-L}^{L} dx^- e^{-i\frac{k\pi}{L}x^-} j^{+a}(x^-) \tag{85}$$

which satisfy $[V_k^a, V_l^b] = if^{abc}V_{k+l}^c + \frac{1}{2}l\delta^{ab}\delta_{k+l,0}$. The currents j^{+a} are defined by point splitting along x^-; however for $A^+ = 0$, the path- ordered exponential included to ensure gauge invariance reduces to one. The algebra may be extended to include the $U(1)$ current $j^+ = (\frac{2}{N})^{\frac{1}{2}} : \psi_R^\dagger \psi_R :$. The transformed operator V_k commutes with the other $SU(N)$ elements, and the related operator $a_k^\dagger \equiv (\frac{2}{k})^{\frac{1}{2}} \epsilon(k) V_k$ satisfies the free boson commutation relations $[a_k, a_k^\dagger] = \delta_{k,l}$.

The interacting part of the Hamiltonian is greatly simplified when expressed in terms of these operators:

$$P_I^- = -\frac{g^2}{16} \int_{-L}^{L} dx^- dy^- |x^- - y^-| j^{+a}(x^-) j^{+a}(y^-) \tag{85}$$

becomes

$$\frac{L}{2\pi}\frac{g^2}{2\pi} \sum_{k=-\infty}^{\infty} \frac{1}{k^2} V_k^a V_{-k}^a. \tag{86}$$

Because $V_0^a = Q^a$, the contribution at $k = 0$ is proportional to the total charge $Q^a Q^a$ and so may be discarded.

The V_k are color-singlet bi-linear operators in ψ_R, and so may be used to create mesonic-like states with momentum $P^+ = \frac{2\pi k}{L}$. In the limit where m/g is zero, the entire Hamiltonian is given by Eq. (86). Because the V_k commute with the V_k^a

which appear in P_I^-,

$$M^2 V_k |0\rangle = \frac{2\pi k}{L}[P^-, V_k]|0\rangle = 0. \tag{85}$$

Not only is the state created by acting with V_k on the vacuum an exactly massless eigenstate in this limit, but states formed by repeated applications are also exactly massless. Furthermore, acting with V_k on an eigenstate of non-zero mass produces a degenerate state of opposite parity. This argument is independent of the value of the numerical momentum K and so gives an exact continuum result.

If the gauge group is $U(N)$ rather than $SU(N)$, the additional term associated with the extra $U(1)$,

$$\frac{L}{2\pi}\frac{g^2}{2\pi}\sum_{k=1}^{\infty}\frac{1}{k}a_k^\dagger a_k, \tag{85}$$

appears in P^-. The a_k satisfy free bosonic commutation relations, and this additional interaction is therefore the discrete light-cone Hamiltonian for free bosons of mass squared $g^2/2\pi$. These formerly massless states created by the $a_k^\dagger$ are promoted to the free massive bosons found in the Schwinger model and are discussed in Refs. 78 and 22. The quark wavefunctions for these states at infinite coupling or zero fermion mass are constant in x, reflecting their point-like character.

Structure Functions for QCD(1+1)[18]

As we have emphasized, when the light-cone Hamiltonian is diagonalized at a finite resolution K, one gets a complete set of eigenvalues corresponding to the total dimension of the Fock state basis. A representative example of the spectrum is shown in Fig. 15 for baryon states ($B = 1$) as a function of the dimensionless variable $\lambda = 1/(1 + \pi m^2/g^2)$. Notice that spectrum automatically includes continuum states with $B = 1$.

The structure functions for the lowest meson and baryon states in SU(3) at two different coupling strengths $m/g = 1.6$ and $m/g = 0.1$ are shown in Figs. 16 and 17. Higher Fock states have a very small probability; representative contributions to the baryon structure functions are shown in Figs. 18 and 19. For comparison, the valence wavefunction of a higher mass state which can be identified as a composite of meson pairs (analogous to a nucleus) is shown in Fig. 20. The interactions of the quarks in the pair state produce Fermi motion beyond $x = 0.5$. Although these results are for one-time one-space theory they do suggest that the sea quark

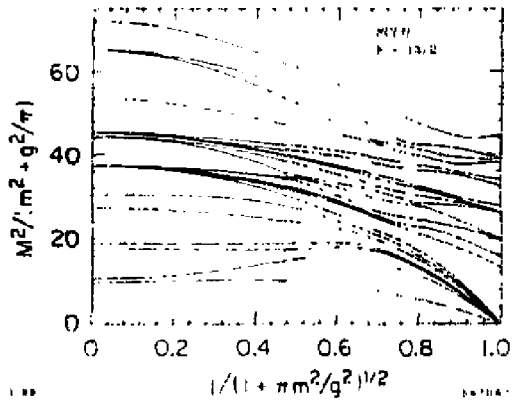

Figure 15. Representative baryon spectrum for QCD in one-space and one-time dimension.[18]

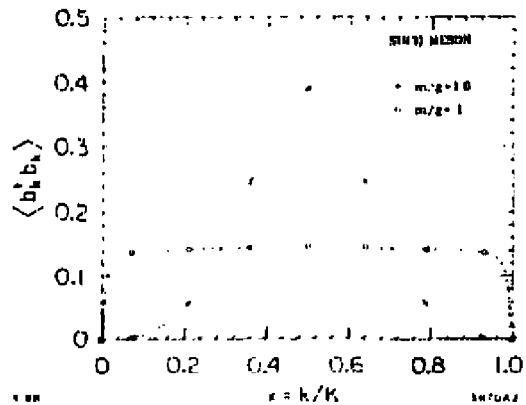

Figure 16. The meson quark momentum distribution in QCD[1+1] computed using DLCQ.[18]

distributions in physical hadrons may be highly structured. We will discuss this possibility further in the next section.

The Heavy Quark Content of the Proton

The DLCQ results for sea quark distributions in QCD(1+1) may have implications for the heavy quark content of physical hadrons. One of the most intriguing unknowns in nucleon structure is the strange and charm quark structure of the

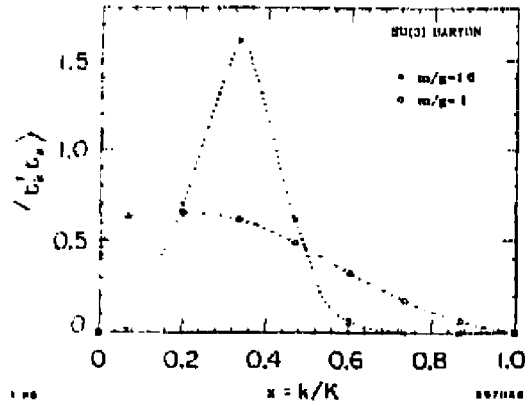

Figure 17. The baryon quark momentum distribution in QCD[1+1] computed using DLCQ.[18]

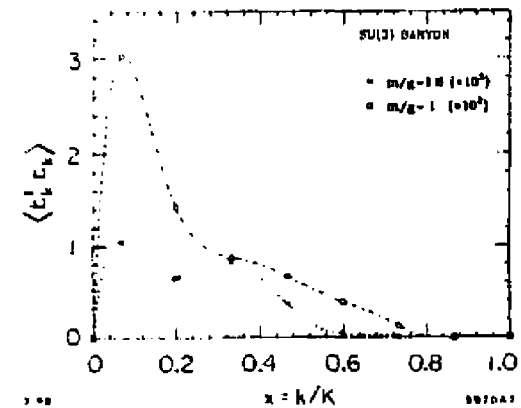

Figure 18. Contribution to the baryon quark momentum distribution from $qqq\overline{qq}$ states for QCD[1+1].[18]

nucleon wavefunction.[79] The EMC spin crisis measurements indicate a significant $s\bar{s}$ content of the proton, with the strange quark spin strongly anti-correlated with the proton spin. Just as striking, the EMC measurements[80] of the charm structure function of the Fe nucleus at large $x_{bj} \sim 0.4$ appear to be considerably larger than that predicted by the conventional photon-gluon fusion model, indicating an anomalous charm content of the nucleon at large values of x. The probability of intrinsic charm has been estimated[80] to be 0.3%.

As emphasized in the previous sections, the physical content of a hadron in

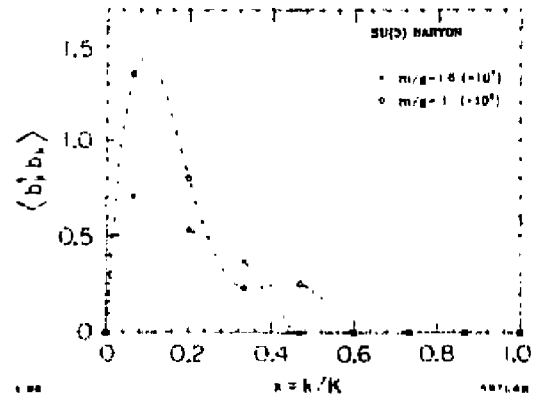

Figure 19. Contribution to the baryon quark momentum distribution from $qqq\bar{q}\bar{q}\bar{q}$ states for QCD[1+1].[18]

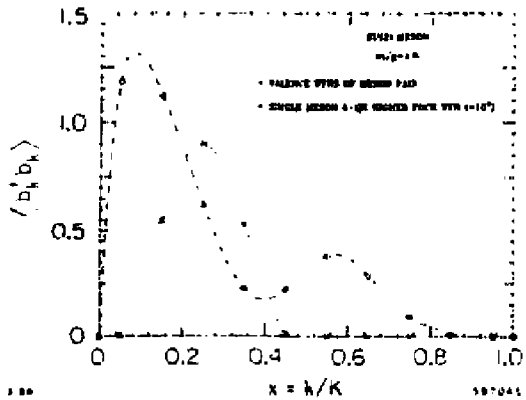

Figure 20. Comparison of the meson quark distributions in the $q\bar{q}q\bar{q}$ Fock state with that of a continuum meson pair state. The structure in the former may be due to the fact that these four-particle wavefunctions are orthogonal.[18]

terms of its quark and gluon constituents, including sea-quark distributions, is represented by its light-cone wavefunctions $\psi_n(x_i, p_{\perp i}, \lambda_i)$, which the projections of the hadron wavefunction on the complete set of Fock states defined at fixed light-cone time $\tau = t + z/c$.[19] Here $x_i = (E_i + p_{Li})/(E + p_L)$, with $\sum_i x_i = 1$, is the fractional (light-cone) momentum carried by parton i. The determination of the light-cone wavefunctions requires diagonalizing the light-cone Hamiltonian on the free Fock basis. As we have discussed, this has, in fact, been done for QCD in one-space and one-time dimension.[18]

In Fig. 21 we show recent results obtained by Hornbostel[81] for the structure functions of the lowest mass meson in QCD(1+1) wavefunctions for $N_C = 3$ and two quark flavors. As seen in the figure, the heavy quark distribution arising from the $q\bar{q}Q\bar{Q}$ Fock component has a two-hump character. The second maximum is expected since the constituents in a bound state tend to have equal velocities. The result is insensitive to the value of the Q^2 of the deep inelastic probe. Thus intrinsic charm is a feature of exact solutions to QCD(1+1). Note that the integrated probability for the Fock states containing heavy quarks falls nominally as g^2/m_Q^4 in this super-renormalizable theory, compared to g^2/m_Q^2 dependence expected in renormalizable theories.

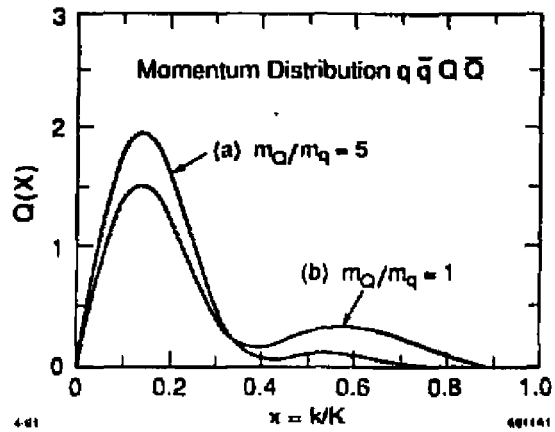

Figure 21. The heavy quark structure function $Q(x) = G_{Q/M}(x)$ of the lightest meson in QCD(1+1) with $N_c = 3$ and $g/m_q = 10$. Two flavors are assumed with (a) $m_Q/m_q = 1.001$ and (b) $m_Q/m_q = 5$. The curves are normalized to unit area. The probability of the $q\bar{q}Q\bar{Q}$ state is 0.56×10^{-2} and 0.11×10^{-4}, respectively. The DLCQ method for diagonalizing the light-cone Hamiltonian is used with anti-periodic boundary conditions. The harmonic resolution is taken at $K = 10/2$. (From Ref. 81.)

In the case of QCD(3+1), we also expect a two-component structure for heavy-quark structure functions of the light hadrons. The low x_F enhancement reflects the fact that the gluon-splitting matrix elements of heavy quark production favor low x. On the other hand, the $Q\bar{Q}q\bar{q}$ wavefunction also favors equal velocity of the constituents in order to minimize the off-shell light-cone energy and the invariant mass of the Fock state constituents. In addition, the non-Abelian effective Lagrangian analysis discussed above allows a heavy quark fluctuation in the bound

state wavefunction to draw momentum from all of the hadron's valence quarks at order $1/m_Q^2$. This implies a significant contribution to heavy quark structure functions at medium to large momentum fraction x. The EMC measurements of the charm structure function of the nucleon appear to support this picture.[80]

It is thus useful to distinguish *extrinsic and intrinsic* contributions to structure functions. The extrinsic contributions are associated with the substructure of a single quark and gluon of the hadron. Such contributions lead to the logarithmic evolution of the structure functions and depend on the momentum transfer scale of the probe. The intrinsic contributions involve at least two constituents and are associated with the bound state dynamics independent of the probe. (See Fig. 22.) The intrinsic gluon distributions[17] are closely related to the retarded mass-dependent part of the bound-state potential of the valence quarks.[19] In addition, because of asymptotic freedom, the hadron wavefunction has only an inverse power $\mathcal{M}^{-2}$ suppression for high mass fluctuations, whether heavy quark pairs or light quark pairs at high invariant mass $\mathcal{M}$. This "intrinsic hardness" of QCD wavefunctions leads to a number of interesting phenomena, including a possible explanation for "cumulative production," high momentum components of the nuclear fragments in nuclear collisions. This is discussed in detail in Ref. 82.

Calculation of the e^+e^- Annihilation Cross Section

An important advantage of the free LC Fock basis is that the electroweak currents have a simple representation. Thus once one diagonalizes the light-cone Hamiltonian, one can immediately compute current matrix elements, such as the proton–anti-proton time-like form factors $\langle 0|j^\mu(0)|\psi\rangle_{p\bar{p}}(s)$ or any given hadronic final state contribution to the total annihilation cross section $\sigma_{e^+e^-}(s)$. This program has recently been carried out explicitly using the DLCQ method and Lanczos tri-diagonalization by Hiller[13] for QED(1+1). A typical result is shown in Fig. 23. It would be interesting to repeat this non-perturbative calculation for a renormalizable theory like the Gross-Neveu model in (1+1) dimensions, and analyze how the channel-by-channel calculation merges into the asymptotic freedom result.

Applications of DLCQ to Gauge Theories in 3+1 Dimensions

The diagonalization of the light-cone Hamiltonian

$$H_{LC}|\psi_i\rangle = M_i^2|\psi_i\rangle\,. \tag{87}$$

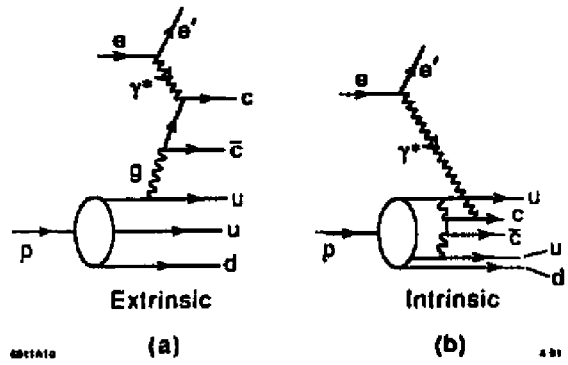

Figure 22. Illustrations of (a) extrinsic (leading twist) and (b) intrinsic (higher twist $\mathcal{O}(\mu^2/m_c^2)$) QCD contributions to the charm structure function of the proton $G_{c/p}(x)$. The magnitude of the intrinsic contribution is controlled by the multi-gluon correlation parameter μ in the proton wavefunction. The intrinsic contribution dominates $G_{c/p}(x)$ at large x.

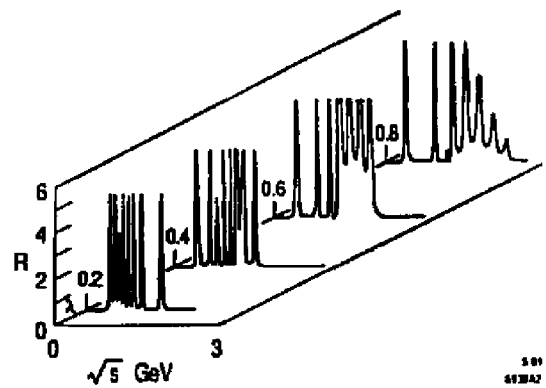

Figure 23. Calculation of $R_{e^+e^-}(s)$ in QED(1+1) using the DLCQ method. The results are shown for different coupling constants. For display purposes, the plot is clipped at $R = 5$. In addition, in order to give finite widths to what would have been δ–functions, the infinitesimal ϵ was set to 0.01 (from Ref. 13).

provides not only the eigenvalues M_i^2 but also the relativistic boost-invariant eigenfunctions $|\psi_i\rangle$. In the following sections we will discuss specific implementations of the DLCQ method for quantum electrodynamics and QCD in 3 + 1 dimensions. Although the QED spectrum is well understood from Bethe Salpeter and other approaches, it is important and interesting to study this system at strong coupling strength for possible clues to confinement and hadronization mechanisms in QCD.[10] Furthermore at moderate α we can make contact with the precision QED

results of Yennie,[83] Lepage, Bodwin, and others, and possibly understand the validity of standard perturbative expansions in QED. However, most important for our purposes, positronium serves as a crucial system to validate the DLCQ methods. In addition to the work discussed here, Kaluża[30] has recently used a DLCQ diagonalization approach to obtain the lepton structure function in positronium.

In the complete formulation of DLCQ, one constructs a complete discretized light-cone Fock basis in momentum space. The LC Hamiltonian can then be visualized as a matrix with a finite number of rows and columns assuming an invariant ultraviolet cut-off. Next, one formulates all necessary model assumptions, in accord with covariance and gauge-invariance, thus obtaining a discrete representation of the quantum filed theory. At any stage, one can go to the continuum limit, convert the matrix equation to an integral equation, and solve it with suitably optimalized numerical methods. One should emphasize, that the regularization scheme of DLCQ[28] explicitly allows for such a procedure, since the regularization scales are equal both for discretization and the continuum, contrary to lattice gauge theory, for example.

Testing Discretized Light Cone Quantization with Positronium

In the simplified DLCQ model[84] we shall discuss here, we will consider only the charge zero sector of QED(3+1) and include only the $J_z = 0$ *electron-positron* ($e\bar{e}$) and the *electron-positron-photon* ($e\bar{e}\gamma$) Fock states, denoted collectively by $|e\bar{e}\rangle$ and $|e\bar{e}\gamma\rangle$, respectively. In effect we have analyzed the muonium system μ^+e^- at equal lepton mass to avoid complications from the annihilation kernels. Even when one restricts the Fock states to one dynamical photon, one is considering a complex non-perturbative problem, similar to ladder approximation in the Bethe-Salpeter formalism. The light-cone approach has the advantage that one obtains the Dirac-Coulomb equation in the heavy muon limit. (In the Bethe-Salpeter approach, one must include all crossed graph irreducible kernels to derive the Dirac equation.) However, it should be emphasized that in any formalism the physics of the Lamb Shift and vertex corrections to the hyperfine interaction cannot occur until one includes the contributions of at least two dynamical photons "in flight."

It is convenient to introduce the projectors $P+Q = \mathbf{1}$, with $P = \sum_i |(e\bar{e})_i\rangle\langle(e\bar{e})_i|$ and $Q = \sum_i |(e\bar{e}\gamma)_i\rangle\langle(e\bar{e}\gamma)_i|$. The index i runs over all discrete light-cone momenta and helicities of the partons (electron e, positron $\bar{e}$ and photon γ) subject to fixed total momenta and to covariant regularization by a sharp momentum cut-off.[28] The Hamiltonian Eq. (87) can then be understood as a block matrix. There are a number of restrictions and simplifications due needed to maintain gauge invariance

when the Fock space is limited in momentum space. The structure of these blocks in terms of matrix elements needs to be discussed in some detail. For example, the matrix elements as depicted in Fig. 24 for the Q-space contain either an instantaneous boson or an instantaneous fermion line. According to the general gauge principle[28,27] for DLCQ, one should include the instantaneous graphs only if the 'instantaneous parton' will be accompanied by a real 'dynamic parton' with the same space-like momentum and in the same Fock space configuration. Otherwise gauge invariance of the scattering amplitudes is violated already on the tree level. Thus, diagram (a) has to be excluded, since there are no $|e\bar{e}\gamma\gamma\rangle$ Fock states in the model, as well as diagram (b) since the two photon states are absent. Actually, only diagram (d) survives the gauge cut-off in the Q-space. Similarly in the P-space, only diagram (a) of Fig. 25 survives.

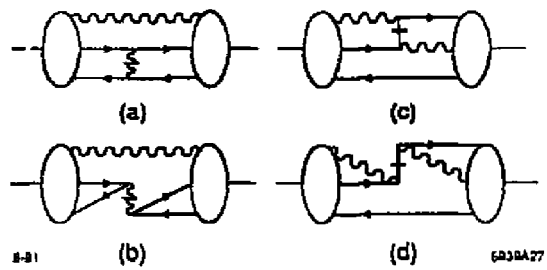

Figure 24. The instantaneous interactions in the Q-space. – Graph (a) and (b): The instantaneous boson interactions $S^{(s)}_{q\bar{q}\to q\bar{q}}$ and $S^{(e)}_{q\bar{q}\to q\bar{q}}$, respectively. Graph (c) and (d): The instantaneous fermion interactions $S^{(s)}_{qq\to qq}$ and $S^{(a)}_{qq\to qq}$, respectively.

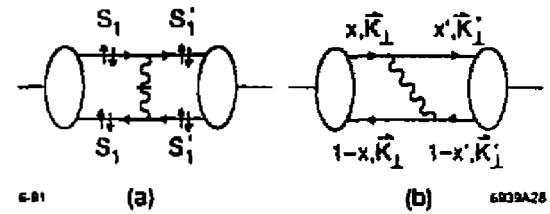

Figure 25. The off-diagonal matrix elements in P-space. – (a): the instantaneous boson graph $S^{(s)}_{q\bar{q}\to q\bar{q}}$; (b): the iterated graph $W = VGV$. – The figure displays also the space-like momentum assignment of the fermions; those of the boson are fixed by momentum conservation. Graph (b) holds for $x > x'$, the corresponding one for $x < x'$ is not shown.

As part of the model, one additional simplification has been made, namely to omit diagram (d) of Fig. 24, *i.e.*

$$S^{(a)}_{q\bar{q}\to g g} = 0 \text{ in } Q\text{-space.} \tag{88}$$

One has no good reason to do so except mathematical simplification, since the Q-space matrix is now rendered diagonal. An equivalent assumption has been made in all of the preceding work.[4,7,20]

By inverting the matrix $(M_i^2 - H_{\rm LC}) \equiv (\omega - H_{\rm LC})$ in the Q-space, *i.e.*

$$Q\,|\psi_i\rangle = Q\frac{1}{\omega - H_{\rm LC}} Q H_{\rm LC} P\,|\psi_i\rangle\,, \tag{89}$$

Eq. (87) can be identically rewritten as

$$H_{\rm eff}(\omega)\,|\psi_i(\omega)\rangle = M_i^2(\omega)\,|\psi_i(\omega)\rangle\,, \tag{90}$$

the 'effective Hamiltonian' acting only in P-space, *i.e.*

$$H_{\rm eff}(\omega) \equiv P H_{\rm LC} P + P H_{\rm LC} Q \frac{1}{\omega - H_{\rm LC}} Q H_{\rm LC} P. \tag{91}$$

Once $|\psi_i(\omega)\rangle = P\,|\psi_i\rangle$ is known, one can calculate the Q-space wave function from Eq. (89) by quadrature.

Despite acting only in P-space, Eq. (90) is not simpler to solve than the full problem, Eq. (87). But it can be approximated easier. Since the Q-space matrix is diagonal by construction, $\omega - H_{\rm LC}$ can be inverted trivially. Characterizing the electron by its Lagrangian mass $m_{\rm F}$, its longitudinal momentum fraction x, its transverse momentum $\vec{k}_\perp$, and by its spin projection s_1, and correspondingly the positron as displayed in Fig. 25, the effective Hamiltonian

$$H_{\rm eff}(\omega) = \frac{m_{\rm F}^2 + \vec{k}_\perp^{\,2}}{x(1-x)} + C + S + W(\omega) = \frac{m_{\rm F}^2 + \vec{k}_\perp^{\,2}}{x(1-x)} + V_{\rm eff}(\omega^*) \tag{92}$$

contains thus the free part, the diagonal contraction terms C in the P-space, the seagull interaction $S = S^{(s)}_{q\bar{q}\to q\bar{q}}$ in the P-space, and the iterated vertex interaction $W(\omega) = V\frac{Q}{\omega - M^2_{e\bar{e}\gamma}}V$. The latter connects the P-space with the Q-space through the vertex interaction $V = V_{q\to qg}$ with the 'energy' denominator $\omega - M^2_{e\bar{e}\gamma}$. Note, that the effective potential $V_{\rm eff}$ is strictly proportional to α.

In general ω should be chosen as the eigenvalue M_i^2. To correct for the violation of gauge invariance by Eq. (88) approximately, however, one replaces the eigenvalue ω with a function of $(x, \vec{k}_\perp)$, *i.e.* with the symmetrized mass (squared)

$$\omega \Rightarrow \omega^* = \frac{1}{2}\left(\frac{m_F^2 + \vec{k}_\perp^2}{x(1-x)} + \frac{m_F^2 + \vec{k}_\perp'^2}{x'(1-x')}\right). \tag{93}$$

This (second ad-hoc) assumption restores the gauge-invariance of the $e\bar{e}$-scattering amplitude in the P-sector, at least. This completes the model.

The projection technique of deriving an effective Hamiltonian is fairly standard in many-body theory,[85] and has been applied to light-cone formulation before.[4,20] Since we have truncated the Fock states, the model can be regarded as a light-cone gauge theory analogue of the Tamm-Dancoff approach[7] used in equal-time theory. A similar approach was applied recently[86,87] to a scalar field model in light-cone coordinates.

The Light-Cone Tamm-Dancoff Equation

In the continuum, the matrix equation (91) becomes an integral equation

$$\left\{\frac{m_F^2 + \vec{k}_\perp^2}{x(1-x)} - M_i^2\right\}\psi_i(x, \vec{k}_\perp, s_1, s_2)$$
$$+ \sum_{s_1', s_2'} \int_D dx' d^2\vec{k}_\perp' \left\langle x, \vec{k}_\perp; s_1, s_2 \middle| V_{\rm eff}(\omega) \middle| x', \vec{k}_\perp'; s_1', s_2' \right\rangle \psi_i(x', \vec{k}_\perp', s_1', s_2') = 0. \tag{94}$$

The finite domain of integration D is set by covariant Fock space regularization,[28]

$$\frac{m_F^2 + \vec{k}_\perp^2}{x(1-x)} \leq \Lambda^2 + 4m_F^2, \tag{95}$$

with given cut-off scale Λ. Combined with Eq. (93), we shall speak of this equation as the 'Light-cone Tamm-Dancoff' equation.

The effective interaction $V_{\rm eff}$, which is also displayed diagrammatically in Figs. 25 and 26, appears to have two kinds of singularities, namely a 'Coulomb singularity' at ($x = x'$ and $\vec{k}_\perp = \vec{k}_\perp'$), and a 'colinear singularity' at ($x = x'$ and $\vec{k}_\perp \neq \vec{k}_\perp'$).

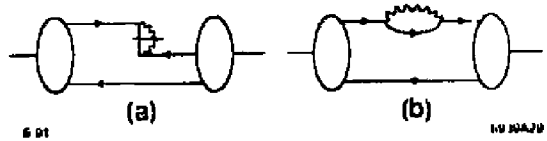

Figure 26. The diagonal matrix elements in P-space. - (a): the instantaneous contraction terms, (b): the iterated graph $W = VGV$ (self-mass diagram).

The latter is caused by the instantaneous interaction

$$\left\langle x, \vec{k}_\perp; s_1, s_2 \right| S \left| x', \vec{k}_\perp'; s_1', s_2' \right\rangle = -\frac{\alpha}{2\pi^2} \frac{2}{(x-x')^2} \delta_{s_1,s_1'} \delta_{s_2,s_2'} \ ,$$

but it will be cancelled by a corresponding term in the iterated vertex interaction $W(\omega)$. Strictly speaking, one should treat the *diagonal* interaction matrix element for $x = x'$ *and* $\vec{k}_\perp = \vec{k}_\perp'$ differently from the *off-diagonal* elements $(x, \vec{k}_\perp) \neq (x', \vec{k}_\perp')$, which is always possible going back to the discretized case. The diagonal matrix element $C + W(\omega)$ is displayed in Fig. 26 and vanishes strictly for $\omega = \omega^*$ due to mass renormalization.[84] One might expect a diagonal contribution from the instantaneous interaction S, but its matrix element vanishes for $x = x'$ in DLCQ.[28]

As an example, consider the off-diagonal matrix element of the iterated vertex interaction $\left\langle x, \vec{k}_\perp; \uparrow, \downarrow \right| W(\omega) \left| x', \vec{k}_\perp'; \uparrow, \downarrow \right\rangle$ for $x > x'$. Straightforward insertion of the matrix elements (See Tables 2a-d) gives

$$W(\omega) = \frac{2\beta}{\mathcal{D}(x,x';\omega)} \vec{\epsilon}_\perp(\uparrow) \cdot \left(\frac{\vec{k}_\perp - \vec{k}_\perp'}{x-x'} - \frac{\vec{k}_\perp'}{x'} \right) \vec{\epsilon}_\perp^*(\uparrow) \cdot \left(\frac{\vec{k}_\perp - \vec{k}_\perp'}{x-x'} + \frac{\vec{k}_\perp'}{1-x'} \right)$$

$$+ \frac{2\beta}{\mathcal{D}(x,x';\omega)} \vec{\epsilon}_\perp(\downarrow) \cdot \left(\frac{\vec{k}_\perp - \vec{k}_\perp'}{x-x'} - \frac{\vec{k}_\perp}{x} \right) \vec{\epsilon}_\perp^*(\downarrow) \cdot \left(\frac{\vec{k}_\perp - \vec{k}_\perp'}{x-x'} + \frac{\vec{k}_\perp}{1-x} \right) .$$

The denominator $\mathcal{D}(x,x';\omega) \equiv -(x-x')\,(\omega - M^2_{e\bar{e}\gamma})$ is introduced for convenience. The polarization sums can be expressed in terms of the transverse scalar and vector products, $\vec{k}_\perp \cdot \vec{k}_\perp'$ and $\vec{k}_\perp \wedge \vec{k}_\perp'$, respectively. One obtains straightforwardly $2(\vec{\epsilon}_\perp(\uparrow) \cdot \vec{k}_\perp)(\vec{\epsilon}_\perp^*(\downarrow) \cdot \vec{k}_\perp') = \vec{k}_\perp \cdot \vec{k}_\perp' - i\vec{k}_\perp \wedge \vec{k}_\perp'$. *The colinear singularities in*

$$W(\omega) = \frac{\alpha}{2\pi^2} \frac{1}{\mathcal{D}(x,x';\omega)} \Big[\frac{\vec{k}_\perp^2}{(x-x')^2} \Big(1 + \frac{x'(1-x')}{x(1-x)} \Big) + \frac{\vec{k}_\perp'^2}{(x-x')^2} \Big(1 + \frac{x(1-x)}{x'(1-x')} \Big)$$

$$- \frac{4\vec{k}_\perp \vec{k}_\perp'}{(x-x')^2} - \frac{\vec{k}_\perp \cdot \vec{k}_\perp' - i\vec{k}_\perp \wedge \vec{k}_\perp'}{x'x} - \frac{\vec{k}_\perp \cdot \vec{k}_\perp' + i\vec{k}_\perp \wedge \vec{k}_\perp'}{(1-x')(1-x)} \Big]$$

cancel against those of S, and the effective interaction becomes finally for $\omega = \omega^*$

$$\left\langle x, \vec{k}_\perp; \uparrow, \downarrow \right| V_{\rm eff}(\omega^*) \left| x', \vec{k}_\perp'; \uparrow, \downarrow \right\rangle = -\frac{\alpha}{2\pi^2} \frac{1}{\mathcal{D}(x,x')} \Big[m_{\rm F}^2 \Big(\frac{1}{x'x} + \frac{1}{(1-x')(1-x)} \Big)$$
$$+ \frac{\vec{k}_\perp^2}{x(1-x)} + \frac{\vec{k}_\perp'^2}{x'(1-x')} + \frac{\vec{k}_\perp \cdot \vec{k}_\perp' - i\vec{k}_\perp \wedge \vec{k}_\perp'}{x'x} + \frac{\vec{k}_\perp \cdot \vec{k}_\perp' + i\vec{k}_\perp \wedge \vec{k}_\perp'}{(1-x')(1-x)} \Big], \tag{96}$$

with $\mathcal{D}(x,x') \equiv \mathcal{D}(x,x';\omega^*)$. The effective potential has no ultraviolet or infrared singularities. Only the usual integrable 'Coulomb singularity' in $\mathcal{D}(x,x')$ remains.

The Light-Cone Coulomb Schrödinger Equation

At this stage, the original matrix equation (87) has been approximated by the Tamm-Dancoff Equation, Eq. (94). For orientation, it is useful to consider the non-relativistic limit ($\vec{k}_\perp'^2 \ll m_{\rm F}^2$ and $(x - \frac{1}{2})^2 \ll 1$). In this limit the TDE, and particularly Eq. (96) are easily converted[4] into the 'Light-Cone Schrödinger equation'

$$\frac{m_{\rm F}^2 + \vec{k}_\perp^2}{x(1-x)} \psi(x, \vec{k}_\perp) - \frac{\alpha}{2\pi^2} \int_D dx' d^2\vec{k}_\perp' \frac{8 m_{\rm F}^2 \, \psi(x', \vec{k}_\perp')}{4m_{\rm F}^2 (x-x')^2 + (\vec{k}_\perp' - \vec{k}_\perp)^2} = M^2 \, \psi(x, \vec{k}_\perp), \tag{97}$$

One should note however, that this equation is kind of a hybrid since the non-relativistic limit is taken only in the potential energy. Therefore, it cannot and does not[84] precisely yield Bohr spectrum. When the non-relativistic limit is taken consistently by replacing the longitudinal momentum fraction with a 'parallel momentum' $k_\parallel \equiv 2m_{\rm F}(x - \frac{1}{2})$, collecting the momenta into a 3-vector $\vec{k} = (k_\parallel, \vec{k}_\perp)$, substituting the kinetic energy $(m_{\rm F}^2 + \vec{k}_\perp^2)/x(1-x)$ by $4m_{\rm F}^2 + 4\vec{k}^2$, and using the *definition* $M_{\rm r}^2 \equiv 4m_{\rm F}^2 + 4m_{\rm F}E$, one arrives straightforwardly at the usual Coulomb Schrödinger equation in momentum space, *i.e.*

$$\frac{\vec{k}^2}{2m_{\rm r}} \psi(\vec{k}) - \frac{\alpha}{2\pi^2} \int_D d^3\vec{k}' \, \frac{1}{(\vec{k} - \vec{k}')^2} \psi(\vec{k}') = E \, \psi(\vec{k}), \tag{98}$$

including the correct reduced mass $m_{\rm r} = m_{\rm F}/2$. Fock space regularization converts itself into a 3-momentum cut-off, *i.e.* the domain of integration D is given by $\vec{k}^2 \leq \Lambda^2/4$.

Solving the Integral Equations

As one sees from the above discussion, even at the level of only one dynamical photon, there are available a whole sequence of approximations: DLCQ-Matrix equation $\Longrightarrow$ Tamm-Dancoff Equation $\Longrightarrow$ Light-Cone Schrödinger equation $\Longrightarrow$ Coulomb Schrödinger equation. Each of these approximation equations have been recently investigated by numerical means.[30,84] the numerical effort turns out to be remarkably small, provided the numerical methods are optimized to the particular problem.

Implementing the Symmetries

A particularly important optimization for numerical solutions is the utilization of the light-cone symmetries. Some approaches to gauge field theory do not respect the elementary symmetries of the Lagrangian, by nature of their construction. However, the exact Lagrangian symmetries need not be violated by DLCQ or its approximations. For example, the Lagrangian is invariant under an arbitrary *rotation* of the coordinate system in the $x-y$-plane, corresponding to conservation of the projection of the total angular momentum J_z. Introducing the coordinates $(\vec{k}_\perp)_x = k_\perp \cos\varphi$ and $(\vec{k}_\perp)_y = k_\perp \sin\varphi$, one can Fourier transform the continuum version of the Tamm-Dancoff Eq. (94), and in particular the effective potential $V_{\rm eff} = V_{\rm eff}(\omega^*)$ according to

$$\frac{1}{2\pi}\int_0^{2\pi} d\varphi e^{-iL_z\varphi}\int_0^{2\pi} d\varphi' e^{+iL'_z\varphi'}\,\langle x, k_\perp, \varphi; s_1, s_2|\, V_{\rm eff}\,|x', k'_\perp, \varphi'; s'_1, s'_2\rangle = \langle x, k_\perp, L_z; s_1, s_2|\,\tilde{V}_{\rm eff}\,|x', k'_\perp, L'_z; s'_1, s'_2\rangle\,. \tag{99}$$

In this way, one replaces the azimuthal angle φ by the projection of the orbital angular momentum $L_z = 0, \pm 1, \ldots$ as a variable, although neither L_z nor $S_z = s_1 + s_2$ are individually a good quantum number. The explicit expressions for the matrix elements of $\tilde{V}_{\rm eff}$, are derived straightforwardly from those in Tables 2a-d. For the case $J_z = 0$, they are compiled in Tables 3 and 4.

Table 3: The matrix elements of the effective interaction for $J_z = 0$ and $x > x'$.

$\frac{\pi}{\alpha}\langle x, k_\perp, J_z, s_1, s_2 \vert \widetilde{V}_{\rm eff}(\omega^*) \vert x', k'_\perp, J_z, s'_1, s'_2\rangle$	Helicity factors
$m_{\rm F}^2 \frac{(x'-x)^2}{(1-x')x'(1-x)x}$ A	$\delta_{-s_2,s'_2}\ \delta_{s_2,s'_1}\ \delta_{s_1,-s'_1}$
$-m_{\rm F}\frac{1}{x'x}s_1\left\{\frac{1}{k_\perp}\ {\rm B} + k_\perp \frac{1-x'}{1-x}\ {\rm A}\right\}$	$\delta_{s_2,s'_2}\ \delta_{s_1,s'_2}\ \delta_{-s_1,s'_1}$
$+m_{\rm F}\frac{1}{x'x}s_1\left\{\frac{1}{k'_\perp}\ {\rm B} + k'_\perp \frac{1-x}{1-x'}\ {\rm A}\right\}$	$\delta_{s_2,s'_2}\ \delta_{s_1,-s'_2}\ \delta_{-s_1,s'_1}$
$+m_{\rm F}\frac{1}{(1-x')(1-x)}s_1\left\{\frac{1}{k_\perp}\ {\rm B} + k_\perp \frac{x'}{x}\ {\rm A}\right\}$	$\delta_{s_2,-s'_2}\ \delta_{-s_1,s'_2}\ \delta_{s_1,s'_1}$
$+m_{\rm F}\frac{1}{(1-x')(1-x)}s_1\left\{\frac{1}{k'_\perp}\ {\rm B} + k'_\perp \frac{x}{x'}\ {\rm A}\right\}$	$\delta_{s_2,-s'_2}\ \delta_{s_1,s'_2}\ \delta_{s_1,s'_1}$
$-\ {\rm A}\left\{m_{\rm F}^2\left(\frac{1}{xx'}+\frac{1}{(1-x)(1-x')}\right)+\frac{k_\perp^2}{x(1-x)}+\frac{k_\perp'^2}{x'(1-x')}\right\}$	$\delta_{s_2,s'_2}\ \delta_{s_2,-s'_1}\ \delta_{s_1,s'_1}$
$-\ {\rm A}\ \frac{1}{xx'(1-x)(1-x')}k_\perp k'_\perp$	$\delta_{s_2,s'_2}\ \delta_{s_1,s'_2}\ \delta_{s_1,s'_1}$
$+\ {\rm B}\left(\frac{1}{xx'}+\frac{1}{(1-x)(1-x')}\right)$	$\delta_{s_2,s'_2}\ \delta_{s_2,-s'_1}\ \delta_{s_1,s'_1}$
$+\ {\rm B}\left(\frac{1}{xx'}+\frac{1}{(1-x)(1-x')}\right)\frac{1}{k_\perp k'_\perp}m_{\rm F}^2$	$\delta_{s_2,s'_2}\ \delta_{s_1,s'_2}\ \delta_{s_1,s'_1}$

Abbreviations:

$$\mathrm{A} = \frac{1}{\sqrt{a^2 - 4k_\perp^2 k_\perp'^2}}; \qquad \mathrm{B} = \frac{1}{2}\left(1 + a\,\mathrm{A}\right);$$

$$a = -(x-x')^2\frac{m_{\rm F}^2}{2}\left(\frac{1}{x'x}+\frac{1}{(1-x')(1-x)}\right) - \left(k_\perp^2 + k_\perp'^2\right)$$

$$+ (x-x')\left\{\frac{k_\perp'^2}{2}\left(\frac{1}{1-x'}-\frac{1}{x'}\right)+\frac{k_\perp^2}{2}\left(\frac{1}{x}-\frac{1}{1-x}\right)\right\}$$

Table 4: The matrix elements of the effective interaction for $J_z = 0$ and $x < x'$.

$\frac{\pi}{\alpha}\left(x, k_\perp, J_z, s_1, s_2\right\vert \widetilde{V}_{\rm eff}(\omega^*) \left\vert x', k'_\perp, J_z, s'_1, s'_2\right)$	Helicity factors
$m_{\rm F}^2 \frac{(x'-x)^2}{(1-x')x'(1-x)x}$ A	δ_{-s_2,s'_2} δ_{s_2,s'_1} $\delta_{s_1,-s'_2}$
$+m_{\rm F}\frac{1}{(1-x')(1-x)}s_1\left\{\frac{1}{k_\perp}\ {\rm B}\ + k_\perp \frac{x'}{x}\ {\rm A}\right\}$	δ_{-s_2,s'_2} δ_{s_2,s'_1} δ_{s_1,s'_2}
$+m_{\rm F}\frac{1}{(1-x')(1-x)}s_1\left\{\frac{1}{k'_\perp}\ {\rm B}\ + k'_\perp \frac{x}{x'}\ {\rm A}\right\}$	δ_{-s_2,s'_2} $\delta_{s_2,-s'_1}$ δ_{s_1,s'_1}
$-m_{\rm F}\frac{1}{x'x}s_1\left\{\frac{1}{k_\perp}\ {\rm B}\ + k_\perp \frac{1-x'}{1-x}\ {\rm A}\right\}$	δ_{s_2,s'_2} δ_{-s_2,s'_1} $\delta_{s_1,-s'_2}$
$+m_{\rm F}\frac{1}{x'x}s_1\left\{\frac{1}{k'_\perp}\ {\rm B}\ + k'_\perp \frac{1-x}{1-x'}\ {\rm A}\right\}$	δ_{s_2,s'_2} δ_{s_2,s'_1} $\delta_{s_1,-s'_2}$
$-\ {\rm A}\left\{m_{\rm F}^2\left(\frac{1}{xx'}+\frac{1}{(1-x)(1-x')}\right)+\frac{k_\perp^2}{x(1-x)}+\frac{k_\perp'^2}{x'(1-x')}\right\}$	δ_{s_2,s'_2} $\delta_{s_2,-s'_1}$ δ_{s_1,s'_1}
$-\ {\rm A}\ \frac{1}{xx'(1-x)(1-x')}k_\perp k'_\perp$	δ_{s_2,s'_2} δ_{s_1,s'_2} δ_{s_1,s'_1}
$+\ {\rm B}\left(\frac{1}{xx'}+\frac{1}{(1-x)(1-x')}\right)$	δ_{s_2,s'_2} $\delta_{s_2,-s'_1}$ δ_{s_1,s'_1}
$+\ {\rm B}\left(\frac{1}{xx'}+\frac{1}{(1-x)(1-x')}\right)m_{\rm F}^2\frac{1}{k_\perp k'_\perp}$	δ_{s_2,s'_2} δ_{s_1,s'_2} δ_{s_1,s'_1}

Abbreviations:

$$\mathrm{A} = \frac{1}{\sqrt{a^2-4k_\perp^2 k_\perp'^2}}; \qquad \mathrm{B} = \frac{1}{2}\left(1 + a\ \mathrm{A}\right);$$

$$a = -(x'-x)^2\left(\frac{1}{x'x}+\frac{1}{(1-x')(1-x)}\right)\frac{m_{\rm F}^2}{2} - \left(k_\perp^2 + k_\perp'^2\right)$$
$$+ (x'-x)\left\{\frac{k_\perp^2}{2}\left(\frac{1}{1-x}-\frac{1}{x}\right)+\frac{k_\perp'^2}{2}\left(\frac{1}{x'}-\frac{1}{1-x'}\right)\right\}$$

The Lagrangian is also invariant under the operation of *charge conjugation* C, *parity* $\mathcal{P}$, and *time reversal* $\mathcal{T}$. Neither $\mathcal{P}$ nor $\mathcal{T}$, however, is an explicit symmetry of the light-cone Hamiltonian, because $\mathcal{P}$ and $\mathcal{T}$ do not leave the $x^+ = 0$ plane invariant. (Parity interchanges x^+ and x^-.) However, $\exp(-i\pi J_3)\mathcal{P}\mathcal{T}$, for example, or $\exp(-i\pi J_1)\mathcal{P}$ are exact symmetries.[18,30,68] In the numerical work[84] quoted below the combined symmetry $\mathcal{P}\mathcal{T}$ with eigenvalues ± 1 will be used.

When including both the rotational and the combined $\mathcal{P}\mathcal{T}$ symmetry, Eq. (94) can be rewritten in terms of $\Psi(x, k_\perp; J_z) \equiv \frac{1}{\sqrt{2\pi}} \int d\varphi e^{iL_z\varphi}\psi(x, \vec{k}_\perp; s_1, s_2)$, *i.e.* the Fourier-transformed wavefunctions. The "coordinate" J_z will be dropped in the sequel for notational simplicity. Since J_z is an exact symmetry, the matrix elements $\langle J_z|\, \tilde{V}_{\rm eff}\, |J_z'\rangle$ with different J_z vanish strictly in the present representation.

Solving the Light-Cone Tamm-Dancoff Equation

How does one solve an equation like (94) in practice? — As a rule, one can evaluate the integrals by Gaussian quadratures, mapping the integral equation onto another matrix equation. By converting the integration over the longitudinal momentum x into a Gaussian sum with weights $\omega_i^{(N)}$, the Tamm-Dancoff Equation (94) becomes

$$\left\{\frac{m_F^2 + k_\perp^2}{x_i(1-x_i)} - M^2\right\}\Psi(x_i, k_\perp) - \sum_{j=1}^{N}\omega_j^{(N)}\int dk_\perp'^2\, \langle x_i, k_\perp|\, \tilde{V}_{\rm eff}\, |x_j, k_\perp'\rangle \Psi(x_i, k_\perp')$$
$$+ C_{cc}(x_i, k_\perp)\Psi(x_i, k_\perp) + \sum_{j=1}^{N}\omega_j^{(N)}\int dk_\perp'^2\, \langle x_i, k_\perp|\, \tilde{V}_{\rm eff}\, |x_j, k_\perp'\rangle \Psi(x_j, k_\perp') = 0. \tag{100}$$

(The domain of summation and integration is the same as in the Tamm-Dancoff Equation as given by Eq. (95).) In this expression two terms which sum to zero are included, *i.e.* $C_{cc}(x, \vec{k}_\perp)\psi(x, \vec{k}_\perp) - C_{cd}(x, \vec{k}_\perp)\psi(x, \vec{k}_\perp)$. With the continuum part defined by

$$C_{cc}(x, k_\perp) \equiv \int_D dx' dk_\perp'^2\, \langle x, k_\perp|\, \tilde{V}_{\rm eff}\, |x', k_\perp'\rangle\ , \tag{101}$$

one easily identifies its discretized partner C_{cd} in Eq. (100). Their sum thus vanishes in the continuum limit.

The reason for introducing the 'Coulomb counter terms' is the following: The kernel of the Tamm-Dancoff Equation is singular, as can be seen explicitly in the

approximate Eqs. (97) and (98). Despite being integrable, this singularity is a numerical nightmare, and is present whenever one deals with a Coulomb-like problem in a momentum-space representation. For example, it is close to impossible to get numerically stable solutions as function of the number of integration points (and resolution) N. However, when the Coulomb terms are added, the singularity in the kernel and in the (discrete) counter term tend to cancel in the vicinity of the singularity, since by construction, they have the same residue. What remains is a smooth function which can be approximated easier. The continuum part of the counterterm restores the original equation. Ideally it should be calculated analytically, or if this turns out too difficult, it can be evaluated numerically with ultra high resolution.

Instead of $x, k_\perp$ (and φ) one can use 'spherical momentum coordinates' r, θ as defined by $k_\perp = \sqrt{\Lambda^2 + 4m_F^2}\sin\theta$ and $x = \frac{1}{2} + r\cos\theta$. The variables r and $\cos\theta$ are discretized in the intervals $[0, \frac{\Lambda}{2\sqrt{\Lambda^2+4m_F^2}}]$ and $[-1, 1]$ with ω_i as the Gaussian weights. In order to get an eigenvalue problem with a symmetric matrix the wavefunction Ψ is substituted by $\Psi(r_i, \cos\theta_j) = \Phi(r_i, \cos\theta_j)/r_i\sqrt{\omega_i\omega_j}$. The actual matrix elements are therefore $\langle r_i, \cos\theta_j | \widetilde{V}_{\rm eff} | r'_k, \theta'_l \rangle \Lambda^2 r_i r'_k \sqrt{\omega_i\omega_j\omega_k\omega_l}$. For convenience the same number of integration points N in r and $\cos\theta$ will be used in the sequel. Further details are given in Ref. 84.

The spectrum of the Tamm-Dancoff Equation obtained using the above method is displayed in Fig. 27 as a function of the resolution. It is remarkable how fast the lowest two eigenvalues approach a limiting value. These two states are identified as the singlet and the triplet state of positronium, as verified by the fact that their wave function has the correct symmetries. It is not surprising to see the comparatively slow convergence of the higher excited states. Although their wave functions in momentum space are also localized near $x \approx \frac{1}{2}$ and $k_\perp \approx 0$, they have more nodal structures. Consequently, more integration points are needed to resolve their structure.

We should emphasize two points. First, the numerical methods are obviously very efficient. For example, only a 25×25 matrix (for $N = 5$) is needed to render the singlet and the triplet state reasonably stable as function of N. This corresponds to only two transverse momentum states. Second, one has established that the longitudinal and transverse continuum limit of DLCQ exists. One should emphasize that the light-cone approach is well-defined, covariant, and numerically very economical. Most of the results have been generated by diagonalizing matrices of dimension as small as 225×225. A particularly important role for achieving this

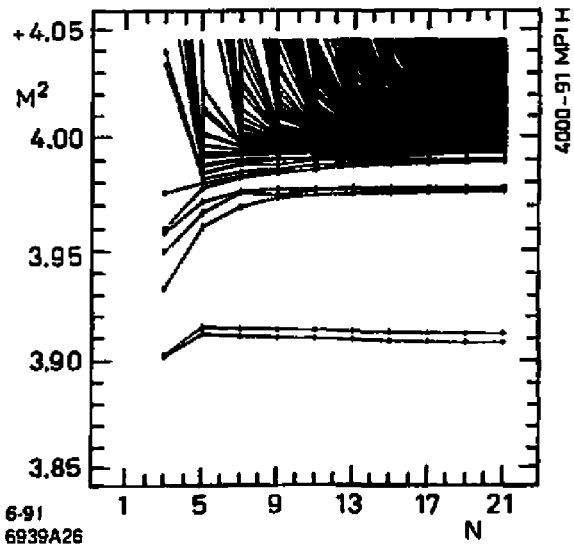

Figure 27. The invariant mass squared eigenvalues of the Tamm-Dancoff equation versus the number of integration points N. – Note the good convergence with N, and the appearance of the hyperfine splitting. Calculations are done for $J_z = 0$, $\Lambda = m$ and $\alpha = 0.3$. The numerically integrated Coulomb counter term for the Tamm-Dancoff equation is included.

result is played by the Coulomb counter terms. In general they are quite necessary for investigating numerically Coulomb-like problems in momentum representation. The methods applied are not only efficient but also precise. The calculation have been done for two vastly different values of the fine structure constant, namely $\alpha = 0.3$ and $\alpha = 1/137$. In order to extract the hyperfine shift the latter requires a numerical stability within ten significant figures (10^{-10}!).

On can also examine the convergence of the low lying spectrum as a function of scale Λ and make quantitative comparisons with analytical results. In Table 5 the binding coefficient of the singlet mass ($B_s \equiv (4(2 - M_s)/\alpha^2)$ and the singlet to triplet mass difference in the form of the hyperfine coefficient ($C_{\rm hf} \equiv (M_t - M_s)/\alpha^4$) are tabulated for five values of Λ and two values of α. The extrapolation to $\Lambda \to \infty$ is made by a Padé approximation. One should emphasize, that the deviation of the calculated mass squared eigenvalues from the free value is extremely small for $\alpha = \frac{1}{137}$. A reliable extraction of the data in Table 5 thus requires numerical accuracy to ten significant figures. The fact that the calculations do not become numerically unstable as a function of Λ is taken as a final and overall indicator

Table 5: The singlet binding and the hyperfine coefficient for the Light-cone Tamm-Dancoff Equation as function of Λ and α. - Calculations are done $N = 15$ integration points, and extrapolated to $\Lambda \to \infty$ with a Padé-Approximand $f(\Lambda) = (c_1 + c_2/\Lambda)/(1 + c_3/\Lambda)$ using the values $\Lambda = 1.0$, 3.0, and 5.0.

$\alpha = \frac{3}{10}$			$\alpha = \frac{1}{137}$		
Λ	B_s	$C_{\rm hf}$	$\Lambda\frac{1}{3\alpha}$	B_s	$C_{\rm hf}$
1.0	1.0503	0.1348	1.0	0.9345	0.1023
2.0	1.1834	0.2888	2.0	0.9922	0.1955
3.0	1.2390	0.3857	3.0	1.0053	0.2366
4.0	1.2723	0.4533	4.0	1.0127	0.2581
5.0	1.2960	0.5037	5.0	1.0211	0.2667
∞	1.4025	0.8317	∞	1.0459	0.3140

that one can master the numerical aspects of the problem.

What should one expect analytically? In an expansion up to order α^4, the singlet and the triplet mass of positronium (excluding annihilation) is given by[89]

$$M_s = 2 - \frac{1}{4}\alpha^2\left(1 + \frac{63}{48}\alpha^2\right) \quad \text{and} \quad M_t = 2 - \frac{1}{4}\alpha^2\left(1 - \frac{1}{48}\alpha^2\right), \tag{102}$$

respectively, where here (and in the following) masses are given in units of the physical electron mass. The hyperfine coefficient is then the Fermi value $(C_{\rm hf})_{\rm Fermi} = \frac{1}{3}$. Bodwin *et al.*[83] have summarized the analytical work for the higher order corrections to the hyperfine shift in positronium:

$$C_{\rm hf} = \frac{1}{2}\left[\frac{2}{3}\left(+\frac{1}{2}\right) - \frac{\alpha}{\pi}\left(\ln 2 + \frac{16}{9}\right) + \frac{5}{12}\alpha^2 \ln\frac{1}{\alpha} + K\alpha^2 + K'\alpha^3\right]. \tag{103}$$

The term $\frac{1}{2}$ is set in parentheses since it originates in the photon annihilation term. The impact of the coefficient K is small; its numerical value[83] is $K = +0.427$. A complete calculation is not yet available for K', except that is contains a $\ln\alpha$ term; it is set zero. Eq. (103) predicts therefore the values $C_{\rm hf} = 0.333$ for $\alpha = \frac{1}{137}$ and $C_{\rm hf} = 0.257$ for $\alpha = 0.3$. It should be noted that part of the higher order

corrections come from contributions in which two dynamical photons are in flight; thus a strict correspondence with the spectrum of light-cone model is not expected.

The numbers in Table 5 agree with the analytical predictions only to first approximation. In particular, they are not as accurate as the recent results of Koniuk *et al.*[90,91] for a corresponding model using *equal time* quantization. Although the present hyperfine shift for $\alpha = \frac{1}{137}$ is reasonably in between the Fermi and the Bodwin *et al.*values, the singlet state is slightly over-bound by four percent — in view of the numerical accuracy a small but significant deviation. For $\alpha = \frac{3}{10}$ the discrepancy is even more accentuated. Instead of $B_s = 1.118$ one gets 1.403, which shows that the α^4 coefficient is overrated by about a factor 3. The hyperfine shift points to the same direction, it is larger than the analytical value by roughly a factor 3.

One must conclude that the Tamm-Dancoff Equation overdoes the relativistic effects. We conjecture that the right correction will come when the ad-hoc assumption, Eq. (88), will be relaxed and the restriction to one dynamical photon is removed.

Summary and Discussion of the Tamm-Dancoff Equation Results

The numerical tests of the light-cone Tamm Dancoff approach in positronium provide some confidence that one can use light-cone Fock methods to solve relativistic bound state problems in gauge theory. The Tamm-Dancoff Equation reproduces the expected Bohr spectrum $M_n \sim 2m(1-B_n\frac{\alpha^2}{4})$ almost quantitatively, as well a the typical relativistic deviations like the hyperfine shift $\nu = \alpha^4 C_{\rm hf}(\alpha)$. The binding coefficients $B_n \sim \frac{1}{n^2}$ are reproduced with small but significant deviations, one percent by order of magnitude. They are much smaller for the physical value $\alpha = 1/137$ than for the very large value $\alpha = 0.3$. Similarly, the hyperfine coefficient for $\alpha = 1/137$ is close to the correct value $C_{\rm hf} \sim \frac{1}{3}$, but for $\alpha = 0.3$ it is almost twice as large.

But the Tamm-Dancoff Equation does not solve the original physical problem. It mistreats it by a so far uncertain approximation, stated in Eq. (88). It is however possible to relax this constraint Eq. (88) and generate the full resolvent without uncontrolled approximations: Quite in general, the full resolvent $G(\omega)$ in the Q-space can be expanded in terms of the free resolvent $G_0(\omega)$ and of the instantaneous annihilation interaction $S^{(a)}$, *i.e.* $G(\omega) = G_0(\omega) + G_0(\omega)S^{(a)}G(\omega)$. With $W(\omega) = VG(\omega)V^\dagger$ the next-to-leading order becomes $W^{(2)}(\omega) = VG_0(\omega)S^{(a)}G_0(\omega)V^\dagger$. The superscript indicates the power of α. Figure 28 collects essentially all possible graphs classified according to whether the two vertices sit on the same or on a

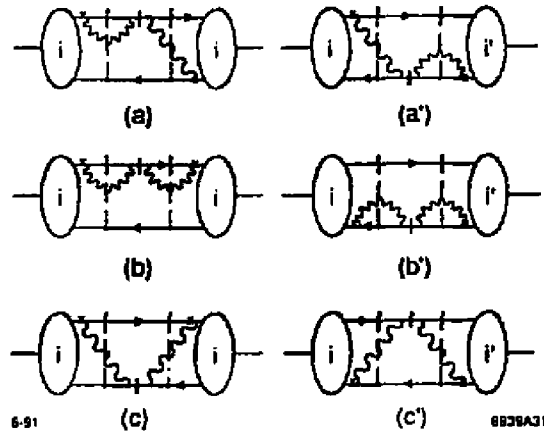

Figure 28. Some typical graphs to order α^2 which begin and end with a vertex interaction $V_{q-qq}(\times)$. The instantaneous interaction $S^{(a)}_{qq-qq}$ is sandwiched in between them. In diagram (a) and (a') the vertices are one different, else they are on the same lines.

different fermion line. Considering the same case as in section 3, graphs 28(a) and 28(a') turn out to vanish, strictly. Graphs 28(b) and 28(b') must be absorbed into mass renormalization, only graphs 28(c) and 28(c') need to be considered. As it turns out they can be re-summed explicitly *to all orders*, with the exact result

$$\widetilde{W}(\omega) = \sum_{n=2}^{\infty} W^{(n)}(\omega) = \frac{1}{1+a} W^{(2)}(\omega).$$

Both a and $W^{(2)}$ diverge logarithmically with the scale Λ. For sufficiently large values one gets by order of magnitude $a \sim \alpha \ln \Lambda/m_F$ and $W^{(2)} \sim \alpha^2 \ln \Lambda/m_F$. The re-summed interaction $\widetilde{W}$ therefore is proportional to α instead of to α^2, and independent of Λ it is probably able to account for the small but significant deviations in the binding coefficients and the hyperfine shift.

The Lanczos Method for DLCQ

The most serious practical difficulty for implementing DLCQ matrix diagonalization for physical theories in 3 + 1 dimensions, is the rapidly growing size of the matrix representation as one increases the size of the Fock basis. Fortunately, the matrix representations of H_{LC} in the free Fock basis are extremely sparse, and one can take advantage of efficient algorithms for diagonalizing such matrices. An

important example of such an algorithm is the Lanczos method, which has been used for DLCQ problems in papers by Hiller,[13] Kaluža,[30] and Hollenberg, *et al.*[29] For example, let H be an $N \times N$ Hermetian matrix. Apply H to a test state vector $|v_1\rangle$. The result is

$$H|v_1\rangle = \alpha_1 |v_1\rangle + \beta_1 |v_2\rangle \ , \tag{104}$$

where $|v_2\rangle$ is orthonormal to $|v_1\rangle$. Applying H to the new state vector gives:

$$H|v_2\rangle = \beta_1 |v_1\rangle + \alpha_2 |v_2\rangle + \beta_2 |v_3\rangle, . \tag{105}$$

where $|v_3\rangle$ is orthonormal to $|v_1\rangle$ and $|v_2\rangle$. However, if we apply H to $|v_3\rangle$ one only gets three non-zero terms:

$$H|v_3\rangle = 0|v_1\rangle + \beta_2 |v_2\rangle + \alpha_3 |v_3\rangle + \beta_3 |v_4\rangle \ . \tag{106}$$

Thus, by construction, $\langle v_i| H |v_j\rangle$ is tri-diagonal, and the eigenvalues of its first $P \times P$ submatrix of this matrix converges rapidly to the lowest P eigenvalues of H. The computer time for obtaining these eigenvalues grows like fN^2 where f is a measure of the sparseness of H. This is much less than the time required for diagonalizing H itself, which grows like N^3. In the work of Hollenberg *et al.* one can handle matrices of sizes approaching $N = 10^6$.

First Applications of DLCQ to QCD(3+1)

The application of the DLCQ method to QCD(3+1) will inevitably be difficult since meaningful numerical results will require Fock states containing two or more gluons. At the least, asymptotic freedom cannot appear in the coupling constant renormalization unless one allows for two or more gluons "in flight." A consistent renormalization program for the non-Abelian theory has not been completely worked out within the non-perturbative framework. However, as an initial exercise to test the power of the Lanczos method, Hollenberg *et al.* have diagonalized the unrenormalized light cone Hamiltonian for QCD(3+1) within the meson Fock classes $|q\bar{q}\rangle$ and $|q\bar{q}g\rangle$ only. Figure 29 shows the result for the lowest meson eigenvalue $\mathcal{M}^2$ as a function of QCD bare coupling g for several values of the quark mass. The Fock space was limited by taking the harmonic resolution $K = 6$; in addition, the ultraviolet cut-off used in this work limited the square of the Fock state invariant mass to 24 GeV^2. The maximum transverse momentum

at $Q_\perp = \frac{\pi N_\perp}{L_\perp} = 1$ GeV, with $N_\perp$ transverse points. The fact that the mass-squared spectrum turns negative at large coupling may possibly be cured by a consistent light-cone Hamiltonian renormalization procedure or the use of the Coulomb singularity trick used for positronium.[84] Another possibility is that negative eigenvalues of the P^- actually represents a cross-over with a negative P^+ spectrum.[92]

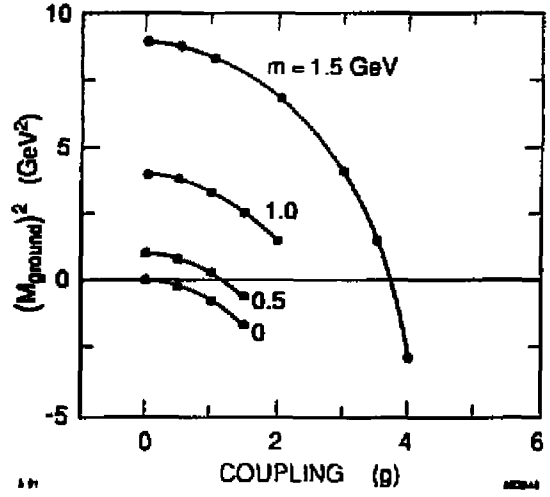

Figure 29. First computation of the low-lying meson spectrum of $QCD(3+1)$ computed using Lanczos diagonalization. Only the lowest two Fock classes are retained. See Ref. 29.

The Light-Cone Vacuum

In the introduction we discussed the remarkable feature that the perturbative vacuum in light-cone perturbation theory can also be an eigenstate of the full Hamiltonian. Let us review the arguments: By definition, the perturbative vacuum is annihilated by the free Hamiltonian: $H_0^{LC}|0\rangle = 0$. In gauge theory the interaction terms in H_{LC} are three-and four-point interactions; for example, in QED, the application on the vacuum of the interaction $H_I^{LC} = \int d^3x e\bar{\psi}\gamma \cdot A\psi$ results in a sum of terms $b^\dagger(\underline{k}_1)a^\dagger(\underline{k}_2)d^\dagger(\underline{k}_3)|0\rangle$. Just as in the discussion of LCPTH, P^+ conservation requires $\sum_{i=1}^3 k_i^+ = 0$. However $k_i^+ = 0$, is incompatible with finite energy for the massive fermions. Thus the total light-cone Hamiltonian also annihilates the perturbative vacuum: $H^{LC}|0\rangle = 0$. In contrast, the state $H|0\rangle$ is a

highly complex composite of pair fluctuations in equal-time quantization.

The apparent simplicity of the vacuum in light-cone quantization is in severe contradiction to normal expectations for the structure of the lowest mass eigenstate of QCD. In the instant form, the QCD vacuum is believed to be a highly structured quark-gluon condensate, which in turn is believed to be connected to color confinement, chiral symmetry breaking, the Goldstone pion, etc.[93] In the standard model, the $W^{\pm}$ and Z bosons acquire their mass through the spontaneous symmetry breaking of the scalar Higgs potential. Thus an immediate question is how one can obtain non-trivial vacuum properties in a light-cone formulation of gauge field theory.[94] This problem has recently been attacked from several directions. In the analyses of Hornbostel and Lenz *et al.*, one can trace the fate of the equal time vacuum as one approaches the $P_z \to \infty$ or equivalently rotate $\theta \to \pi/2$ as the evolution parameter $\tau = t\cos\theta + \frac{z}{c}\sin\theta$ approaches time on the light-cone. As shown in Refs. 23 and 94, one finds that for theories that allow spontaneously symmetry breaking, there is a degeneracy of light-cone vacua, and the true vacuum state can differ from the perturbative vacuum through the addition of zero mode quanta with $k^+ = k^- = k_\perp = 0$.

An illuminating analysis of the influence of zero modes in $QED(1+1)$ has been given by Werner, Heinzl and Krusche.[95] They show that although it is correct to impose the gauge condition $A^+ = 0$ on the particle sector of the Fock space, one must allow for $A^+ \neq 0$ if $k^+ = 0$. Allowing for this degree of freedom, one obtains a series of topological θ vacua on the light-cone which reproduce the known features of the massless Schwinger model including a non-zero chiral condensate. However, the effect of the infrared zero mode quanta decouples from the physics of zero charge bound states, so that the physical spectrum in one-space one-time gauge theories is independent of the choice of vacuum. The freedom in having a non-zero value for A^+ at $k^+ = 0$ can also be understood by using the gauge $\partial^+ A^+ \sim k^+ A^+ = 0$.[46]

It is thus anticipated that zero mode quanta are important for understanding the light-cone vacuum for QCD in physical space-time. In particular, the non-Abelian four-point interaction term

$$H_I^{LC} = -\tfrac{1}{2} g^2 \int d^3\underline{x} Tr\{[A^\mu, A^\nu][A^\mu, A^\nu]\} \tag{107}$$

plays a unique and an essential role, since $H_I^{LC}|0\rangle \neq 0$ as long as one allows for zero mode gluon fields in the Fock space. Thus the true light-cone vacuum $|\Omega\rangle$ is not necessarily identical to the perturbative vacuum $|0\rangle$. In fact the zero mode

excitations of H_f^{LC} produce a color-singlet gluon condensate $\langle\Omega|G_{\mu\nu}G^{\mu\nu}|\Omega\rangle \neq 0$ of the type postulated in the QCD sum rule analyses. The effect of such condensates will be to introduce "soft" insertions into the quark and gluon propagators and their effective masses $m(p^2)$, and to modify the perturbative interactions at large distances. (See Fig. 30). Thus unlike the one-space one-time theory, the zero-mode gluon excitations do affect the color-singlet bound states. On the other hand, such zero mode corrections to vacuum cannot appear in Abelian QED(3+1) as long as a non-zero fermion mass appears in the free Hamiltonian.

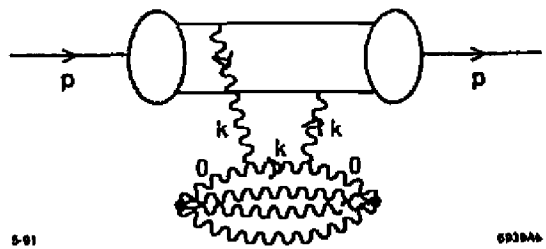

Figure 30. Effect of a zero-mode gluon condensate on quark and gluon propagators.

Advantages of Discretized Light-Cone Quantization

As we have discussed in these lectures, the method of discretized light-cone quantization provides a relativistic, frame-independent discrete representation of quantum field theory amenable to computer simulation. In principle, the method reduces the light-cone Hamiltonian to diagonal form and has the remarkable feature of generating the complete spectrum of the theory: bound states and continuum states alike. DLCQ is also useful for studying relativistic many-body problems in relativistic nuclear and atomic physics. In the nonrelativistic limit the theory is equivalent to the many-body Schrödinger theory. As we have reviewed in these lectures, DLCQ has been successfully applied to a number of field theories in one-space and one-time dimension, providing not only the bound-state spectrum of these theories, but also the light-cone wavefunctions needed to compute structure functions, intrinsic sea-quark distributions, and the e^+e^- annihilation cross section.

Although our primary has been to apply light-cone methods to non-perturbative problems in QCD in physical space-time, it is important to first validate these techniques– particularly the renormalization program–in the much simpler Abelian

theory of QED. In the proceeding sections we have quantized quantum electrodynamics on the light-cone in a discretized form which in principle allows practical numerical solutions for obtaining its spectrum and wavefunctions at arbitrary coupling strength α. We also have discuss a frame-independent and approximately gauge-invariant particle number truncation of the Fock basis which is useful both for computational purposes and physical approximations. In this method[28] ultraviolet and infrared regularizations are kept independent of the discretization procedure, and are identical to that of the continuum theory. One thus obtains a finite discrete representation of the gauge theory which is faithful to the continuum theory and is completely independent of the choice of Lorentz frame. Hopefully, these techniques will be applicable to non-Abelian gauge theories, including quantum chromodynamics in physical space-time.

The recent applications of DLCQ to the positronium spectrum are encouraging, but they also show formidable numerical difficulties as the number of Fock states and level of discreteness grows. Whether QCD can be solved using such methods — considering its large number of degrees of freedom is unclear.

Nevertheless, DLCQ has the potential for solving important non-perturbative problems in gauge theories. It has a number of intrinsic advantages:

- The formalism is independent of the Lorentz frame – only relative momentum coordinates appear. The computer does not know the Lorentz frame!
- Fermions and derivatives are treated exactly; there is no fermion doubling problem.
- The ultraviolet and infrared regulators are introduced in DLCQ as Lorentz invariant momentum space cut-offs of the continuum theory. They are thus independent of the discretization.
- The field theoretic and renormalization properties of the discretized theory are faithful to the continuum theory. No non-linear terms are introduced by the discretization.
- One can use the exact global symmetries of the continuum Lagrangian to pre-diagonalize the Fock sectors.
- The discretization is denumerable; there is no over-counting. The minimum number of physical degrees of freedom are used because of the light-cone gauge. No Gupta-Bleuler or Faddeev-Popov ghosts occur and unitarity is explicit.
- Gauge invariance is lost in a Hamiltonian theory. However, the truncation can be introduced in such a way as to minimize explicit breaking of the gauge

symmetries.

- The output is the full color-singlet spectrum of the theory, both bound states and continuum, together with their respective light-cone wavefunctions.

There are, however, a number of difficulties that need to be resolved:

- The number of degrees of freedom in the representation of the light-cone Hamiltonian increases rapidly with the maximum number of particles in the Fock state. Although heavy quark bound states probably only involve a minimal number of gluons in flight, this is probably not true for light hadrons.
- Some problems of ultraviolet and infrared regulation remain. Although Pauli-Villars ghost states and finite photon mass can be used to regulate Abelian theories, it is not suitable method in non-Abelian theories.[73] This problem may possibly be avoided by working with finite but broken, super-symmetric theories. A cutoff in the invariant mass of the Fock state introduces extra renormalization terms compatible with the light-cone Lorentz symmetries.
- The renormalization procedure is not completely understood in the context of non-perturbative problems. However, a non-perturbative recursive representation for electron mass renormalization has been successfully tested in QED(3+1).
- The Coulomb singularity in the effective gluon-exchange potential is poorly approximated in the discrete form. An analytic trick must be used to speed convergence. Such a method has been tested successfully in the case of the positronium spectrum in QED(3+1).
- The light-cone gauge introduces extra divergences at $k^+ \to 0$ which in principle cancel between instantaneous gluon exchange and gluon propagation. However, this cancellation requires relating instantaneous potential terms to higher gluon number Fock states.
- The vacuum in QCD is not likely to be trivial since the four-point interaction term in $g^2 G_{\mu\nu}^2$ can introduce new zero-mode color-singlet states which mix with the free vacuum state. Thus a special treatment of the QCD vacuum is required. In the case of zero mass quarks, there may be additional mixing of the perturbative vacuum with fermion zero-modes. Since the zero-mode $k^\mu = 0$ states have no spatial structure, the light-cone vacuum is evidently much simpler than that of the equal-time theory. In the case of massless fermions, chiral symmetry could be spontaneous broken by fermion pair zero-modes which form a chiral condensate.

Acknowledgements

Much of the material presented in these lectures is based on collaborations with Kent Hornbostel, Andrew Tang, Peter Lepage, Matjaz Kaluža, Michael Krautgärtner, Thomas Eller, and Frank Wölz. We particularly thank Alex Langnau and Matthias Burkardt for many valuable discussions and suggestions. We also wish to thank Professors H. Mitter and his colleagues for their work in organizing an outstanding Winter School in Schladming.

REFERENCES

1. A. S. Kronfeld and D. M. Photiadis, Phys. Rev. D31, 2939 (1985).
2. G. Martinelli and C. T. Sachrajda, Phys. Lett. B217, 319 (1989).
3. V. L. Chernyak, A.R. Zhitnitskii, Phys. Rept. 112, 173 (1984). See also M. Gari and N. G. Stephanis, Phys. Lett. B175, 462 (1986), and references therein.
4. G. P. Lepage and S. J. Brodsky, Phys. Rev. D22, 2157 (1980); Phys. Lett. 87B, 359 (1979); Phys. Rev. Lett. 43, 545, 1625(E) (1979).
5. See P. Kroll, Wuppertal University preprint WU-B-90-17 (1990), and references therein.
6. For a review, see S. J. Brodsky, SLAC-PUB 5529 (1991), to be published in the proceedings of the Lake Louise Winter Institute (1991).
7. I. Tamm, J. Phys (USSR) 9, 449 (1945). S. M. Dancoff, Phys. Rev. 78, 382 (1950).
8. We shall use the conventional term "light-cone quantization" as the equivalent to the front-form and null-plane quantization. For further discussion, see P. L. Chung, W. N. Polyzou, F. Coester, and B. D. Keister, Phys. Rev. C37, 2000 (1988), and references therein.
9. P.A.M. Dirac, Rev. Mod. Phys. 21, 392 (1949).
10. Gribov has emphasized the interesting alternative possibility that hadrons in QCD are actually bound states of light quarks with *negative* kinetic energy. This removes the exclusion of negative k^+ in the Fock basis and thus would have profound consequences for light-cone quantization. See V. N. Gribov, Lund preprint, LU TP 91-7 (1991).
11. For a discussion of renormalization in light-cone perturbation theory, see S. J. Brodsky, R. Roskies and R. Suaya, Phys. Rev. D8, 4574 (1974), and also Ref. 4.
12. M. Burkardt, A. Langnau, SLAC-PUB-5394, (1990), and to be published.
13. J. R. Hiller, University of Minnesota preprints (1990), and Phys. Rev. D43,2418 (1991).
14. S. D. Drell and T. M. Yan, Phys. Rev. Lett. 24, 181 (1970).
15. S. J. Brodsky and S. D. Drell, Phys. Rev. D22, 2236 (1980).
16. G. P. Lepage and B. A. Thacker, CLNS-87/114, (1987). See also G. P. Lepage and W. Caswell, Phys. Lett. 167B, 437 (1986).

17. S. J. Brodsky and I. A. Schmidt, Phys. Lett.B234,144 (1990); Phys. Rev. D43, 179 (1991).
18. K. Hornbostel, S. J. Brodsky, H. C. Pauli, Phys. Rev. D41, 3814 (1990).
19. G. P. Lepage, S. J. Brodsky, T. Huang, P. B. Mackenzie, published in the *Proceedings of the Banff Summer Institute*, 1981.
20. S. J. Brodsky, G. P. Lepage, in *Perturbative Quantum Chromodynamics*, p. 93, edited by A. H. Mueller (World Scientific, Singapore, 1989).
21. H. C. Pauli and S. J. Brodsky, Phys. Rev. D32, 1993 (1985); Phys. Rev. D32, 2001 (1985).
22. T. Eller, H. C. Pauli, S. J. Brodsky, Phys. Rev. D35, 1493 (1987).
23. A. Harindranath and J. P. Vary, Phys. Rev. D36, 1141 (1987).
24. M. Burkardt, Nucl. Phys. A504, 762 (1989).
25. R. J. Perry, A. Harindranath, K. G. Wilson, Phys. Rev. Letters 65, 2959 (1990), R. J. Perry, and A. Harindranath, Ohio State University preprint (1990).
26. D. Mustaki, S. Pinsky, J. Shigemitsu, K. Wilson, Ohio State University preprint (1990).
27. A. C. Tang, SLAC-351 (1990).
28. A. C. Tang, S. J. Brodsky, and H. C. Pauli, SLAC-PUB-5425 (1991), to be published in Phys. Rev. D.
29. L. C. L. Hollenberg, K. Higashijima, R. C. Warner, B. H. J. McKellar, KEK-TH-280, (1991).
30. M. Kaluža, University of Heidelberg thesis, and to be published (1990).
31. J. R. Klauder, H. Leutwyler, and L. Streit, Nuovo Cimento us 59 315 (1969).
32. J. B. Kogut and D. E. Soper, Phys. Rev. D1 2901 (1970)
33. F. Rohrlich, Acta Phys. Austriaca, Suppl. VIII, 2777 (1971).
34. H. Leutwyler, Nucl. Phys. B76, 413 (1974).
35. A. Casher, Phys. Rev. D14, 452 (1976).
36. S. J. Chang, R. G. Root, T. M. Yan, Phys. Rev. D7, 1133 (1973); S. J. Chang, T. M. Yan, Phys. Rev. D7, 1147 (1973).
37. S. J. Brodsky, C. R. Ji, SLAC-PUB-3747, (1985).
38. G. McCartor, Z. Phys. C41, 271 (1988); and SMU preprint SMUTH/91-02 (1991).
39. E. V. Prokhvatilov and V. A. Franke, Sovj. J. Nucl. Phys. 49, 688 (1989).

40. V. A. Franke, Y. V. Novozhilov, and E. V. Prokhvatilov, Letters in Mathematical Physics 5, 239 (1981).

41. A. M. Annenkova, E. V. Prokhvatilov, and V. A. Franke Zielona Gora Pedag. Univ. preprint - WSP-IF 89-01 (1990).

42. V. A. Karmanov, Nucl. Phys. B166, 378 (1980).

43. V. A. Karmanov, Nuclear Physics, A362, 331 (1981).

44. V. N. Pervushin, Nuclear Physics B15, 197 (1990).

45. G. McCartor, Z. Phys. C41 271, (1988).

46. F. Lenz, in the proceedings of the NATO Advanced Summer Institute on Nonperturbative Quantum Field Theory Cargese, France, Aug 8-18, 1989. Edited by D. Vautherin, F. Lenz, and J.W. Negele. Plenum Press, N. Y. (1990).

47. S. Weinberg, Phys. Rev. 150, 1313 (1966).

48. S. D. Drell, D. Levy, T. M. Yan, Phys. Rev. 187, 2159 (1969); Phys. Rev. D1, 1035 (1970); Phys. Rev. D1, 1617 (1970).

49. L. Susskind, Phys. Rev. 165, 1535 (1968); L. Susskind, G. Frye, Phys. Rev. 164, 2003 (1967).

50. J. D. Bjorken, J. B. Kogut, D. E. Soper, Phys. Rev. D3, 1382 (1971); J. B. Kogut, D. E. Soper, Phys. Rev. D1, 2901 (1970).

51. S. J. Brodsky, R. Roskies, R. Suaya, Phys. Rev. D8, 4574 (1973).

52. General QCD analyses of exclusive processes are given in Ref. 4, S. J. Brodsky and G. P. Lepage, SLAC-PUB-2294, presented at the Workshop on Current Topics in High Energy Physics, Cal Tech (Feb. 1979), S. J. Brodsky, in the Proc. of the La Jolla Inst. Summer Workshop on QCD, La Jolla (1978), A. V. Efremov and A. V. Radyushkin, Phys. Lett. B94, 245 (1980), V. L. Chernyak, V. G. Serbo, and A. R. Zhitnitskii, Yad. Fiz. 31, 1069 (1980), S. J. Brodsky, Y. Frishman, G. P. Lepage, and C. Sachrajda, Phys. Lett. 91B, 239 (1980), and A. Duncan and A. H. Mueller, Phys. Rev. D21, 1636 (1980).

53. QCD predictions for the pion form factor at asymptotic Q^2 were first obtained by V. L. Chernyak, A. R. Zhitnitskii, and V. G. Serbo, JETP Lett. 26, 594 (1977), D. R. Jackson, Ph.D. Thesis, Cal Tech (1977), and G. Farrar and D. Jackson, Phys. Rev. Lett. 43, 246 (1979). See also A. M. Polyakov, Proc. of the Int. Symp. on Lepton and Photon Interactions at High Energies, Stanford (1975), and G. Parisi, Phys. Lett. 84B, 225 (1979). See also S. J.

Brodsky and G. P. Lepage, in *High Energy Physics–19[illegible] Proceedings of the XXth International Conference, Madison, Wisconsin, [illegible]* by L. Durand and L. G. Pondrom (AIP, New York, 1981); p. 568. A. [illegible]hov and A. V. Radyushkin, Rev. Nuovo Cimento 3, 1 (1980); Phys. Lett. 94B, 245 (1980). V. L. Chernyak and A. R. Zhitnitsky, JETP Lett. 25, 11 (1977); G. Parisi, Phys. Lett. 43, 246 (1979); M. K. Chase, Nucl. Phys. B167, 125 (1980).

54. S. J. Brodsky, G. R. Farrar, Phys. Rev. D11, 1309 (1975).
55. A. Kronfeld and B. Nizic, Fermilab-Pub 91/64-T (1991). The Compton scattering data are from M. Shupe *et al.*, Phys. Rev. D19, 1921 (1979).
56. P. Stoler, Phys. Rev. Lett. 66, 1003 (1991); and to be published in Phys. Rev. D.
57. C. E. Carlson and J. L. Poor, Phys. Rev. D38, 2758 (1988).
58. N. Isgur and C. H. Llewellyn Smith, Phys. Lett. B217, 535 (1989)
59. J. Hansper, R. Eckardt, and M. F. Gari *et al.*, Ruhr-Universität Bochum preprint (1991).
60. A. Szczepaniak, L. Mankiewicz Univ. of Florida Preprint (1991).
61. S. J. Brodsky, SLAC-PUB-5529 (1991).
62. J. Botts, Nucl. Phys. B353 20 (1991).
63. P. V. Landshoff, Phys. Rev. D10, 1024 (1974).
64. S. J. Brodsky, G. P. Lepage, and P. B. Mackenzie Phys. Rev. D28, 228 (1983). For a recent discussion of the scale-fixing problem in QCD, see J. C. Collins, ANL-HEP-CP-90-58 (1990).
65. W. Kwong, P. B. Mackenzie, R. Rosenfeld, and J. L. Rosner Phys. Rev. D37 3210,(1988).
66. A. Szczepaniak, E. M. Henley, S. J. Brodsky, Phys.Lett. B243, 287 (1990).
67. S. J. Brodsky, G. P. Lepage, and S. A. A. Zaidi, Phys. Rev. D23, 1152 (1981).
68. As noted by U. Dokshitser and A. Mueller (private communication), virtual loop corrections related to the Sudakov form factor due to the difference in the overall heavy quark mass scale M_b^2 and the hard scattering scale can also modify the hard scattering amplitude. However, such corrections are not expected to be large.
69. D. Bartoletta *et al.*, Phys. Rev. Lett. 62 2436 (1989).
70. S. G. Gorishny, A. L. Kataev, and S. A. Larin, Phys. Lett. B212, 238 (1988).
71. We follow here the notation and discussion of D. Soper, Phys. Rev. D4 1620, (1971); and K. Hornbostel, CLNS-90-1038, (1990).

72. A. Langnau, to be published.

73. It also should be noted that in Gribov's approach to quark confinement, Pauli-Villars or dimensional regulation cannot even be used in principle for strong coupling problems in QCD because of the way it eliminates the negative energy sea. See Ref. 10.

74. S. J. Brodsky, Y. Frishman, G. P. Lepage and C. Sachrajda, Phys. Lett. 91B, 239 (1980).

75. *SU(N)* gauge theories, restricted to one spatial dimension and time have been studied extensively at large N; see e.g. G. 't Hooft, Nucl. Phys. B75, 461 (1974); C. G. Callan, N. Coote, and D. J. Gross, Phys. Rev. D13, 1649 (1976); M. B. Einhorn, Phys. Rev. D14, 3451 (1976); and I. Bars and M. B. Green, Phys. Rev. D17, 537 (1978).

76. C. J. Burden and C. J. Hamer, Phys. Rev. D37, 479 (1988), and references therein.

77. Y. Frishman and J. Sonnenschein, Nucl. Phys. B294, 801 (1987), and Nucl. Phys. B301, 346 (1988).

78. Bergknoff, H., Nucl. Phys. B122, 215 (1977).

79. For a recent discussion and further references, see C. S. Kim, Nucl. Phys. B353, 87 (1991).

80. J. J. Aubert, *et al.*, Nucl. Phys. B213, 31 (1983). See also E. Hoffmann and R. Moore, Z. Phys. C20, 71 (1983).

81. K. Hornbostel, private communication; S. J. Brodsky and K. Hornbostel, to be published.

82. S. J. Brodsky and P. Hoyer, SLAC-PUB-5422, (1991).

83. G. T. Bodwin, D. R. Yennie, and M. A. Gregorio, Rev. Mod. Phys. 56, 723 (1985).

84. M. Krautgärtner, H. C. Pauli, and F. Wölz, Heidelberg preprint MPIH-V4-1991.

85. P. M. Morse and H. Feshbach, *Methods in Theoretical Physics*, 2 Vols, Mc Graw-Hill, New York, N.Y., 1953.

86. M. Sawicki, Phys Rev. D32, 2666 (1985).

87. M. Sawicki, Phys. Rev. D33, 1103 (1986).

88. L. Mankiewicz, private communication.

89. H. A. Bethe and E. E. Salpeter, *Quantum Mechanics of One- and Two-Electron Atoms*, Springer, Heidelberg, 1957.

90. W. Dykshoorn, R. Koniuk, and R. Muñoz-Tapia, Phys. Rev. A41, 60 (1990).
91. W. Dykshoorn and R. Koniuk, Phys. Rev. A41, 64 (1990).
92. We thank V. Gribov for an illuminating discussion on this point.
93. See, for example, M. H. Thoma and H. J. Mang, Z. Phys. C44, 349 (1989).
94. St. Glazek, Phys. Rev. D38 3277 (1988).
95. Th. Heinzl, St. Krusche, and E. Werner, Regensburg preprint TPR 90-44.